HOKKAIDO UNIVERSITY

Title	Studies on the biological activities of mottled skate (Raja pulchra) by-products and their possible industrial applications
Author(s)	李, 雯
Degree Grantor	北海道大学
Degree Name	博士(水産科学)
Dissertation Number	甲第14184号
Issue Date	2020-09-25
DOI	https://doi.org/10.14943/doctoral.k14184
Doc URL	https://hdl.handle.net/2115/96128
Type	doctoral thesis
File Information	Li_Wen.pdf

Hokkaido University Collection of Scholarly and Academic Papers : HUSCAP

Studies on the biological activities of mottled skate (*Raja pulchra*) by-products and their possible industrial applications

(カスベ（エイ）加工由来副生物の生物活性およびその産業応用に関する研究)

北海道大学大学院水産科学院

海洋応用生命科学専攻

Graduate School of Fisheries Sciences

Division of Marine Life Science

李 雯

Li Wen

2020 年

Contents

I. General introduction 4

1. Potential bioactive compounds in fish cartilage 6

1.1. Chondroitin sulfate (CS) 6

1.2. Type II collagen (C-II) 12

1.3. Other products 19

2. Potential fish cartilage sources for industrialization 22

2.1. Cartilaginous fish 22

2.2. Cultured bony fish 25

2.3. Other bony fish 26

3. Advantages and disadvantages of fish cartilage as a resource 27

4. The objective of the research in this thesis 29

Tables 31

II. Anti-obesity effects of chondroitin sulfate oligosaccharides from the skate *Raja pulchra* 34

1. Introduction 34

2. Materials and methods 36

2.1. Materials 36

2.2. *In vitro* pancreatic lipase assay 37

2.3. Endotoxin detection and reduction 39

2.4. Cell culture experiment 40

2.5. *In vivo* experiment 41

2.6. Statistical analyses 43

3. Results and discussions 43

3.1. Effects of CSs on pancreatic lipase activity 43

3.2. Endotoxin levels of CSs after endotoxin-reduction treatment 45

3.3. Effect of CSs on 3T3-L1 proliferation/metabolism 46

3.4. Effect of CSs on lipid accumulation in 3T3-L1 adipocytes 48

3.5. *In vivo* effect of CSo 50

4. Conclusion 54
Tables and figures 56
III. Free radical scavenging activity of type II collagen peptides and chondroitin sulfate oligosaccharides from by-products of the mottled skate *Raja pulchra*..... 66
1. Introduction 66
2. Materials and methods 69
2.1. Materials 69
2.2. Enzymatic hydrolysis of skate C-II 70
2.3. 2,2-diphenyl-1-picrylhydrazyl (DPPH) radical scavenging assay 71
2.4. 2,2-azino-bis(3-ethylbenzothiazoline-6-sulfonic acid) (ABTS) radical scavenging assay 72
2.5. Molecular weight distribution analysis 73
2.6. Preparation of segments with different molecular weight 73
2.7. Contents of non-enzymatic browning products and total flavonoid 74
2.8. Cytotoxicity 75
2.9. Statistical analyses 76
3. Results and discussions 76
3.1. Yields and tricine-SDS-PAGE 76
3.2. Antioxidant activity of CPs 77
3.3. Antioxidant activities of CSs 80
3.4. Evaluation of *in vitro* cytotoxicity 83
4. Conclusion 84
Figures 85
VI. Wound healing activity of by-product of skate chondroitin sulfate production 93
1. Introduction 93
2. Materials and methods 96
2.1. Materials 96
2.2. Antioxidant assays in tube 97

2.3. Molecular weight distribution of peptides 97
2.4. Cell culture experiment 98
2.5. CCK-8 assay 98
2.6. Cell viability/activity assay under oxidative stress 99
2.7. Measurement of intracellular ROS levels 99
2.8. Fibroblast proliferation/metabolism assay 100
2.9. Gene expression assay 101
2.10. Scratch assay 102
2.11. Gel-contraction assay in a 3-D culture model 103
2.12. Statistical analyses 104
3. Results and discussions 104
3.1. Antioxidant activity of BP-sCS 104
3.2. Effect of BP-sCS on L929 fibroblast activity 108
4. Conclusion 114
Figures 116
V. General discussion 127
1. Three key aspects toward the future realization of more efficient usage of skate cartilage by-products 129
1.1. Skate production and its sustainability 129
1.2. New fish-processing model to use up by-products toward the zero-discard 130
1.3. Market demand 134
2. Significance and influences of fish-cartilage products for our society 135
Figure 139
References 140
Acknowledgments 167

Chapter I

General introduction

Bone and cartilage comprise the endoskeleton of vertebrates. During embryonic development in most vertebrates, hyaline cartilage develops first, and this is subsequently replaced by endochondral bone (Seidel et al., 2017). However, cartilaginous fish, such as sharks, rays, and their relatives, retain the cartilaginous skeleton into adulthood and consequently lack bony tissue at any stage of their life cycle (cf. Hall, 1982; Seidel et al., 2017).

Cartilage is a gel-like tissue produced by chondrocytes that originate from mesenchymal precursor cells (Seidel et al., 2017; Witten et al., 2010). The extracellular matrix (ECM), which is abundant in proteoglycans and collagen, comprise 90% of the dry weight of cartilage (Knudson & Knudson, 2001; Witten et al., 2010). Proteoglycans are complex macromolecules comprised of a core protein and glycosaminoglycan (GAG) side chain(s) (Merly & Smith, 2013). The major GAGs in cartilage are chondroitin sulfate (CS), keratan sulfate (KS), dermatan sulfate (DS), and heparan sulfate (HS) (cf. Vázquez et al., 2013). The varieties of collagen are named types I–XXIX (Sotelo et al., 2016), and they play different roles in tissues. Hereafter, the different types of collagen are referred to as C-I, C-II, and so on, using Roman numerals to show collagen type. In cartilaginous tissues, C-II is the primary type (Witten et al.,

2010). Depending on the location and degree of maturation, other collagen types, such as C-I, C-X, and C-XI, are also present (Cumming et al., 2019; Dai et al., 2018; Knudson & Knudson, 2001; Witten et al., 2010).

Since GAGs and collagen regulate cell development and activities in the cartilage (Knudson & Knudson, 2001), these compounds have found roles in functional foods, pharmaceuticals, and cosmetics (cf. Silvipriya et al., 2015; cf. Volpi, 2019), and research into the bioactivity of animal cartilaginous tissues is receiving increased attention. For example, CS and C-II extracted from animal cartilage are prescribed to improve osteoarthritis (OA) symptoms (Dai et al., 2018; cf. Volpi, 2019); oral administration reduces the associated inflammation reactions (Cantley et al., 2013; Dai et al., 2018). CS is recommended as a symptomatic slow-acting drug for OA (SYSADOA) in Europe, and in dietary supplements in the United States, for the treatment of knee, hand and hip OA (Restaino et al., 2019). OA is a global health issue with high incidence and economic impact. Due to an aging population and rising obesity, OA is predicted to rise dramatically in the future (cf. Volpi, 2019). Since the regeneration of cartilage is extremely limited, demand for CS and C-II products that relieve OA symptoms is increasing.

Various animals provide a resource for cartilage, including terrestrial mammals (bovines and porcines), poultry (chicken), fish (cartilaginous and bony fish), marine invertebrates (squid), and amphibians (giant salamander) (Miyazaki et al., 2015; cf.

Silvipriya et al., 2015; cf. Volpi, 2019; Zhu et al., 2018), though commercial production of bioactive compounds mainly involves mammals and poultry. Although cartilage products from fish processing by-products have gained growing attention because of their high safety and activities, the use of fish-derived cartilage resources has fallen behind that from terrestrial vertebrates in scientific research and market share.

In this chapter, progress in research and application of fish cartilaginous tissues are addressed, with comparisons to those from terrestrial vertebrates where appropriate.

1. Potential bioactive compounds in fish cartilage

The primary commercial sources of cartilage are terrestrial vertebrates such as bovines, porcines, and chickens, yet although fish cartilage shows great potential for industrial use, data on the bioactivity of compounds obtained from fish cartilage are scarce. In this part, I discuss the structure, production method, and bioactivity of compounds obtained from fish cartilage and compare them with those obtained from the cartilage of terrestrial vertebrates.

1.1. Chondroitin sulfate (CS)

1.1.1. CS characteristics

In both terrestrial vertebrates and fish, CS is the major GAG in the extracellular matrix of the cartilage, and it is covalently linked to a protein core to form a proteoglycan. CS is a polysaccharide chain having a repetitive disaccharide unit composed of -4GlcAβ1-3GalNAcβ1- (GlcA: glucuronic acid, GalNAc: N-acetyl-galactosamine) (Restaino et al., 2017). It is characterized by differences in sulfation, including non-sulfated disaccharides (CS-O), mono-sulfated (CS-A: di-4S CS and CS-C: di-6S CS), and di-sulfated units (CS-D: di-2,6S CS and CS-E: di-4,6S CS) (cf. Restaino et al., 2019). CS formulation varies with tissue, organ, and species (Volpi, 2007). Data on CS formulation and molecular weight differ somewhat depending on research conditions and are impacted by processing and purification methods (cf. Martel-Pelletier et al., 2015; Volpi, 2007). During manufacturing, desulfation and depolymerization may occur (cf. Martel-Pelletier et al., 2015). Table 1 summarizes the formulations of CS derived from animal cartilage. CS from cartilaginous fish is characterized by a high percentage of di-sulfated disaccharides and CS-C, whereas that from terrestrial vertebrates contains either no or trace amounts of di-sulfated disaccharides and a higher percentage of CS-A (Arima et al., 2013; Maccari et al., 2015; Restaino et al., 2017). The formulation of CS from bony fish cartilage is more complex. In salmon, the CS formulation is similar to that of cartilaginous fish, whereas in sturgeon the formulation shows the characteristics of CS from terrestrial vertebrates (Im et al., 2010; Maccari et al., 2015; Restaino et al., 2017). CSs from different tissues also

have different formulations in fish. For example, CS from bony fish bone contains a high percentage of CS-A and di-sulfated disaccharides (Arima et al., 2013; Restaino et al., 2017). Notably, CS from monkfish bone contains high CS-E, which is a typical characteristic of squid CS (Maccari et al., 2015). Some reports give conflicting data; for example, the ratio of CS-C/CS-A in skate cartilage CS is given as either “more than 2” or as “near 1” (Volpi, 2007). In summary, CS formulations from different fish species and tissues differ, a factor that requires adequate study in the future since CS formulations influence CS bioactivity.

1.1.2. CS extraction and purification

CS is extracted and purified from animal cartilaginous tissues; microbial production alternatives, as in the case of hyaluronic acid, have proved difficult (cf. Schiraldi et al., 2010; Schiraldi et al.2012). In general, CS extraction and purification include three steps: hydrolysis of cartilage, selective precipitation of CS, and purification of CS. First, fish cartilage is hydrolyzed by chemical methods or proteases (Murado et al., 2010; cf. Vázquez et al., 2013). Considering environmental protection, enzymatic hydrolysis using proteases, such as papain, subtilisin, and other peptidases, is recommended (Hashiguchi et al., 2011; Novoa-Carballal et al., 2017; cf. Vázquez et al., 2013). After protein fraction breakdown and cartilage structure degradation, the CS fraction is selectively precipitated by alcoholic treatment, usually using ethanol

(Murado et al., 2010; cf. Vázquez et al., 2013). The redissolved CS sediment is purified by column chromatography or ultrafiltration membranes. Hashiguchi et al. (2011) used gel filtration and anion-exchange chromatography to purify ray CS, while rabbitfish (*Chimaera monstrosa*) CS was purified in the last stage using membrane technologies (Vázquez et al., 2019). Ultrafiltration membranes are more suitable for large scale production because they are cheaper, simpler, easier to scale-up, and provide satisfactory efficiency (Vázquez et al., 2019).

1.1.3. CS bioactivity

I summarize the bioactivity of CSs obtained from the cartilage of mammals and chicken, and then consider fish CSs (Table 2).

CS derived from the cartilage of terrestrial vertebrates is mainly used for the treatment of OA (cf. Schiraldi et al., 2010). OA is the most common form of arthritis, whose characteristics are degeneration and inflammation of the cartilage in joints. The beneficial effects of CS in the treatment of OA symptoms include reduction of apoptosis of chondrocytes, increased synthesis of articular cartilage proteoglycans, and reduction in inflammation reactions (Cantley et al., 2013). As already stated, CS is recommended as a SYSADOA in Europe, and in the United States as a dietary supplement for the treatment of knee, hand, and hip OA (Restaino et al., 2019). As a food supplement, the daily CS recommended dosage is between 800 and 1200 mg (Restaino et al., 2019).

CS from terrestrial vertebrates also has the following effects: neuroprotection (Egea et al., 2010), antioxidation (cf. Campo et al., 2006; Canas et al., 2007), inflammation modulation (Melgar-Lesmes et al., 2016), wound healing (Zou et al., 2009), antithrombotic (Bjornsson et al., 1982), metal chelation (Ajisaka et al., 2016), and intestinal microbiota modulation (Shang et al., 2016). For example, bovine or porcine CS have found therapeutic use in diseases of the central nervous system (CNS) (Canas et al., 2007; Egea et al., 2010). Canas et al. (2007) reported CS-A of bovine or porcine cartilage protects neuroblastoma SH-SY5Y cells from oxidative stress by inducing heme oxygenase-1, the dominant antioxidant enzyme in cells. Moreover, CS shows great promise in applications involving medical biomaterials since it combines with other polymers to form cellular scaffolds for cartilage and bone regeneration. A scaffold made of poly(ethylene glycol) containing bovine trachea CS enhances chondrogenic gene expression and cartilage-specific matrix production compared to a scaffold without CS (Varghese et al., 2008). CS-based nanocarriers are used for drug/gene delivery with the advantages of directional transmission (cf. Zhao et al., 2015).

Table 2 summarizes the reported biological activities of fish CSs. First, fish-derived CSs are useful for OA treatment due to their anti-inflammatory and cartilage regenerative activities. For example, oral administration of CS from shark fins had an anti-inflammatory effect and reduced OA symptoms (Volpi, 2002). Shark CS-C

increased C-II mRNA expression in a three-dimensional culture of porcine chondrocytes (Nishimoto et al., 2005). Second, fish-derived CSs find application in the nervous system; for example, shark and ray cartilage CSs have neurite outgrowth-promoting activity through the HGF signaling pathway (Hashiguchi et al., 2011; Nadanaka et al., 1998). Third, fish-derived CSs are potential health supplements. Skate (*Raja kenojei*) CS shows anti-inflammation activity through attenuation of lipopolysaccharide-induced liver damage in mice. Shark (*Mustelus mustelus*) CS has anticoagulant activity and can be used in the prevention and treatment of thromboembolic diseases (Krichen et al., 2018). Sturgeon (*Acipenser baerii* × *Acipenser schrenckii*) CS also acted as a strong antithrombotic through its anticoagulant, anti-platelet, and thrombolysis activities (Gui et al., 2015). Sturgeon (*A. sinensis*) CS has wound healing activity; it increases fibroblast adhesion and induces their proliferation and migration through its action on MAPK signaling pathways (Im et al., 2010). Fourth, fish CS is suitable for medical biomaterials. For example, shark CS nanoparticles incorporated into chitosan-poly(hydroxybutyrate-co-valerate) hydrogels significantly enhanced the viability and chondrogenic differentiation of mesenchymal stem cells, which offer great potential for nucleus pulposus tissue engineering (Nair et al., 2015).

Interestingly, anti-obesity action of CS has been reported using CS from salmon (Han et al., 2000). Since bovine CS modulates obesity-related inflammation (Melgar-Lesmes et al., 2016; Stabler et al., 2017), CS can be used in functional foods for chronic

health problems.

CS in its original form (polysaccharide) has low absorptivity in the digestive tract, which probably detracts from its potential in health foods or medications (Wang et al., 2016; Yamada et al., 2013). Therefore, CS oligosaccharides with low molecular weight have been developed. For example, from the skate (*R. pulchra*), CS oligosaccharides that have 2–14 sugar units were prepared by hydrolysis of CS polysaccharides with a subcritical water microreaction system (Yamada et al., 2013). Low molecular weight shark CS (2000–5000) possessed neuroprotective properties against toxic effects induced by amyloid-beta peptides both *in vitro* and *in vivo* that are beneficial for preventing Alzheimer's disease (Zhang et al., 2015).

Based on their sulfation patterns, CSs from different origins provide specific biological functions (cf. Volpi, 2019). Since CSs from fish cartilage show different sulfation patterns compared to those from terrestrial vertebrates, there is a possibility that some of the reported biological activities of fish CSs are specific. As shown in Table 2, some of the activities were reported only in fish CS. However, in the future, more detailed comparative studies are needed to elucidate the bioactivities specific to CSs from different fish species.

1.2. Type II collagen (C-II)

1.2.1. C-II characteristics

Collagen accounts for approximately 30% of total protein in animals and is present in at least 29 different types, each with a distinctive amino acid sequence and molecular structure (Sotelo et al., 2016). C-I accounts for 80%–85% of the collagen in the body (cf. Subhan et al., 2015). To date, most research on fish collagen has been based on C-I extracted from the skin. However, C-II is the most abundant type of collagen in the ECM of vertebrate cartilage (Merly & Smith, 2013) and is the most important component in the development and maturation process of chondrocytes in articular cartilage (Dai et al., 2018). Thus, as described later, C-II or C-II-derived biomaterials are suited to mimicking the microenvironment around chondrocytes in the human body and for use in the treatment of and research into arthritis. C-II is also one of the most common types of collagen found in cosmetics and supplements (cf. Felician et al., 2018). Therefore, fish-derived C-II should also be a focus of research.

Fish C-II molecules consist of a homotrimer of α chains, which contrasts with the existence of two types of α chain in mammalian C-I and three types of α chain in fish C-I (Zhang et al., 2014, 2016, 2019). In common with mammalian C-II, a characteristic feature of fish C-II is that it binds more glycosides than C-I. Zhang et al. (2019) showed that notochord C-II from Amur sturgeon (*A. schrenckii*) contained 31.8 μg/mg galactose and 33.7 μg/mg glucose, whereas skin C-I contains only 2.08 μg/mg galactose and 2.64 μg/mg glucose. The molecular denaturation temperature and the ability to assemble into

fibrils also differ between C-I and C-II, both of which are also common in fish and other vertebrates. C-II has superior thermal stability to C-I in sturgeons (Zhang et al., 2014, 2019). C-II has a longer lag time for assembly, slower fibril formation speed, and lower fibril formation rate than C-I in humans, calf, and sturgeon (Birk & Silver, 1984; Fertala et al., 1994; Meng et al., 2020; Zhang et al., 2019). Fibrils formed from C-II are thinner and shorter (Zhang et al., 2019).

The principal differences between fish and other animal collagens include denaturation temperature and glycosylation (Bu et al., 2017; cf. Subhan et al., 2015). Generally, C-II from land animal species that maintain a high body temperature had higher amounts of imino acids and superior thermal stability than those from fish, whose habitat temperature, and therefore body temperature, was lower (Cao et al., 2013). For example, C-II from chicken sternal cartilage has a higher imino acid content (about 232 residues per 1000 total residues) than C-II from shark cartilage (156 residues per 1000 total residues) and shows a higher denaturation temperature (Cao & Xu, 2008; Jeevithan et al., 2014) (Table 3). A higher imino acid content usually confers a more stable helical structure. However, C-IIs from sturgeons have similar imino acid content to those from land animals yet show lower denaturation temperature (Table 3). The relationship between the denaturation temperature and structural characterization of fish C-II needs further study.

Glycosylation patterns of collagen are crucial factors for immunologic tolerance

(Bu et al., 2017). Fish C-IIs express 5%–30% glycosylation, and this percentage may vary from species to species (Bu et al., 2017). As already stated, Zhang et al. (2019) reported the glycosylation patterns of C-I and C-II in Amur sturgeon; however, the glycosylation patterns of fish C-II and the function of specific carbohydrate chains linked to collagens are not well understood (Merly & Smith, 2013).

1.2.2. C-II extraction and purification

Before C-II from fish and terrestrial vertebrate cartilage can be extracted, it is necessary to remove non-collagenous substances. Usually, NaOH and/or EDTA is used as a pretreatment (Dai et al., 2018; Jeevithan et al., 2015; Mizuta et al., 2003). Then, C-II is extracted by hydrolysis of cartilage with proteases and purified by salting out or gel-filtration column chromatography (Jeevithan et al., 2018; Zhang et al., 2014). For extraction, pepsin in an acidic solution is commonly used. Native C-II molecules from cartilage are composed of three identical α-chains with telopeptides that construct inter-molecular crosslinks. The telopeptides also possess immunogenicity (Cao et al., 2013). Pepsin cuts telopeptides making C-II molecules more soluble and reducing their immunogenicity (Cao et al., 2013). Fish C-II extraction and purification should always be conducted at low temperature to reduce denaturation.

One of the characteristic features of the collagen obtained from both cartilaginous fish and bony fish is that it contains not only C-II but also other types. Contamination

by other types of collagen arises from the characteristic morphological features of fish cartilaginous tissues. The primary cartilage in cartilaginous fish is hyaline-like cartilage that persists throughout life and is never converted to or replaced by bone. Instead, mineralized tiles (tesserae) cover the outer cartilage surface to provide stiffness (Seidel et al., 2017). The calcified surface and the cartilage core contain different collagens, C-I and C-II, respectively (Seidel et al., 2017). Bony fish cartilaginous tissues include not only hyaline cartilage but also tissues intermediate between “bone and cartilage” or “connective tissue and cartilage” (Witten et al., 2010). These bone-like cartilages and cartilage-like connective tissues cause difficulties in teleost cartilage identification. Also, because fish grow throughout life, many cartilaginous tissues may not be fully differentiated (Witten et al., 2010). Thus, there is always a possibility of getting complex mixtures of cartilaginous tissues from bony fish, consisting of different types of collagen.

Here, I mention a characteristic teleost cartilage-related tissue, the notochord. The notochord is a rod-like tissue that develops anteroposteriorly and functions as an axial skeleton in the embryonic stages until other tissues, such as vertebral bones or cartilage, replaces it. The notochord, known as vesicular cartilage, has the same matrix components as hyaline cartilage (derived from chondrocytes) but is produced by notochord cells (Witten et al., 2010). The notochord is a unique tissue that expresses only C-II, making it a good source of C-II with minimal C-I contamination (Zhang et

al., 2019). In sturgeon species, because of incompletely developed vertebral cartilage, the notochord exists throughout life.

1.2.3. C-II bioactivity

Since research and application of fish C-II are limited, I first summarize information on C-II from animals of terrestrial origin, and then move on to fish C-II.

Collagen is widely used in foods, cosmetics, pharmaceuticals, and biomaterials (cf. Hashim et al., 2015; cf. Silvipriya et al., 2015). Currently, health supplements are the most frequent applications of C-II from terrestrial vertebrates. As a collagen supplement, C-II helps in reducing the destruction of body C-II, modulating the inflammatory response, and increasing joint flexibility (cf. Hashim et al., 2015). One of the most significant functions of C-II in supplements is for the treatment of arthritis, including OA and rheumatoid arthritis (RA). RA is a systemic autoimmune disease that involves hyperplasia of synovial tissues and structural damage to cartilage, bone, and ligaments (Cho et al., 2007). Many reports have shown the effectiveness of oral administration of C-IIs against RA symptoms. For example, oral administration of bovine C-II suppresses pro-inflammatory cytokine expression of T cells in arthritis-induced mice (Ju et al., 2008). In a double-blind, placebo-controlled trial, oral treatment with chicken C-II showed positive effects in the relief of RA symptoms (Barnett et al., 1998). In a randomized, double-blind trial, patients taking chicken C-II for three months

showed a decrease in joint swelling and tenderness (Trentham et al., 1993). Additionally, squid C-II induced cartilage repair in an osteoarthritis-induced cartilage lesion model *in vitro* and *in vivo* (Dai et al., 2018).

The function of C-II as a biomaterial is a current research focus in cartilage tissue engineering. C-II is the natural scaffold of chondrocytes, regulating chondrogenic differentiation of multipotent stem cells and supporting cartilage repair *in vitro* (Calderon et al., 2010; Raabe et al., 2010). A porous scaffold made of porcine C-II can increase rates of biosynthesis of cartilage matrix by chondrocytes (Lee et al., 2003). Porcine C-II sponge supports chondrocytes to maintain their phenotype and promote re-differentiation (Francioli et al., 2010). In hydrogel based on C-II and activated CS, chondrocytes survived well and showed round or oval morphology, and the surrounding matrix was remolded by the embedded chondrocytes (Gao et al., 2018). This hydrogel was injectable and was useful for delivering chondrocytes for cartilage regeneration (Gao et al., 2018). However, provision of a sufficient and stable supply of medical-grade C-II in the market, and clinical trials of C-II-derived scaffolds for cartilage regenerative medicine, remain future challenges.

Research on the bioactivity of fish C-II is in its infancy. The information that does exists is limited almost entirely to shark C-II, and is mainly divided into three categories. First, in line with terrestrial sources, C-II from blue shark (*Prionace glauca*) and whale shark (*Rhincodon typus*) cartilage have anti-inflammatory activity (Bu et al.,

2017; Jeevithan et al., 2016b). Chen et al. (2012) showed that oral administration of C-II from blue shark suppresses RA in experimentally-induced RA model rats. Second, whale shark C-II stimulates osteogenesis and suppresses osteoclastogenesis when used as cellular scaffolds (Jeevithan et al., 2018), and blue shark C-II scaffold promotes osteoblast cell formation (Jeevithan et al., 2016a). Third, whale shark C-II has antioxidant activity (Jeevithan, 2015). As described in Section 3, sharks are threatened by overfishing, therefore, research on the bioactivities of C-II derived from fish species other than sharks is crucial in the future.

1.3. Other products

1.3.1. Proteoglycans

Proteoglycans (PG) are biopolymers consisting of a core protein covalently attached to GAG chains (Ono et al., 2018). PGs can be extracted from cartilage using acetic acid (Kobayashi et al., 2017). The predominant PG in cartilage is aggrecan that binds CS as GAG chains (Knudson & Knudson, 2001). In mammals, the core protein of aggrecan has multiple functional domains, including three globular domains, G1, G2, and G3 (cf. Kiani et al., 2002). A region for attachment of GAG chains (the attachment domain) separates the G2 and G3 domains (cf. Kiani et al., 2002; Knudson & Knudson, 2001). The CS attachment domain in mammalian aggrecan is the repeating amino acid

sequence containing serine–glycine (Kakizaki et al., 2011; cf. Kiani et al., 2002;). However, unlike mammalian aggrecans, the apparent repetitive sequence is not seen in zebrafish, pufferfish, and salmon aggrecans (Kakizaki et al., 2011). This may indicate the specificity of fish PGs.

I found that research on the bioactivity of cartilage PG was limited to salmon nasal cartilage PG. PG from salmon (*Oncorhynchus keta*) nasal cartilage is aggrecan with a 143-kDa core protein and GAG chains (Ono et al., 2018). The disaccharide units in the GAG chains contain 60% CS-C (Ono et al., 2018). Salmon PG has an immunomodulatory effect. Oral administration of PG attenuates allergic responses in a respiratory inflammation mouse model, regulates collagen-induced arthritis, and reduces obesity-induced inflammation (Hirose et al., 2017; Ono et al., 2018). Considering the low intestinal absorptivity of PG, the immunomodulatory effect of PG possibly comes from its effect on the intestinal microbiota, since daily oral administration of salmon PG enhances probiotics and short-chain fatty acid-producing bacteria (Asano et al., 2013; Ono et al., 2018). Salmon PG also has anti-angiogenesis activity arising through the inhibition of endothelial cell adhesion and production of matrix metalloproteinases (Kobayashi et al., 2017). The anti-angiogenesis activity of PGs may explain why cartilage lacks blood vessels (Kobayashi et al., 2017). I believe that PG from salmon nasal cartilage will show other forms of biological activity, and that it has great potential for medical application since PG is involved in the regulation of cellular activities

(Hirose et al., 2017; Kobayashi et al., 2017). The results of studies into the biological activity of PGs from other fish species will open a new window for the future industrial application of PGs.

1.3.2. Cartilage hydrolysate and peptides

Tissues or proteins are commonly hydrolyzed by enzymes, such as papain, pepsin, trypsin, and other peptidases, to obtain tissue hydrolysates or peptides (cf. Felician et al., 2018). Bioactive peptides usually have 3–40 amino acid residues, and their activities are based on amino acid composition and molecular weight (cf. Wijesekara et al., 2011). Over the years, many researchers have tried to obtain tissue hydrolysates and peptides from fish-processing waste and have studied their biological activities. These activities include antioxidative, anti-hypertensive, anti-inflammatory, anti-proliferative, anti-coagulant, calcium-binding, anti-obesity, anti-diabetic, anti-cancer, and so on (cf. Halim et al., 2016; cf. Wijesekara et al., 2011). Several researchers have demonstrated antioxidant activity of fish cartilage-derived hydrolysates or peptides (Li et al., 2017; Pan et al., 2016; Tao et al., 2018). For example, three peptides isolated from shark (*M. griseus*) cartilage hydrolysate scavenge radicals, inhibit lipid peroxidation, and protect H_2O_2-stressed HepG2 cells (Tao et al., 2018). Antioxidant peptides from skate (*R. porosa*) cartilage have also been reported (Pan et al., 2016). The alcalase-hydrolyzed cartilage of shark (*P. glauca*) exerts anti-hyperuricemic activity after oral administration

to rats (Murota et al., 2014). These results suggest that fish cartilage hydrolysates or peptides have potential as functional foods or in other fields. Key bioactive substances in fish cartilage hydrolysates or peptides remain to be clarified, and there is an ample possibility that the key bioactive substances are CS and C-II.

1.3.3. Other derivatives

In addition to the products that I have discussed, fish cartilage can be used in the production of cartilage powder, gelatin, various GAGs, and others (Jeevithan et al., 2014; Knudson & Knudson, 2001). Their biological activities deserve further study. However, the possible industrialization of these products needs to be considered from the viewpoints of extraction and purification complexity, cost, and stability, sufficiency, and sustainability of the supply of raw materials (cf. Olsen et al., 2014)

2. Potential fish cartilage sources for industrialization

2.1. Cartilaginous fish

Cartilage is the primary skeletal tissue in Chondrichthyes (cartilaginous fish), including sharks, skates, rays, and relatives. Therefore, cartilaginous fish have been the primary candidate as the source of fish cartilage.

Until now, the cartilage of sharks has been the major sources of commercial "marine CS". However, due to overfishing, commercial mass killing of sharks is not supported by international treaties (Arima et al., 2013; Sotelo et al., 2016). Some researchers have found that by-catch during fishing operations includes a certain quantity of low-value sharks (e.g. lantern shark and catshark) worthy of exploitation (Novoa-Carballal et al., 2017; Sotelo et al., 2016). These species generally become “discards” that are not retained on board during fishing operations because their relatively low commercial value makes it unprofitable to bring them to shore (Blanco et al., 2015; Sotelo et al., 2016). However, fishery discards are currently controversial, and the European Commission has published rules that prohibit discards (Sotelo et al., 2016; Vázquez et al., 2018). Therefore, in Europe, the wise use of by-catch sharks is an alternative for dealing with shark discards.

Another example is the dominant by-catch species in Chinese fisheries, the blue shark (*P. glauca*). The amount of cartilage remaining after consumption of the fresh or frozen meat appears to be increasing and forms a resource that should be utilized (Bu et al., 2017).

Regardless, shark catches are decreasing worldwide and have become controversial; thus, alternatives to shark cartilage have been widely sought. Other major cartilaginous fish, skates and rays, are an alternative resource because these species are the target of commercial fisheries. Skate or ray fin has become a popular food in many

countries. For example, Hongtak, made from the pectoral fins of skate (*R. kenojei*), is an indigenous fermented product in Korea (Mizuta et al., 2003). Skate (Kasube) fin is a familiar food in Hokkaido, Japan, and there are various recipes in restaurants, including boiled, deep-fried, or sashimi. In Spain, 2581 t of skate and rays were landed at the Port of Vigo in the year 2008 (Murado et al., 2010). Skate are also commercially harvested on both coasts of North America. In Alaska, skate (family Rajidae) are not overfished, and the development of skate fisheries is encouraged (Farrugia et al., 2015). Seafood exporters are interested in buying skate from Alaska to sell in Asia (Farrugia et al., 2015).

Since only the fins of skate and rays are used as food, 50%–80% of their carcasses end up as waste following industrial processing (Farrugia et al., 2015; Murado et al., 2010). In particular, the head and axial skeleton of skate, which are rich in cartilage, are mostly discarded. In terms of the availability of raw materials, skate and ray cartilage could be an alternative to that from shark.

Another potential source of cartilage would be the ancient cartilaginous chimera fish. Rabbit fish (*C. monstrosa*) appears as by-catch in deep-water North Atlantic trawlers, and its cartilage has been studied with a view to isolating CS (Vázquez et al., 2019).

Cartilaginous fish have low rates of potential population increase with little capacity to recover from threats such as overfishing, pollution, and habitat destruction

(Cavanagh & Gibson, 2007). The sustainability of the cartilaginous fish fisheries depends on future demand and management.

2.2. Cultured bony fish

Thanks to their abundance and extensive culture programs, bony fish could serve as an excellent new source for commercial CS and collagen (Maccari et al., 2015).

Sturgeons are the top-rated source of cartilage among the bony fish because of their cartilaginous skeleton and notochord. Sturgeons are primitive bony fish and have a characteristic skeleton whose major component is cartilage, similar to chondrichthyans (Zhang et al., 2016). The natural sturgeon population is severely threatened by overfishing, habitat degradation, and pollution (Bronzi et al., 2019). However, there is now a trend towards sturgeon aquaculture to substitute the production from fisheries, with the practice now widely adopted in China, Russia, the Middle East, the Far East, Europe, and Japan (Bronzi et al. 2019), with China accounting for approximately 80% of global production (Gui et al., 2015). Globally, sturgeon fisheries are valuable for production of the luxury food, caviar. However, since a long cultivation period is required to obtain caviar, the production cost of sturgeon is higher than that of other fish (Zhang et al., 2014). Utilization of by-products could support further growth of the sturgeon aquaculture industry.

Aquaculture of Salmonids (particularly Atlantic salmon *Salmo salar* and rainbow trout *Oncorhynchus mykiss*) is a major contributor to the world production of farmed finfish. Atlantic salmon is the most commonly farmed salmonid, and its production exceeds 2m t annually (FAO, Cultured Aquatic Species Information Programme). Salmon farming is significant in Chile, Norway, Scotland, Canada, and the Faroe Islands, and the primary consumption occurs in the United States and Europe (FAO, Cultured Aquatic Species Information Programme). Because salmon is a high-yielding species, the major by-product of the salmon processing industry is the nasal cartilage.

As research on the active compounds in fish cartilage continues, opportunities to develop new industries using cartilage from cultured bony fish will significantly increase.

2.3. Other bony fish

Collagen from the nasal cartilage of hoki (*Macruronus novaezelandiae*) has been studied for potential application in cartilage scaffolds (Cumming et al., 2019). Hoki in New Zealand is an essential commercial deep-water species making up the largest tonnage fishery (Cumming et al., 2019). Furthermore, New Zealand hoki is considered one of the best-managed trawl fisheries in the world, certified as sustainable by the Marine Stewardship Council (MSC). Therefore, nasal cartilage from hoki represents a

sustainable by-product resource.

Bioactive compounds derived from fish cartilage have been investigated only in a limited number of species. More research is needed to find alternative fish cartilage sources and new bioactive substances that can be applied in the pharmaceutical and nutraceutical industries.

3. Advantages and disadvantages of fish cartilage as a resource

The most prominent benefit of the industrial use of fish cartilage is that it decreases the waste of the fish-processing industry. In the last couple of decades, the cumulative total production from capture fisheries and aquaculture has continuously increased (FAO, 2018). The trend towards more processing of fish products within the supply chain is creating increasing quantities of by-products (FAO, 2018). By-products may constitute as much as 50%–70% of fish weight after industrial processing (FAO, 2018; cf. Olsen et al., 2014). Cartilage has been regarded as a low-value fish processing by-product and discarded. Recently, researchers have focused on transforming this waste into isolated bioactive components to provide value-added products (cf. Ferraro et al., 2010; cf. Olsen et al., 2014). This strategy can mitigate environmental pollution from solid waste, improve the economic profit of fishery and aquaculture industries, and could result in the production of more food from limited resources (cf. Ferraro et al.,

2010; cf. Olsen et al., 2014).

The second benefit is the broader acceptance of the use of fish cartilage in society. Fish cartilage has a much lower risk of contamination with zoonotic diseases (such as bovine spongiform encephalopathy and influenza) than the traditional sources of cartilage (bovine, porcine, and chicken cartilage) (cf. Volpi, 2019). Also, fish cartilage has fewer religious restrictions.

Third, the cartilage content in fish species is higher than in terrestrial species. Mammalian cartilage represents only 0.6% of the body weight, whereas that in cartilaginous fish represents 6%–8% (Blanco et al., 2015).

Taken together, cartilage from fish by-products is a valuable resource. Moreover, the ecological diversity of fish gives different characteristics and properties to the isolated bioactive compounds. For example, gelatins extracted from warm-water fish have a thermal stability similar to that of mammalian gelatins, whereas gelatins from cold-water fish are less thermally stable (cf. Ferraro et al., 2010). The bioactive compounds isolated from fish cartilage may also show diverse characteristics, suggesting more flexible usage of the compounds. Those whose properties are close to those for to mammalian equivalents could act as substitutes, whereas those with specific characteristics could form the basis of new products to fill gaps in the market.

Though the use of fish cartilage has many advantages, only a few high-value products have been established and sold in large quantities, indicating a considerable

gap between research and the market. Like other fish by-products, there are two main disadvantages of fish cartilage: the supply of raw materials from specific species is insufficient and irregular; and the high price of fish products relative to those from mammals, probably due to the higher cost of production (cf. Olsen et al., 2014).

4. The objective of the research in this thesis

As already described, shark cartilage is the primary source of marine cartilage now. However, shark catches are decreasing worldwide, owing to over-fishing (FAO, international plan of action for conservation and management of sharks, 2014). Therefore, this project tried to develop a new cartilage source – skate cartilage.

In northern Hokkaido, skate fishery is one of the essential industries. After landing the skate, their fins are processed as food, and a massive volume of cartilaginous by-products is generated. Although the commercial production of skate-CS containing functional foods for healthier joints has already implemented (Nishimura et al., 2018), diversification of products having different functionalities will make the skate-cartilage industry more developed. Therefore, I set the objective of the research in this thesis to find new bioactivities of compounds contained in the skate cartilage. I used the skate *Raja pulchra* as a model species, which is the dominant species of the skate fishery in northern Hokkaido.

The cartilage of *Raja pulchra* contains CS polysaccharides, C-II, non-collagenous proteins, and minerals. Therefore, firstly, I investigated the anti-obesity functions of CS *in vitro* and *in vivo* in Chapter II. In this study, CS polysaccharides were obtained after the enzyme hydrolysis of the cartilage and were further hydrolyzed to oligosaccharides using a subcritical water microreaction system (Yamada et al., 2013). Secondly, I evaluated the antioxidant activities of CS and C-II peptides in Chapter III. Finally, I intended to find the biological activity in the by-product of CS production. After isolating CS polysaccharides from the skate cartilage, the rest of the material contains C-II peptides, non-collagenous peptides, minerals, and a small amount of CS polysaccharides. I named it as by-products of skate chondroitin sulfate production (BP-sCS) and studied its wound healing activity in Chapter IV. In Chapter V, as a general discussion, I discussed three key aspects toward the future realization of more efficient usage of skate cartilage by-products and general significances and influences of the fish cartilage products for our society.

Tables

Table 1

The CS formulations of cartilage of different origins.

	Mammal			**Poultry**	**Cartilaginous fish**			**Bony fish**		
	Bovine	Pig	Whale	Chicken	Shark	Skate	Chimaera	Salmon	Sturgeon	Bone†
CS-C/CS-A	0.5–1	< 0.5	0.5–1	< 0.5	> 1	> 1	> 1	> 1	< 0.5	0.5–1
Di-sulfated (%)	< 0.5	< 0.5	< 0.5	< 0.5	>10	1–10	>10	0.5–1	< 0.5	1–10
References	[1, 2]	[1]	[1]	[1]	[1-4]	[5]	[6]	[3]	[7, 8]	[3]

†, the data are obtained from bones of bony fishes (salmon, tuna, monkfish, codfish).

References: [1] Restaino et al., 2019; [2] Volpi, 2007; [3] Maccari et al., 2015; [4] Vázquez et al., 2018; [5] Hashiguchi et al., 2011; [6] Vázquez et al., 2019; [7] Im et al., 2010; [8] Yamagata et al., 1987.

Table 2

The bioactivities of fish-derived CS.

Sources	Activities
Shark	anti-inflammation [1, 2, 3], cartilage regeneration [4], neurite outgrowth promoting activity [5], cell activation [6, 7], anticoagulant [8]
Skate	neuritogenic activity [9], anti-inflammation [10]
Salmon	anti-obesity* [11], anti-oxidant [12], metal chelation [13]
Sturgeon	wound healing [14], antithrombotic activity [15]
Shark CS oligosaccharide	neuroprotective properties [16]

*, activities reported in fish CSs only.

Reference: [1] Surapaneni et al., 2014; [2] Volpi, 2002; [3] Imada et al., 2010; [4] Nishimoto et al., 2005; [5] Nadanaka et al., 1998; [6] Volpi et al., 1993; [7] Nair et al., 2015; [8] Krichen et al., 2018; [9] Hashiguchi et al., 2011; [10] Song et al., 2017; [11] Han et al., 2000; [12] Ajisaka et al., 2016; [13] Uchisawa et al., 2001; [14] Im et al., 2010; [15] Gui et al., 2015; [16] Zhang et al., 2015.

Table 3

Imino acid and denaturation temperature of fish-derived pepsin soluble type II collagen.

Sources	Imino acid/ 1000 residues	Denaturation temperature (℃)	References
Silvertip shark *Carcharhinus albimarginatus* skeleton	156	31.25	[1]
Whale shark *Rhincodon typus* cartilage	155	34.02	[2]
Skate *Raja kenojei* fin cartilage	188	-	[3]
Amur sturgeon *Acipenser schrenckii* cartilage	226	35.71	[4]
Amur sturgeon *Acipenser schrenckii* notochord	232	33.5	[5]
Bester sturgeon *Huso huso*× *Acipenser ruthenus* notochord	212	36.3	[6]
Chick sternal cartilage	232	43.8	[7]
Bovine articular cartilage	206	38	[8]
Squid cartilage	171	31.9	[9]

-: no data

Reference: [1] Jeevithan et al., 2014; [2] Jeevithan et al., 2015; [3] Mizuta et al., 2013; [4] Liang et al., 2014; [5] Zhang et al., 2019; [6] Zhang et al., 2014; [7] Cao & Xu, 2008; [8] Herbage et al., 1977; [9] Dai et al., 2018.

Chapter II

Anti-obesity effects of chondroitin sulfate oligosaccharides from the skate *Raja pulchra*

1. Introduction

Chondroitin sulfate (CS) is a polysaccharide chain consisting of a repeated disaccharide unit composed of glucuronic acid (GlcA) and N-acetylgalactosamine (GalNAc). It is a ubiquitous component of the cell surface and extracellular matrix (Hashiguchi et al., 2011; cf. Kwok et al., 2012). The different types of sulfation of the disaccharide subunits lead to the generation of distinct types of CS. For example, sulfation at C-4 of GalNAc is present in CS-A and sulfation at C-6 of GalNAc is present in CS-C (Kwok et al., 2012). CS has multiple biological effects, including anti-angiogenic (Kobayashi et al., 2017), immunological activity (Melgar-Lesmes et al., 2016), and neurite outgrowth-promoting activity (Hashiguchi et al., 2011). The potency of CS with regard to each of these depends on their type and molecular weight (MWt), which varies according to their origin and methods of production and purification (cf. Martel-Pelletier et al., 2015; Volpi, 2007). Several types of CS have been isolated from various natural sources, including terrestrial vertebrates and marine species, such as cows, pigs, chickens, sharks, and skates.

Recently, a new anti-obesity bioactivity of salmon nasal CS has been reported (Han et al., 2000). Obesity is a key component of metabolic syndrome and is a growing threat to public health. It usually results from an imbalance in energy intake and consumption (Zhang & Lu, 2012), and therefore inhibition of the intestinal absorption of dietary fats is one of the most effective ways of treating obesity. Pancreatic lipase (EC3.1.1.3) plays a key role in the digestion of 50%–70% of dietary fat (cf. Garza et al., 2011). Therefore, inhibition of this enzyme would reduce intestinal fat absorption, making it a potential target for the treatment of obesity. Han et al. (2000) showed that salmon nasal CS inhibits pancreatic lipase activity *in vitro* and that oral administration results in lower fat storage in mice fed a high-fat diet.

Another effective way of preventing or ameliorating obesity is to inhibit fat storage, and the regulation of adipocyte proliferation, differentiation, and metabolism is crucial for this purpose. However, prior studies of the effect of CS in adipocytes have been limited to evaluating the effect of one type of CS only, fucosylated CS from sea cucumbers (Xu et al., 2015).

As I described in Chapter I, CS polysaccharides could be obtained from skate head and axial cartilages, which are the waste of the skate-processing industry. The absorption of CS polysaccharides from the digestive system is generally very low (Yamada et al., 2013). However, CS oligosaccharides prepared from skate CS could be effectively absorbed from the intestine of rats (personal communication). Thus, orally

administered CS oligosaccharides may be able to influence adipocyte proliferation, differentiation, and metabolism. Moreover, a new, low-cost method using a subcritical water microreaction system to produce skate CS oligosaccharides has been developed (Yamada et al., 2013). Thus, oral administration of skate CS oligosaccharides is now possible and may be beneficial for obesity.

In this study, I used CS oligosaccharides produced from the head and axial cartilages of the skate *Raja pulchra*, a major catch in northern Hokkaido, and investigated their anti-obesity effects *in vitro* and *in vivo*. Their lipase- and adipocyte-inhibitory effects were also compared with those of CSs of other MWts and origins. I hypothesized that intestinally absorbable skate CS oligosaccharides have stronger adipocyte-inhibitory activity and a weaker lipase-inhibitory activity than high MWt CS polysaccharides; and that CSs of different origin have differing anti-obesity potencies.

2. Materials and methods

2.1. Materials

CS polysaccharides from skate cartilage (CSp, purity 70%) and its oligosaccharides, containing 2–14 sugar units (CSo, purity 80%), were obtained from Marukyo Bio Foods Co. Ltd. (Wakkanai, Hokkaido, Japan). CSo was produced by

hydrolysis of the CSp using a subcritical water microreaction system (Yamada et al., 2013). High-purity CSp (H-CSp) and high-purity CSo (H-CSo, 6–14 sugar units) were respectively purified from the CSp and CSo using ethanol and activated charcoal treatments by Marukyo Bio Foods Co (purity 83.1 and 86.3%, respectively). These CSs were obtained as CS sodium salt. Thus, the CSp and CSo contained CS, minerals, and a small amount of peptides (≤ 10%). In contrast, the H-CSp and H-CSo contained only CS and minerals. Pure chondroitin sulfate sodium salt from shark and bovine cartilage (shark CS and bovine CS) were purchased from Sigma-Aldrich (Saint Louis, MO; Lot BCBN1883V and Lot SLBR4195V, respectively). The compositions and MWts of skate, shark, and bovine CSs are summarized in Table 1.

2.2. *In vitro* pancreatic lipase assay

The lipase inhibitory activities of the CSs were quantified using a para-nitrophenyl phosphate (pNPP) assay, according to the method of Zhang et al. (2012), with minor modifications. In the assay, the pNPP was hydrolyzed by pancreatic lipase to release *para*-nitrophenol, a colored substance that can be quantified according to its absorbance at 405 nm. Lipase type II from porcine pancreas (Sigma-Aldrich) was dissolved in 50 mM Tris-HCl buffer (pH 8.0) at a concentration of 1.2 mg/ml and then centrifuged at 5,940 × *g* for 10 min to remove the insoluble components. The CSs were dissolved in

deionized water at concentrations of 5 or 50 mg/ml. Orlistat (Sigma-Aldrich) is a lipase inhibitor that was used as a positive control. It was dissolved in DMSO at a concentration of 1000 mM and then diluted in deionized water to a concentration of 100 mM.

Two types of reaction buffer were prepared. Reaction buffer 1 contained 50 mM Tris-HCl buffer (pH 8.0), 0.2% (w/v) sodium deoxycholate, 0.02% (w/v) lecithin (L-α-phosphatidylcholine, Sigma-Aldrich), and 5 mM $CaCl_2$. In Reaction buffer 2, 0.1% (w/v) gum arabic (Sigma-Aldrich) was used instead of the lecithin and $CaCl_2$. pNPP (Sigma-Aldrich) was dissolved in Reaction buffer at a concentration of 0.79 mM.

Lipase inhibitory activity was measured as follows. First, the reaction buffer (30 µl per well) and the lipase solution (50 µl per well) were added to a 96-well microplate and pre-incubated for 10 min at 37°C. Simultaneously, the pNPP solution (650 µl per tube) and the CS solution (130 µl per tube) were mixed and pre-incubated. The reaction was started by adding 120 µl of the pNPP-CS mixture into each well, and then the plate was incubated at 37°C. After 30 min (reaction buffer 1) or 10 min (reaction buffer 2), the absorbance at 405 nm was measured using a microplate reader (Infinite F50R, Tecan Japan Co., Ltd., Kawasaki, Japan). Each experiment was carried out in triplicate.

The inhibition rate (%) was calculated using the following equation:

$$\text{Inhibition rate (\%)} = \left(1 - \frac{\mathrm{B} - \mathrm{b}}{\mathrm{A} - \mathrm{a}}\right) \times 100\%,$$

where A is an absorbance of the negative control (without sample but with lipase), a is the absorbance of the negative blank control (without sample and lipase), B is the experimental absorbance (with sample and lipase), and b is the absorbance of the experimental blank (with sample but without lipase).

2.3. Endotoxin detection and reduction

Endotoxin is composed of lipopolysaccharides that are contained in the outer membrane of certain gram-negative bacteria, which are known to evoke an inflammatory response by cells (Morris et al., 2014). Therefore, before the experiment, the endotoxin levels present in the CSs were reduced using an EndotoxinOUT™ Kit (G-Bioscience, St. Lewis, MO). Briefly, freeze-dried CSs were dissolved in endotoxin-free water (EFW) to 10 mg/ml, and a 1-ml sample was applied to a kit column. After incubating at room temperature for 30–60 min, the sample was eluted three times with 1 ml EFW. The eluate was lyophilized and then the recovery rate, which is the percentage of the dry masses of the sample before and after the treatment, was calculated. The endotoxin levels in CSs were measured using a *Limulus amebocyte* lysate (LAL) assay (ES-24S® Kit, lot No.24S16004; Seikagaku Corp., Tokyo, Japan), according to the manufacturer's instructions. Control Standard Endotoxin (CSE, Lot No.249025; Associates of Cape Cod Incorporated, E. Falmouth, MA) was used as a

standard.

2.4. Cell culture experiment

The mouse 3T3-L1 preadipocyte cell line was obtained from the RIKEN Cell Bank (Tsukuba, Japan), and cultured in 96- or 48-well plates coated with 0.03% porcine skin collagen (Cellmatrix type I-C, Nitta Gelatin Inc., Osaka, Japan) in an atmosphere of 5% CO_2 at 37°C. First, cells were cultured in Preadipocyte expansion medium (Dulbecco's modified Eagle's medium containing high glucose [DMEM], GIBCO, Grand Island, NY) containing 10% newborn calf serum (NCS, Lot 1751586; GIBCO) and 1% penicillin/streptomycin (GIBCO). Two days after reaching confluence, cells were induced to differentiate for 2 days in Differentiation medium consisting of 1.0 μM dexamethasone (DEX, Sigma-Aldrich), 0.5 mM 3-isobutyl-1-methylxanthine (IBMX, Sigma-Aldrich), 1 μg/ml insulin (Sigma-Aldrich), and 10% fetal bovine serum (FBS, Lot. No 451456, GIBCO) in DMEM. Subsequently, the culture medium was changed to Adipocyte maintenance medium consisting of DMEM, 10% FBS, and 1 μg/ml insulin for 8 days. The endotoxin-reduced CSs dissolved in EFW were added to the culture medium at various concentrations and time points. EFW was used as a negative control.

Cell proliferation/metabolism was assessed using Cell Counting Kit-8 (CCK-8, Dojindo, Kumamoto, Japan), which measures total metabolic activity in the well, and

provides an estimate of total cell number if cellular metabolism is assumed to be stable during the experiment. However, because it is not sure if cell metabolism is not affected by the addition of CS, the terms “cell number/metabolism” or “cell proliferation/metabolism” will be used to denote this measurement in this Chapter. After discarding the culture medium, 10% (v/v) CCK-8 solution in culture medium was added to each well, and following incubation at 37°C for 15 min, the absorbance at 450 nm was measured using the microplate reader. Data are expressed as the relative absorbance normalized to the absorbance of the control well.

Cellular triglyceride (TG) content was measured using a Triglyceride E-Test kit (Wako Pure Chemical Co., Osaka, Japan). After differentiation, cells in 48-well plates were washed twice with 0.1 M phosphate-buffered saline (PBS) and treated with trypsin-EDTA (GIBCO) until the majority of cells were floating in the medium. Cells were then collected by centrifugation and resuspended in PBS. The cell suspension was then frozen (−30°C, 30 min) and thawed (37°C, 30 min) three times and centrifuged to obtain the supernatant. Finally, the TG content of the supernatant was determined using the kit, and the absorbance was measured at 600 nm using the microplate reader.

Cellular morphology was examined under a microscope (DMI600B, Leica, Wetzlar, Germany) and photographed.

2.5. *In vivo* experiment

In vivo experiments were carried out at the New Drug Research Center Inc. (Eniwa, Hokkaido, Japan) and approved by the animal experiment committee of the New Drug Research Center Inc. (Permit Number 171030C). Four-week-old male C57B/6J mice (Charles River Laboratories Japan, Inc., Yokohama, Japan) were housed at a controlled environmental condition (22±3°C and 50±20% humidity) under a 12–12 h light-dark condition. The obesity model mice were established by feeding a high-fat diet (HFD) (60% kcal fat content, D12492, Research Diets Inc., New Brunswick, NJ). Following the acclimation for 7 days, mice were randomly divided into 3 groups (8 mice each): A-group mice were fed normal diet (ND) (D12450J, Research Diets Inc.) and orally administered 5 ml/kg/day distilled water; B-group mice were fed HFD and orally administered 5 ml/kg/day distilled water; C-group mice were fed HFD and orally administered 50 mg/5 ml/kg/day CSo (Table 3). Animals had free access to ND or HFD and water. Body weight was measured, and food consumption was calculated weekly for 8 weeks. After 8 weeks of treatment, feces were collected during the last 24 h. Blood samples were collected and centrifuged at 3000 rpm for 15 min, and then serum was obtained. After the mice were sacrificed, liver and adipose tissues (epididymal fat, perirenal and retroperitoneal fat, and mesenteric fat) were excised, weighted, and kept frozen at -70°C until analyses.

Total fat in feces and livers were extracted with chloroform-methanol-water

(2:2:1), and the extracts were concentrated under a nitrogen stream. The triglyceride (TG) contents of the extracts and sera were determined using a Triglyceride E-Test kit (Wako Pure Chemical Co.). The endotoxin levels in the serum were estimated using ES-24S® Kit (Seikagaku Corp.).

2.6. Statistical analyses

Data are expressed as means ± standard errors. Statistical analyses were performed using Grubbs test for outliers, Student's *t*-test, the Tukey-Kramer test, and the Steel-Dwass test after ANOVA, in Microsoft Excel add-in statistical software (SSRI, Tokyo, Japan). Significance was set at $P < 0.05$. The tendency was accepted at $P < 0.1$.

3. Results and discussions

3.1. Effects of CSs on pancreatic lipase activity

The CSs dose-dependently inhibited the hydrolysis of pNPP emulsified with lecithin by pancreatic lipase (Fig. 1A). The inhibitory effects of the preparations were also observed when the substrate pNPP was emulsified with gum arabic (Fig. 1B), but the efficiency was lower than when lecithin was used as an emulsifier. These results

were similar to those obtained using salmon nasal cartilage CS (Han et al., 2000) and suggest that skate CSs also efficiently inhibit the interaction between the pancreatic lipase and the substrate in the presence of lecithin. It is possible that when CSs bind to the substrate, lecithin is likely to strengthen the binding as in the case of lipase inhibitory action of chitosan (Han et al., 1999), but gum arabic has no such effects. A similar effect was also observed in the report of Han et al. (2000), in which the lipase-inhibitory activity of salmon nasal CS is higher in lecithin-emulsified experiments than in gum arabic-emulsified experiments.

The present assay, using lecithin as an emulsifier, also revealed that the skate CSp yielded 50% inhibition of the pancreatic lipase activity at a concentration of 50 mg/ml but that its potency was significantly lower than those of shark and bovine CSs. In addition, the skate CSp had a greater effect than skate CSo at the same concentration. These results imply that the inhibition of pancreatic lipase by CS depends on its origin and MWts. However, at 5 mg/ml the inhibitory activities were similar among all the CS preparations. High-purity CSo also showed a dose-dependent inhibition of lipase (data not shown).

Orlistat, which showed the strongest inhibitory activity in the present lipase assay, is the only clinically approved drug for obesity treatment in Europe (Zhang & Lu, 2012). However, some adverse effects have been reported in patients undergoing orlistat therapy (cf. Garza et al., 2011). Hence, CS preparations, including those derived from

skate CS, may be candidates to replace orlistat as clinical inhibitors of pancreatic lipase.

In summary, lipase inhibition assays have shown that skate CSp is a natural inhibitor of pancreatic lipase and a candidate for inclusion in functional foods, which may have an impact in the intestinal tract. In addition to its potent lipase inhibitory activity, the low absorption of the CSp in the gut (Yamada et al., 2013) could further increase its usefulness. In contrast, the higher absorption of the CSo would be expected in the gut (Yamada et al., 2013) and it was a less potent lipase inhibitor than CSp. Therefore, the direct effects of CSo on adipocyte metabolism was evaluated using a cell culture system.

3.2. Endotoxin levels of CSs after endotoxin-reduction treatment

The endotoxin content of the CSs before and after the endotoxin-reduction treatment is shown in Table 2. The CSs of different origins had contrasting endotoxin contents, which may relate to the methods of production and purification used for each. The endotoxin levels of the H-CSo and H-CSp were low, suggesting that the purification with ethanol and activated carbon had an endotoxin-reducing effect.

After the endotoxin-reduction chromatography, the recovery rates for the CSs were more than 75%. Their endotoxin levels were significantly lower after the treatment, becoming < 0.4 ng/mg. A low concentration of LPS (≤ 1 ng/ml) did not induce the

production of the inflammatory mediators, interleukin (IL)-6, tumor necrosis factor α, and IL-33, in human monocytic cells (Morris et al., 2014). Because the maximum concentration of CS used in the present cell culture experiment was 1 mg/ml, I judged that all CSs were suitable for use in cell culture experiments after the endotoxin-reduction step. The endotoxin level of the CSo was reduced by 97.6% by the treatment, which was a much greater reduction than was achieved with the other CSs. This might be because CSo has a simpler structure, higher solubility in water, and lower viscosity.

3.3. Effect of CSs on 3T3-L1 proliferation/metabolism

To compare the effects of CSs on adipocytes, high-purity samples (H-CSo, H-CSp, shark, and bovine CSs) were used in cell culture experiments.

First, 3T3-L1 preadipocytes were treated with H-CSo at various concentrations (10, 100, or 1000 μg/ml) during the preadipocyte expansion period (Days 1–8) and the cell number/metabolism was estimated using CCK-8 (Figs. 2A–C). In addition, CS polysaccharides of various origins were tested at 1000 μg/ml. During Days 3–8, no significant effects of H-CSo were observed on cell proliferation/metabolism, except for a small difference at a dose of 100 μg/ml on Day 3. In contrast, H-CSp and shark CS significantly enhanced 3T3-L1 preadipocyte proliferation/metabolism. These data indicate that skate and shark CS-polysaccharides accelerate preadipocyte

proliferation/metabolism, but CS oligosaccharides and bovine CS do not. The explanation could be that the formulation of the bovine CS is different from that of the skate and shark preparations (Table 1). Nevertheless, these data suggest that the effect of CSs on preadipocyte proliferation/metabolism depends on their origin and MWts.

Next, the CSs were added to the culture during the adipocyte differentiation and maintenance periods. CCK-8 assays were conducted at the end of the 2-day differentiation period (the start of the maintenance period) and at the end of the 8-day maintenance period (Fig. 3). During the differentiation period, 1000 μg/ml H-CSp significantly increased preadipocyte number/metabolism over that of the EFW control group. However, a significant difference was not induced by the addition of other CSs. During the adipocyte maintenance period, the number/metabolism of cells in the EFW group remained constant. In contrast, there was a downward trend in the number/metabolism of cells during the maintenance period in all CS-treated groups. At the end of the maintenance period, the number/metabolism of cells in wells treated with 1000 μg/ml H-CSo, H-CSp, shark CS, or bovine CS was significantly lower than at the beginning of this period.

These data indicate that the CSs have differing effects on cell proliferation/metabolism, depending on the differentiation stage of the adipocytes: they tend to enhance the proliferation/metabolism of preadipocytes but suppress the number/metabolism of differentiated adipocytes. Two previous studies of the anti-

obesity actions of CSs (Han et al., 2000; Xu et al., 2015) did not investigate the effects of CSs on the proliferation of adipocytes. Therefore, to my knowledge, this is the first report of the effects of CSs on the proliferation of adipogenic cells.

3.4. Effect of CSs on lipid accumulation in 3T3-L1 adipocytes

CSs were added to cultures during the adipocyte differentiation and maintenance periods to evaluate their effects on lipid accumulation, with adipocyte TG content being measured at the end of the maintenance period. As shown in Fig. 4, all CSs tended to inhibit lipid accumulation when compared with the EFW control wells. H-CSo significantly reduced TG content when added at 10 μg/ml, and both H-CSp and shark CS significantly reduced TG content at higher concentrations. In particular, the lipid content of cells treated with shark CS at 1000 μg/ml was below the detection limit. However, the inhibitory effect of bovine CS was weaker: the TG content in bovine CS-treated cells was not significantly different from the control, suggesting that the effect of CS to inhibit lipid accumulation depends on its origin.

It has been previously reported that glucagon-like peptide 1 affects lipid droplet size and number in 3T3-L1 cells (Yang et al., 2013). The lipid droplet size in 1000 μg/ml H-CSo-treated cells was smaller than that of control cells (Fig. 5). These data indicate that high concentrations of H-CSo inhibit the development of lipid

droplets in differentiating adipocytes. Also, larger spaces can be observed between adipocytes in cells treated with 1000 μg/ml H-CSo (Fig. 5). These larger spaces could be the result of reductions in cell number during the maintenance period, consistent with the CCK-8 data. Therefore, skate CS oligosaccharides have inhibitory effects on mature adipocytes.

In contrast to the cell morphology observed following the treatment of cells with other types of CS, spindle-shaped cells without lipid droplets were observed in cells treated with 1000 μg/ml H-CSp (Fig. 5), accompanied by a clear separation between cells. Such morphological characteristics are shared with undifferentiated preadipocytes. These data suggest that H-CSp inhibits adipocyte differentiation and causes changes in cell morphology, while H-CSo affects lipid droplet accumulation in maturing adipocytes. Therefore, the mechanisms suppressing differentiation of 3T3-L1 adipocytes depend on the MWts of the skate CS. These results also explain the contrasting effects of similar doses of H-CSo and H-CSp on cell morphology. When preadipocytes differentiate into adipocytes, the synthesis and secretion of proteoglycans create a loose extracellular space between cells (Calvo et al.,1991). Because CS is a major component of proteoglycans, the addition of H-CSp (more than 50 sugar units) may provide a negative feedback signal to suppress the differentiation of adipocytes. However, H-CSo (6–14 sugar units) may not have the same effect. Presently, the mechanisms of H-CSo to reduce lipid droplets are unknown. My working hypothesis is

that H-CSo binds to cell surface receptor, such as Toll-like receptor 2, to inhibit related-gene PPARγ expression, and then inhibit lipid accumulation in mature adipocytes (cf. Wahli et al., 2012; Wu et al, 2018; Xu et al., 2015). The mechanism will be investigated in the future.

In summary, 3T3-L1 culture experiments revealed that skate CS inhibits proliferation/metabolism of maturing adipocytes and reduces the accumulation of lipid droplets, although in contrast it activates preadipocyte proliferation/metabolism at higher concentrations. Although both H-CSp, H-CSo, and shark CS inhibit lipid accumulation, H-CSo would be more appropriate for oral administration, because it passes through the digestive system more readily (Wang et al., 2016; Yamada et al., 2013). Moreover, H-CSo has higher water solubility and lower viscosity. Taken together, the present findings suggest that H-CSo could be an appropriate material for inclusion in anti-obesity functional foods.

3.5. *In vivo* effect of CSo

The anti-obesity effects of CSo were studied using animal experiments. In this experiment, one mouse in C group (HFD with CSo 50 mg/kg) was excluded as an outlier because its growth rate was extremely high (Grubbs test for outliers, $P < 0.01$).

As shown in Fig. 6A, consumption of HFD for 8 weeks (B group) showed a

significant gain of body weight compared with A group (fed ND). In contrast, the body weight of mice in the C group was at the same level as A group during the early stage (weeks 1–5). After 5 weeks, the body weight of mice in C group was higher than A group but significantly lower than the B group, indicating that CSo prevented weight gain when mice were fed HFD.

From the results of Fig. 6B, HFD decreased food consumption per week at the early stage in both B and C groups. From 5 weeks, however, the B-group mice returned to the normal level of food consumption. The C-group mice also returned their appetite except for the significantly lower food consumption on week 7 compared with A group. There was no significant difference in food consumption between group B and C at any time point. CSo may influence mice appetite. Appetite-related hormone levels could be studied to confirm the relationships between the appetite and CSo intake in the future.

As shown in Table 4, HFD caused mice to increase the weight of adipose tissues. HFD also increased the total TG content of the liver and feces. Compared with the B group, however, C group shows significantly lower liver weight with a decreasing tendency of total TG content of the liver. At the same time, adipose tissues around the kidney and posterior abdominal in C-group mice also showed a decreasing trend than the B group. Serum TG concentrations among the three groups were not significantly different. These results suggest that CS slows down the accumulation of lipids induced by HFD, supporting the results of the present adipocyte-culture experiments. In

addition, the total TG content of feces in C group was tended to increase compared with B group, suggesting that CSo inhibited the absorption of TG, which is in line with its lipase-inhibitory activity.

Obesity leads to metabolic disorders and chronic inflammation. High endotoxin level in plasma is a marker of metabolic endotoxemia and inflammatory disorders, which relate with liver lipogenesis, insulin sensitivity, and so on (Cani et al., 2009). The present mouse experiment (Table 4) showed that the serum endotoxin levels of the B group were significantly higher than A group. Oral administration of CSo inhibited HFD-induced hyperendotoxemia: the serum endotoxin level of C group was statistically similar levels with A group. This result indicated that CSo could help to adjust metabolism and inflammatory disorders induced by HFD.

As a whole, skate CS oligosaccharides can ameliorate obesity in HFD-induced obese mice through inhibition of lipid absorption and accumulation.

To the best of my knowledge, the anti-obesity effects of CS have only been reported for salmon nasal CS (Han et al., 2000) and fucosylated CS of sea cucumber (Li et al., 2018; Xu et al., 2015). CS from salmon nasal cartilage inhibited lipase activity, and its oral administration evoked a significant reduction in body weight and parametrial adipose tissue mass (Han et al., 2000). However, any direct effect of salmon CS on adipocytes has not been established. Since the salmon nasal cartilage CS has high MWts (89800) (Han et al., 2000), its intestinal absorbability could be low; and thus, the

major mechanism of anti-obesity action of salmon nasal cartilage CS is supposed to be inhibition of intestinal lipid absorption. In fucosylated CS (average MWt: 21530), anti-adipogenic effects on cultured adipocytes and anti-obesity effects on high-fat-high-sucrose diet mice were shown (Xu et al., 2015). Also, the anti-obesity action of depolymerized fucosylated CS (MWt: 4300) in high-fat diet mice was shown recently (Li et al., 2018). The fucosylated CS, however, has chondroitin sulfate E backbone with fucose branches, which is different from CSs from vertebrates. So, this study is the first to certify the *in vitro* anti-adipogenic and *in vivo* anti-obesity effects of vertebrate-type CS oligosaccharides with high intestinal absorbability.

This study is also the first to demonstrate the contrasting effects of skate CSs of differing MWts at various time points. CS polysaccharides, which are not significantly absorbed from the intestine, showed stronger inhibition of intestinal lipid digestion, whereas CS oligosaccharides, which are more readily absorbed, inhibited lipid accumulation by adipocytes at lower concentrations. This is noteworthy because the skate CSs with different MWts could be used for different purposes: high MWt CS as an inhibitor of pancreatic lipase in the intestine and CS oligosaccharides as inhibitors of lipid accumulation in differentiating adipocytes. Therefore, a combined preparation of both types may be effective as an anti-obesity functional food.

Moreover, this is the first report regarding the differing potency of CSs from different species. To the best of my knowledge, skate and shark CSs have similar

formulation, but the formulation of bovine CS differs (Table 1). The present data show similar effects of skate and shark CS on preadipocyte proliferation and adipocyte lipid accumulation, which is in accordance with their similar formulation. It is well known that CSs that are formulated differently have differing bioactivities. For example, some CSs have anti-inflammatory effects, while others have weaker effects, and others are pro-inflammatory (cf. Martel-Pelletier et al., 2015). In addition, the specific effect of H-CSp on the morphology of the 3T3-L1 cells may relate to its high proportion of non-sulfated and mono-sulfated disaccharides and its lower proportion of di-sulfated disaccharides compared with other CSs. Because CSs of different origins have distinct formulations and structures, further comparative studies are needed to understand the relationships between CS structure and biological potency.

4. Conclusion

This study clearly demonstrates the anti-obesity effects of skate CS oligosaccharides *in vitro* and *in vivo*. Skate CS oligosaccharides have a lipase-inhibitory activity to inhibit the absorption of TG in the intestine and have an adipocyte-inhibitory activity to reduce lipid accumulation. It can control weight gain and adjust metabolic disorders in HFD mice. The MWt of the CS affected the skate CS mode of action: high MWt CS (CS polysaccharides), which cannot be intestinally absorbed, had stronger

lipase inhibitory activity, which would be expected to inhibit dietary fat absorption in the intestine, whereas low MWt CS (CS oligosaccharides), which are more readily absorbed, suppressed adipocyte lipid accumulation at a lower dose. These results suggest that a formulation containing both CSs may be effective as an anti-obesity functional food. Also, the present study has shown that CS preparations all inhibit lipase, but their potency depends on their origin, as does their effect on adipocytes. Thus, the origin of CS is a key factor in its bioactivity.

Tables and figures

Table 1

The formulations and molecular weights of CSs of different origins.

	Formulations (%)					Molecular weight
	ΔDi-0s	ΔDi-4s (CS-A)	ΔDi-6s (CS-C)	ΔDi-2,6s (CS-D)	ΔDi-4,6s (CS-E)	
CSp	6.5	26.6	60.9	6.5	0.1	10,000–250,000
CSo	10.8	8.5	71.9	8.8	n.d.	460–3,400
Shark CS	3.0	29.0	50.0	15.0	2.0	10,000–250,000
Bovine CS	6.0	61.0	33.0	n.d.	n.d.	10,000–40,000

Data of formulations for CS polysaccharides (CSp) and thermally hydrolyzed CS oligosaccharides (CSo) were obtained from Marukyo Bio Foods Co. Ltd, and for shark CS and bovine CS were obtained from the report of Volpi (2007). Data of molecular weights for CSp, shark CS, and bovine CS were obtained by 16.5% tricine-SDS-PAGE stained with Alcian blue. Data of molecular weight for CSo was obtained from Marukyo Bio Foods Co. Ltd. n.d. = not detected.

Table 2

The endotoxin levels present in CSs before and after the endotoxin-reduction treatment.

	Endotoxin levels ng/mg (EU/mg)	
	Before the treatment	After the treatment
CSo	1.67 (13.36)	0.04 (0.32)
CSp	2.67 (21.36)	0.40 (3.20)
Shark CS	3.63 (29.04)	0.38 (3.12)
Bovine CS	0.33 (2.64)	0.10 (0.80)
H-CSo	0.01 (0.08)	-
H-CSp	0.15 (1.20)	0.06 (0.48)

- : no data (no need for endotoxin-reduction treatment).

The potency of the standard endotoxin used in the experiment was 8 EU/ng.

CSo, thermally hydrolyzed CS oligosaccharides; CSp, CS polysaccharides; H-CSo, high-purity CS oligosaccharides; H-CSp, high-purity CS polysaccharides.

Table 3

The information of the diet for three animal groups.

	A-group	B-group	C-group
Sample	5 ml/kg/day distilled water	5 ml/kg/day distilled water	50 mg/5 ml/kg/day CS oligosaccharides (CSo)
	Normal diet (ND)	High-fat diet (HFD)	
Protein (kcal%)	20	20	
Carbohydrate (kcal%)	70	20	
Fat (kcal%)	10	60	

Table 4

The effect of thermally hydrolyzed CS oligosaccharides (CSo) on tissues wet weight, total TG content, and endotoxin level in the HFD fed mice model.

		A: ND + DW	B: HFD + DW	C: HFD + CSo in DW
Tissues wet weight (g/individual)	Liver	0.9332 ±0.0191	0.9883±0.0153	0.9041±0.0219$^{\#}$
	Epididymal fat	0.4603±0.0221	1.5500±0.0304**	1.2725±0.1197**
	Perirenal and retroperitoneal fat	0.1274±0.0159	0.5953±0.0116**	0.4680±0.0475**†
	Mesenteric fat	0.1922±0.0215	0.3560±0.0191**	0.3314±0.0401**
Total TG (mg)	Liver	0.0069±0.0008	0.0128±0.0009**	0.0101±0.0007*†
	Feces	0.0010±0.0003	0.0018±0.0001	0.0026±0.0004*†
Serum TG concentration (mg/dl)		73.5±7.6	82.4±3.0	73.3±3.5
Serum endotoxin level (pg/ml)		46.00±1.70	55.30±1.51**	51.70±1.89

Data are expressed as mean ± standard errors (n=7 or 8). *$p < 0.05$ and **$p < 0.01$ compared with A group. #$p < 0.05$ compared with B group. †$p < 0.1$ shows tendency of decrease in C group compared with B group.

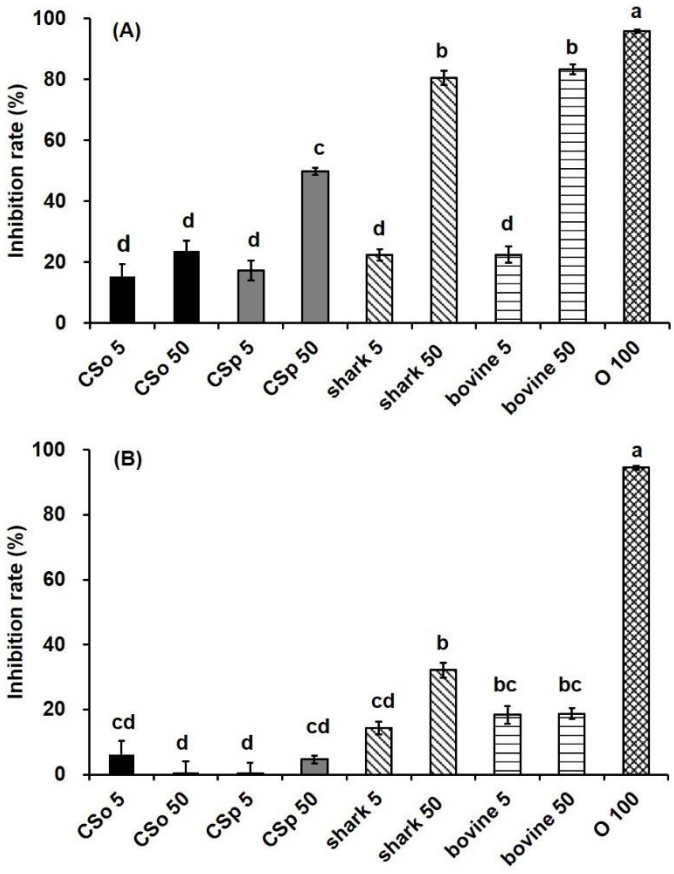


Fig. 1. Effects of CSs on pancreatic lipase activity.

(A) pNPP emulsified with lecithin was used as a substrate. The reaction time was 30 min. (B) pNPP emulsified with gum arabic was used as a substrate. The reaction time was 10 min. The columns and vertical bars show the mean values and standard errors, respectively (n=3). Different letters indicate statistical difference ($p < 0.05$). CSo 5, thermally hydrolyzed CS oligosaccharides (CSo) 5 mg/ml; CSo 50, CSo 50 mg/ml; CSp 5, CS polysaccharides (CSp) 5 mg/ml; CSp 50, CSp 50 mg/ml; shark 5, shark CS 5 mg/ml; shark 50, shark CS 50 mg/ml; bovine 5, bovine CS 5 mg/ml; bovine 50, bovine CS 50 mg/ml; O 100, orlistat 100 mM.

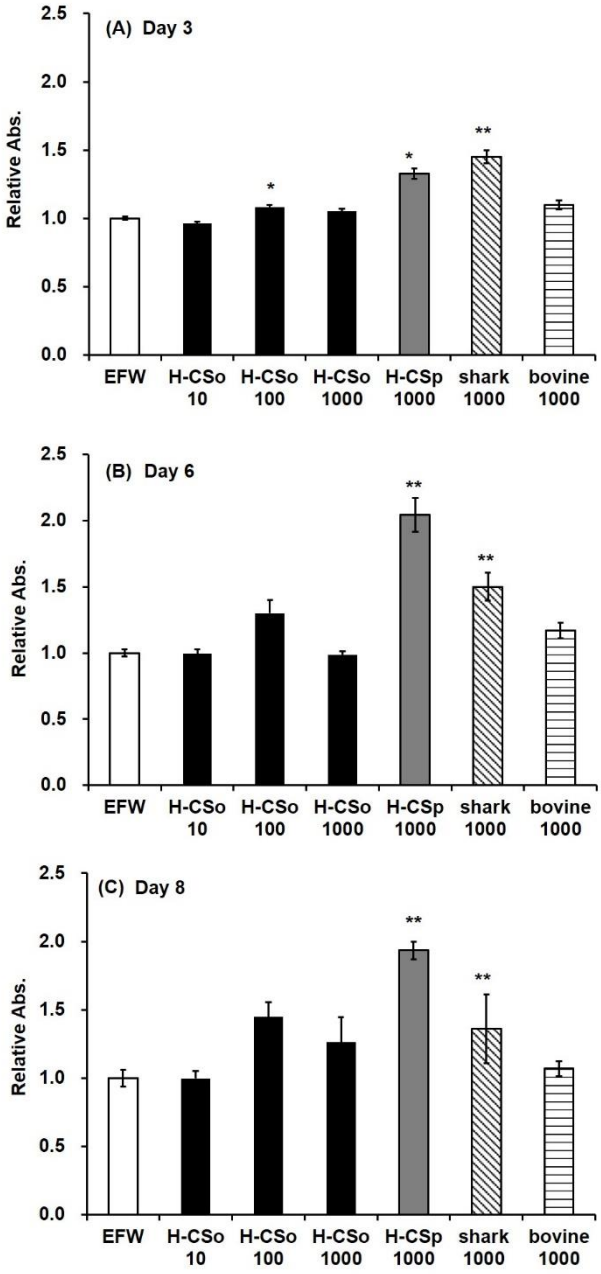


Fig. 2. Effect of CSs on 3T3-L1 proliferation.

Values are expressed relative to the corresponding EFW control. The columns and bars show the mean values and standard errors, respectively (n=10). * $p < 0.05$ and ** $p < 0.01$ compared with the control group (EFW). EFW, endotoxin-free water; H-CSo 10, high-purity CS oligosaccharides (H-CSo) 10 μg/ml; H-CSo 100, H-CSo 100 μg/ml; H-CSo 1000, H-CSo 1000 μg/ml; H-CSp 1000, high-purity CS polysaccharides 1000 μg/ml; shark 1000, shark CS 1000 μg/ml; bovine 1000, bovine 1000 μg/ml.

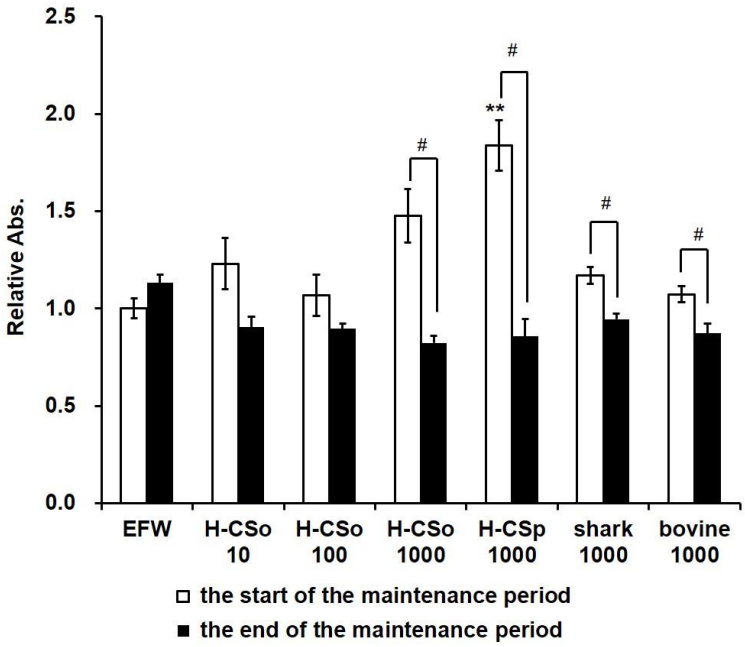


Fig. 3. Effect of CSs on 3T3-L1 adipocyte proliferation during the adipocyte maintenance period.

Two days after the cells reached confluence, they were treated to induce their differentiation into mature adipocytes. After 2 days (at the start of the maintenance period), the culture medium was changed to Adipocyte maintenance medium, and the cells were cultured for a further 8 days. Values are expressed relative to their corresponding EFW control at the start of the maintenance period. The columns and bars show the mean values and standard errors, respectively (n=10). ** p <0.01 compared with the control group (EFW) (Steel-Dwass test) and # p < 0.01 compared with the start of the maintenance period (Student's t-test).

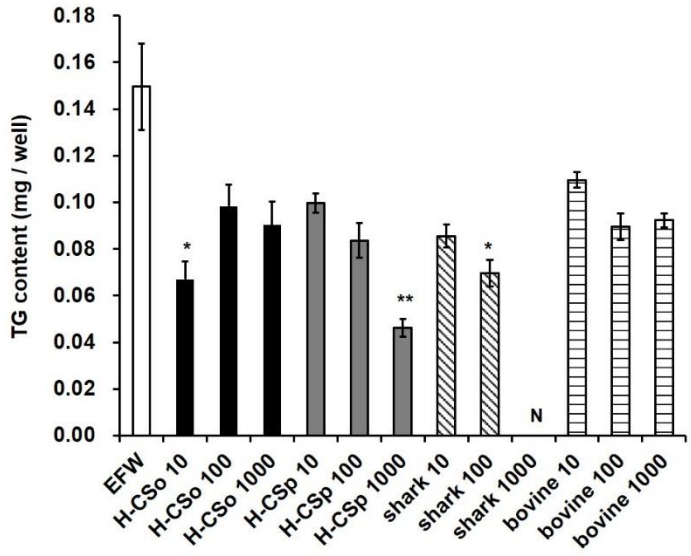


Fig. 4. Effect of CSs on lipid accumulation in 3T3-L1 adipocytes.

The columns and bars show the mean values and standard errors, respectively (n=3). * $p < 0.05$ and **$p < 0.01$ compared with the EFW control. N, below detection limit; EFW, endotoxin-free water; H-CSo 10, high-purity CS oligosaccharides (H-CSo) 10 μg/ml; H-CSo 100, H-CSo 100μg/ml; H-CSo 1000, H-CSo 1000 μg/ml; H-CSp 10, high-purity CS polysaccharides (H-CSp) 10 μg/ml; H-CSp 100, H-CSp 100 μg/ml; H-CSp1000, H-CSp 1000 μg/ml; shark 10, shark CS 10 μg/ml; shark 100, shark CS 100 μg/ml; shark 1000, shark CS 1000 μg/ml; bovine 10, bovine 10 CS μg/ml; bovine 100, bovine CS 100 μg/ml; bovine 1000, bovine CS 1000 μg/ml.

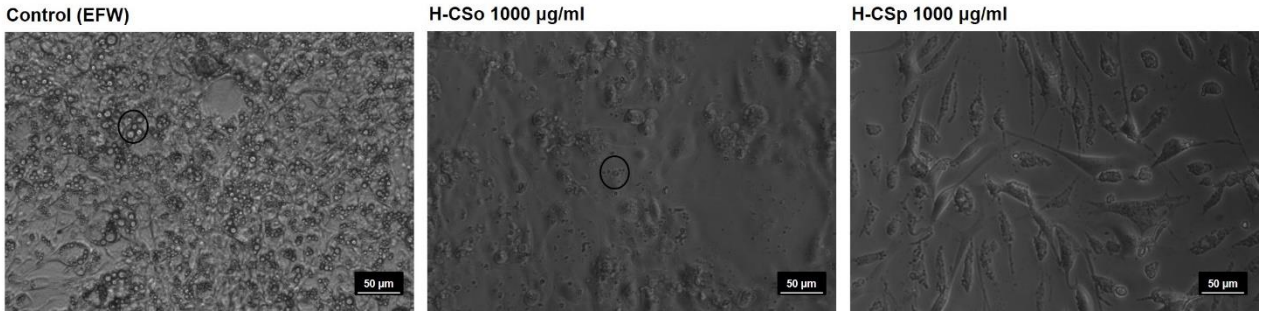


Fig. 5. Effect of high-purity CS oligosaccharides (H-CSo) and high-purity CS polysaccharides (H-CSp) on 3T3-L1 adipocyte morphology and lipid droplets.

Photomicrographs of 3T3-L1 adipocytes at the end of the culture period. Lipid droplets were observed by phase contrast microscopy. Circle, lipid droplets. Bars, 50 µm.

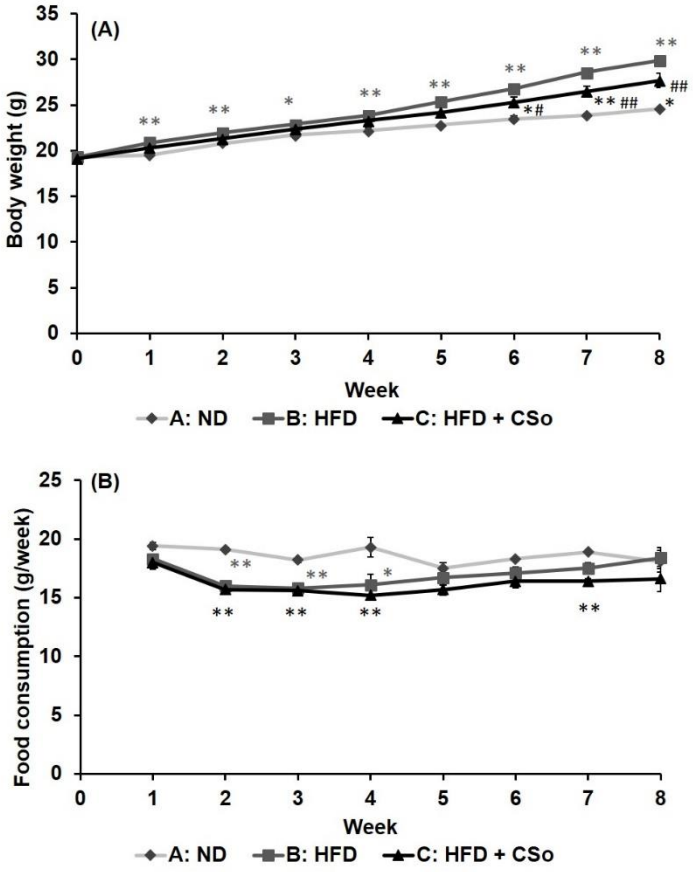


Fig. 6. Effect of thermally hydrolyzed CS oligosaccharides (CSo) on body weight (A) and food consumption (B) in HFD fed mice model.

The date and bars show the mean values and standard errors, respectively (n=7 or 8). * $p < 0.05$ and ** $p < 0.01$ compared with A group. # $p < 0.05$ and ## $p < 0.01$ indicate significant difference between B and C groups.

Chapter III

Free radical scavenging activity of type II collagen peptides and chondroitin sulfate oligosaccharides from by-products of the mottled skate *Raja pulchra*

1. Introduction

Capture fisheries and aquaculture products are essential sources of food worldwide. The total fish production continues to increase and was 171 metric tons in 2016 (FAO, The state of world fisheries and aquaculture, 2018). However, in industrial fish processing, up to 70% of fish weight ends up as by-products (FAO, 2018), which is eliminated as urban solid waste or is discarded into the sea (Lopes et al., 2015). Thus, the by-products of fish processing cause serious environmental problems and result in financial loss. The methods of disposing the by-products are also expensive in Australia and other countries (cf. Pal & Suresh et al., 2016). The FAO (2018) report claims that fish by-products represent a significant additional source of nutrition, and the currently available advanced processing technologies can be used to efficiently harness the nutrients from these by-products. In addition, fish by-products have excellent bioavailability and do not cause any common human diseases; furthermore, their consumption is not prohibited on religious grounds. Thus, they can be developed as

value-added products to boost the efficiency of the fish processing industry and reduce health care costs (cf. Pal & Suresh et al., 2016).

Fifty percent of the carcasses of the mottled skate, *Raja pulchra*, which is an important marine commercial fish in northern Hokkaido, end up as by-products in industrial skate processing (unpublished observation). The by-products include head and axial cartilage that contains type II collagen (C-II) associated with proteoglycans binding chondroitin sulfate (CS) chain (Murado et al., 2010). As I described in Chapter I, the skate cartilage is a practical new alternative resource of the marine cartilage.

Recently, CS polysaccharides (CSp) were isolated and purified from the mottled skate cartilage via enzymatic hydrolysis. To improve the intestinal absorptivity and water solubility of CSp, the CS oligosaccharides were produced via thermal hydrolysis of CSp using a subcritical water microreaction system (Yamada et al., 2013). The bioavailability of CSp is poor, whereas the intestinal absorptivity of the thermally-hydrolyzed CS oligosaccharides (CSo) was improved 40-fold (personal communication). With the exception of CSp, the rest of the skate cartilage is mostly composed of C-II, which accounts for nearly 60% of the dry cartilage weight. However, its industrial usage has not yet been investigated.

CS and collagen peptides (CP) possess multiple bioactivities, which vary according to their origin and molecular weights (MWts) (cf. Martel-Pelletier et al., 2015; cf. Pal & Suresh et al., 2016). To maximize the use of the existing resources, I focused on the

bioactivities CSp, CSo, and type II CP, all of which can be produced from the cartilage of the mottled skate. I have already revealed the anti-obesity actions of the skate CSp and CSo (Chapter II). However, the bioactivity of the type II CP of mottled skate cartilage is not known.

In the human body, regular cellular metabolism results in the production of reactive oxygen species (ROS) (Canas et al., 2007). Factors such as UV and stress increase ROS levels *in vivo*. Overproduction of ROS leads to cell damage and is related to many diseases and aging, such as skin aging, rheumatoid arthritis, Alzheimer's diseases, and others (Canas et al., 2007). Dietary supplementation of antioxidants can reduce ROS levels in our bodies. However, the application of artificial antioxidants is restricted owing to their potential adverse effects on human health (Pan et al., 2016). Therefore, pharmaceutical and food industries tend to use natural antioxidants. Several studies have shown that the hydrolysates/peptides from marine by-products possess antioxidant activity (cf. Pal & Suresh et al., 2016; Sila & Bougatet, 2016).

Three antioxidant peptides were isolated from the protein hydrolysate of the cartilage of the skate, *Raja porosa* (Pan et al., 2016). However, only the non-collagenous peptides were identified. In addition, Li et al. (2013) reported antioxidant activities of type II CP prepared from the cartilages of *Sphyrna lewini*, *Dasyatis akajei*, and *Raja porosa* via trypsin digestion. However, the effects of different enzymatic hydrolysis on the antioxidant activities of type II CP are not yet clear.

The present study aims to evaluate the potential of the cartilage of mottled skate as a source of antioxidants in functional foods. Firstly, I obtained type II CP using three enzymes and compared their antioxidant activities for optimization of the effeciencies. I also determined the relationships between the molecular weight (MWt) distribution of type II CP and antioxidant activities. Later, I analyzed the antioxidant activity of CSo and identified the molecules possibly contributing to this activity. The present results will be a driving force for the industrialization of the skate by-products and may contribute to the substantial reduction of waste discards.

2. Materials and methods

2.1. Materials

Mottled skate cartilage, CSp (purity 70%) and CSo having 2–14 sugar units (purity 80%) from the mottled skate cartilage were obtained from Marukyo Bio Foods Co. Ltd. (Wakkanai, Hokkaido, Japan). High-purity CSp (H-CSp) and high-purity CSo (H-CSo, 6–14 sugar units) were respectively purified from the CSp and CSo using ethanol and activated charcoal treatments by Marukyo Bio Foods Co (purity 83.1 and 86.3%, respectively). The components of purified CSp and CSo other than CS were mineral and water. Triglycine was purchased from Sigma-Aldrich (Saint Louis, MO, USA).

Precision Plus protein^{TM} All Blue Standards (Protein marker) was obtained from Bio-Red (Hercules, CA, USA). Other chemicals were purchased from Wako Pure Chemical Co. (Osaka, Japan) unless otherwise noticed.

2.2. Enzymatic hydrolysis of skate C-II

Skate C-II was extracted according to the method of Zhang et al. (2014) with minor modifications. The cartilage powder was stirred continuously in a solution of HCl (pH 2.0) containing 0.1% (w/v) pepsin for 48 h at 4°C. The mixtures were centrifuged at 10,000 × *g* for 30 min to obtain the supernatants and the residue was re-extracted under the same conditions. The supernatants were precipitated by adding NaCl to a final concentration of 1 M. The resulting precipitate was dissolved in HCl solution (pH 2.0). This process was repeated thrice to purify collagen. The purified collagen was dialyzed against 50 volumes of distilled water for 24 h with two changes of water. The dialysate was sequentially filtered with 3.0, 0.8, and 0.45 μm membrane filters (Advantec, Tokyo, Japan). All the steps of extraction and purification were processed at 4°C or in an ice-bath. The filtrate was lyophilized using a freeze-dryer (FDU-830, Tokyo Rikakikai Co., Ltd., Tokyo, Japan).

The purified collagen was suspended in water and denatured at 60°C for 1 h. Then, the gelatin was digested with trypsin or chymotrypsin (2.5% w/w) at 37°C for 4 h, or

with papain (2.5% w/w) at 50°C for 4 h. After the digestion, the samples were boiled for 10 min to inactivate the enzymes. After filtration via a 0.22 μm filter membrane, the samples were lyophilized using the freeze-dryer. The lyophilized samples were subjected to electrophoresis on 15.5% Tricine-sodium dodecyl sulfate (SDS)-polyacrylamide gel (Schägger & Von Jagow, 1987) and stained using 0.1% Coomassie Brilliant Blue (CBB) R250 and 0.25% Alcian blue (Cowman et al., 1984). The percentage of the dry weight of peptides obtained compared to the dry weight of the initial collagen was calculated as the peptide yield.

2.3. 2,2-diphenyl-1-picrylhydrazyl (DPPH) radical scavenging assay

DPPH (Tokyo Chemical Industry, Tokyo, Japan) was dissolved in methanol to the final concentration of 115 μM. Each sample was dissolved in deionized water to a concentration of 0.625–5 mg/ml. L (+)-ascorbic acid (VC) was used as the positive control. The sample solution (500 μl) was reacted with DPPH methanol solution (500 μl) in the dark at room temperature (21–23°C) for 30 min and the absorbance was measured at 517 nm using a microplate reader (Infinite F50R, Tecan Japan, Kawasaki, Japan). Each measurement was performed in triplicate and the percentage scavenging effect was calculated as follows:

$$\text{DPPH radical scavenging activity (\%)} = (A_b - A_s)/A_b \times 100,$$

where A_b and A_s indicate the absorbance of deionized water and the sample solution, respectively.

2.4. 2,2-azino-bis(3-ethylbenzothiazoline-6-sulfonic acid) (ABTS) radical scavenging assay

ABTS (PubChem CID 16240279; 7 mM) and potassium persulfate (2.45 mM $K_2S_2O_8$) solutions (2:1 v/v) were reacted in the dark at room temperature (21–23°C) for 12–16 h to generate the ABTS radical solution. The solution was diluted with phosphate-buffered saline (PBS, pH 7.4) to an absorbance of 0.70±0.02 at 734 nm, and the 500 µl aliquot was reacted with 500 µl of the sample solution for 10 min at room temperature (21–23°C), followed by measurement of the absorbance at 734 nm using the microplate reader. Each sample was dissolved in deionized water to a concentration of 0.04–5 mg/ml. VC was used as the positive control. Each measurement was performed in triplicate, and the percentage scavenging effect was calculated as follows:

$$\text{ABTS radical scavenging activity (\%)} = (A_b - A_s)/A_b \times 100,$$

where A_b and A_s indicate the absorbance of deionized water and the sample solution, respectively.

2.5. Molecular weight distribution analysis

Molecular weight (MWt) distributions of CPs were determined by size exclusion chromatography on a TSKgel G2500PW column (7.5 mm × 30 cm, Tosoh Co., Tokyo, Japan) with the UV detection at 214 nm. The mobile phase was 35% acetonitrile in 0.05% TFA (pH 2.1) at a flow rate of 0.6 ml/min. A MWt calibration curve was obtained using the following standards: insulin (5700), vitamin B_{12} (1355), and triglycine (189). A 30-μl aliquot of samples or standards was injected into the high performance liquid chromatography (HPLC) system (SCL-10AVP, Shimadzu Corporation, Tokyo, Japan). The percentage of each MWt fraction was calculated as follows:

$$\text{MWt fraction (\%)} = (S_x/S_{total}) \times 100\%,$$

where S_x and S_{total} indicate the area of each fraction (> 5000, 3000–5000, 1000–3000, and < 1000) and the total area of the chromatogram, respectively.

2.6. Preparation of segments with different molecular weight

Papain-hydrolyzed CP (Pa-CP) was separated using the ultrafiltration membrane with the MWt cutoff (MWCO) of 3000 and 10000 (Merck Millipore Ltd., Darmstadt, Germany). A 5-ml aliquot of Pa-CP solution was centrifuged at 4,000 × *g* for 20 min and then eluted with 5 ml deionized water at 4,000 × *g* for 20 min. This process was

repeated several times to obtain the < 3000 peptides. Then, the > 3000 peptides were added to the 10000 MWCO tube and eluted several times with deionized water to separate the 3000–10000 and > 10000 peptides. The collected peptides were freeze-dried.

2.7. Contents of non-enzymatic browning products and total flavonoid

The production of CSo by thermal hydrolysis possibly accompanies the non-enzymatic browning reaction, which includes the Maillard and caramelization reactions, since the CSo shows slight brown color. Thus, the intermediate and the final products of the non-enzymatic browning reaction were estimated by the UV-absorbance and browning intensity of the sample solutions at 294 nm and 420 nm, respectively, using the microplate reader (Ajandouz et al., 2001). The total flavonoid contents of the samples were determined using aluminum chloride ($AlCl_3$), according to the method of Pontis et al. (2014), with minor modifications. In the assay, $AlCl_3$ was dissolved in methanol to a concentration of 5% (w/v). A 0.5-ml sample solution was mixed with 0.75 ml of 5% $AlCl_3$-methanol solution. After 30 min of incubation, the absorbance at 437 nm was measured against a methanol blank. Each experiment was performed in triplicate. The absorbance (ΔA) was calculated using the following equation:

$$\Delta A = A_t - A_b,$$

where A_t is the absorbance of the sample reacted with $AlCl_3$-methanol solution, and A_b is the absorbance of the sample reacted with methanol solution.

2.8. Cytotoxicity

The mouse L929 fibroblast cell line was obtained from the Riken Cell Bank (Tsukuba, Japan). Cells were cultured in 96-well plates in an atmosphere of 5% CO_2 at 37°C. The culture medium was minimum essential medium (MEM, Gibco, Grand Island, NY, USA) containing 5% fetal bovine serum (FBS, Lot. No 451456, Gibco) and 1% penicillin/streptomycin (Gibco). Cells were seeded at the density of 2×10^4 cells/well. After 24 h of incubation, the culture medium was changed to that containing the samples. Samples (CSo and Pa-CP, endotoxin levels < 1 ng/mg) were dissolved in endotoxin-free water (EFW) and were added to the culture medium at the concentration of 1 mg/ml. EFW was used as the negative control.

Following the 48-h incubation with the samples, the cell number/metabolism was assessed using the cell counting kit-8 (CCK-8, Dojindo, Kumamoto, Japan), as described in Chapter II, Section 2.4. The incubation time for the assay was set to 30 min in this experiment.

2.9. Statistical analyses

Data were expressed as means ± standard errors. Statistical analyses were performed using the Tukey-Kramer test after analysis of variance (ANOVA) of the Microsoft Excel add-in statistical software (SSRI, Tokyo, Japan). Experiments were repeated twice to confirm the reproducibility of the results and the representative results have been presented in this report.

3. Results and discussions

3.1. Yields and tricine-SDS-PAGE

Yields of trypsin-CP (Tr-CP), chymotrypsin-CP (Ch-CP), and papain-CP (Pa-CP) were 83, 85, and 91%, respectively. In the tricine-SDS-polyacrylamide gel, CBB and Alcian blue stained peptides and acidic polysaccharides with more than six sugar, respectively (Cowman et al., 1984). The CPs showed no positive reaction with the Alcian blue stain, suggesting that the CPs did not contain reactive CS (Fig. 1A). Pa-CP showed smear after CBB staining with no clear bands, whereas Tr- and Ch-CPs showed several bands at > 20 kDa (Fig. 1B). These data indicated that Pa-CP contained more peptides of lower MWts than Tr- and Ch-CPs. Alcian blue staining showed that CSp and

CSo contained sugars of different MWts (Fig. 1A). Smear stains of CBB were observed in CSp and CSo (Fig. 1B), showing that these samples contained peptides. These CSs were obtained as CS sodium salt. Thus, CSp and CSo contain CS, minerals, and peptides. The preliminary measurement revealed that the peptides accounted for less than 10% of the dry weight of these samples. In contrast, H-CSp and H-CSo contained only CS and minerals (data not shown).

3.2. Antioxidant activity of CPs

3.2.1. Free radical scavenging activity of CPs

The three enzymatically hydrolyzed CPs showed free radical scavenging activity in a dose-dependent manner (Fig. 2). The results of the DPPH radical scavenging assay (Fig. 2A) showed that the activity of Pa-CP was the strongest among the three products. Ch-CP also showed DPPH radical scavenging activity; however, Tr-CP showed almost no activity.

Notably, all CPs showed strong ABTS radical scavenging activity, and scavenged almost all ABTS radicals when the concentration was > 1 mg/ml (Fig. 2B). The ABTS radical scavenging activities varied negligibly among the three CPs.

3.2.2. Relationship between the antioxidant activity and MWt distribution of CPs

The dominant MWt of Tr-CP and Ch-CP were 3000–5000 and > 5000, respectively (Fig. 3). Pa-CP contained more smaller peptides: the sum of < 1000 and 1000–3000 peptides of Pa-CP (48%) was higher than those of Tr-CP (36%) and Ch-CP (12%). This might be because the cleavage specificity of papain was broader than those of trypsin and chymotrypsin. This result is consistent with that obtained with tricine-SDS-PAGE (Fig. 1).

The higher antioxidant activity of Pa-CP is attributed in part to its smaller MWt, as lower MWt peptides have been shown to exert significantly higher antioxidant activities in previous studies (Sila et al., 2016; cf. Zou et al., 2016). For example, the tilapia skin hydrolysate fractions with MWts below 1000 showed the highest free radical scavenging capacity (Zheng et al., 2018). Small MWt peptides may contain more exposed bioactive groups than high MWt peptides, which may contact the free radicals. For example, amino or carboxyl groups in amino acid side chains can act as hydrogen donors to convert free radicals to stable molecules (Amiri et al., 2013).

To further confirm the relationship between the MWts of peptides and antioxidant activity of CP, Pa-CP was divided into three segments with MWts of > 10000, 3000–10000, and < 3000. The results of the ABTS assay (Fig. 4) showed that Pa-CP of < 3000 MWt possessed stronger free radical scavenging activities than high MWt Pa-CP. This further proved that lower MWt CP possessed higher antioxidant activity.

Studies on the radical scavenging activity of type II CP in fish species are limited. Meng (2019) showed DPPH, ABTS, and OH- radical scavenging activities of type II CP from sturgeon notochord. Li et al. (2013) reported antioxidant activity of cartilage collagen hydrolysates from cartilaginous fish (*Sphyrna lewini*, *Dasyatis akjei*, and *Raja porosa*). They also showed that DPPH-radical scavenging activity was higher in lower-MWt peptides. However, this report has several differences with our study: first, the SDS-PAGE result of this study showed existence of many protein bands other than the α, β, and γ bands of type II collagen, suggesting relatively lower purity of collagen than ours; second, the study only used the enzyme trypsin, and enzyme ratio to the collagen is 33% (w/w), which is much higher than our study (2.5%); and third, the trypsin-hydrolysates contained the peptides whose MWt are more than 60000, whereas the hydrolysate in our study is less than 50000. Hence, this is the first study to demonstrate the antioxidant effect of high-purity and low MWt type II CP derived from the skate cartilage and the relationship between their MWts and activity.

Papain is comparatively less expensive than other proteolytic enzymes. Considering the cost of production, Pa-CP is suitable for large-scale production. Furthermore, peptides of < 3000 MWt were more stable during gastrointestinal digestion than those with larger MWts (cf. Zou et al., 2016). Therefore, < 3000 Pa-CP from skate cartilage can be an excellent and inexpensive antioxidant for human health.

3.3. Antioxidant activities of CSs

3.3.1. Free radical scavenging activity of CSp, H-CSp, CSo, and H-CSo

Figure 5 shows the DPPH and ABTS radical scavenging activities of CSp, H-CSp, CSo, and H-CSo. H-CSp showed almost no DPPH and ABTS radical scavenging activities, suggesting that the CS in its native form possesses no free radical scavenging activity. These results were mostly in agreement with those of Ajisaka et al. (2016). This results strongly suggest that the antioxidant activity of CS does not arise due to its direct action on free radicals, but indirectly via its chelating activity.

Unlike H-CSp, CSp possesses radical scavenging activities (Fig. 5). As CSp contains a small amount of peptides (Fig. 1), the activity of CSp may result from these peptides. H-CSo possesses low but significant antioxidant activity. The precise reason underlying the increase in antioxidant activity with breakdown of CS polysaccharides into oligosaccharides is not known. Arai et al. (1999) reported the production of neutralizing molecules via the decomposition of glycosaminoglycans by ROS, which may subsequently act as radical scavengers. Therefore, I speculated that CS oligosaccharides with low molecular weight and simple structure may be easily decomposed by ROS to produce more radical scavengers.

CSo possesses stronger radical scavenging activities than H-CSo (Fig. 5). Notably, the difference between the DPPH radical scavenging activities of CSo and H-CSo was

higher than that between the CSp and H-CSp (Fig. 5A). This indicated that the high activity of H-CSo may not be due only to the peptides.

3.3.2. Non-enzymatic browning products in CSo

I noticed that CSo is produced in acidic and high-temperature environments, the materials contain both sugar and peptides, and CSo is brown in color. Thus, the production of oligosaccharides possibly accompanies the non-enzymatic browning reaction (cf. Kroh, 1994), which includes the Maillard and caramelization reactions. In the reaction process, high UV-absorbing but colorless compounds such as aldehydes, ketones are formed in the intermediate stages, whereas the brown polymers e.g. melanoidins are produced in the final stages (Ajandouz et al., 2001). As these compounds have free radical scavenging activity (Benjakul et al., 2005; Liu et al., 2012), the products of the non-enzymatic browning reaction are the candidate antioxidants in CSo. The intermediate products show UV-absorbance at 294 nm, whereas the final products absorb at 420 nm. At both wavelengths, CSo showed higher absorbance in a dose-dependent manner, than that of Pa-CP and H-CSo (Fig. 6). These results strongly suggest that the excellent antioxidant activity of CSo is partially due to the intermediate and final products of the non-enzymatic browning reaction. Considering that the sample mainly consisted of oligosaccharides, the caramelization reaction must be the major reaction during the high-temperature hydrolysis.

3.3.3. Total flavonoid content of CSo

The intermediate products of the non-enzymatic browning reaction generated via sugar dehydration, sugar fragmentation, or amino acid degradation (Nie et al., 2013) are small molecules, such as furans, ketones, and phenols (Liu et al., 2012; Su et al., 2011). I determined the total flavonoid content of CSo, assuming that they were generated during the non-enzymatic browning reaction, as flavonoids are one of the phenols and good antioxidants. The results showed that CSo had considerably higher absorbance than H-CSo (Fig. 7), suggesting that CSo contained flavonoid-like products that are probably produced via the non-enzymatic browning reaction.

To the best of my knowledge, this is the first study to investigate in detail the non-enzymatic browning reaction in CS processing. The CSo used in this study comprises not only CS oligosaccharides, but other bioactive compounds. The CSo exhibited potent free radical scavenging activity and high intestinal absorptivity. Thus, its oral administration as an antioxidant must be beneficial for human health. However, the effect of the final browning product (melanoidin) on human health is controversial (cf. Bastos & Gugliucci, 2015); hence, the amount of melanoidin intake should be limited even if it is shown to possess antioxidant activity (cf. Bastos & Gugliucci, 2015). Therefore, the intermediate and final compounds of the non-enzymatic browning reaction should be identified and quantified in the future.

3.4. Evaluation of *in vitro* cytotoxicity

To further confirm that Pa-CP and CSo are suitable as antioxidant functional food ingredients, their cytotoxicity in the mouse L929 fibroblast cell model was evaluated. I have already shown that high-purity CS oligosaccharides promote cell proliferation (Chapter II, Section 3.3). However, I was concerned regarding the cytotoxicity of CSo, which included the intermediate and final products of the non-enzymatic browning reaction. In this study, the metabolism of mouse L929 fibroblasts was assessed using the CCK-8 assay after culturing the cells in direct contact with high concentrations of CSo and Pa-CP (1 mg/ml). The results showed that the cellular activities of both the CSo and Pa-CP groups were similar to that of the control group after 48 h of incubation (Fig. 8), indicating that even the high dose of CSo and Pa-CP were not cytotoxic. The results obtained using Pa-CP is in line with those of previous studies that showed absence of cytotoxicity of antioxidant peptides from marine by-products (cf. Pal & Suresh., 2016; Sila et al., 2016).

Taken together, the results of the cytotoxicity assay indicated that skate cartilage-derived Pa-CP and CSo can be used as antioxidants for functional foods. Further analysis of their functionality using *in vivo* models is needed to confirm their value as antioxidants.

4. Conclusion

To maximize the use of resources and to improve the efficiency of the fishery processing industry, the antioxidant components of skate cartilage were investigated in this study. The results showed the high free radical scavenging activities of Pa-CP and CSo from skate by-products. The antioxidant activity of Pa-CP was related to their MWts; the < 3000 Pa-CP showed stronger antioxidant activity than larger peptides. Pure CS, independent of its MWt, showed almost no free radical scavenging activity, whereas the thermally-hydrolyzed CS oligosaccharides showed excellent antioxidant activity because of the non-enzymatic browning products that were produced during the thermal hydrolysis. CSo possibly included flavonoid-like products as antioxidants. Furthermore, CSo and Pa-CP were not cytotoxic and may show high intestinal absorptivity. Therefore, they can act as valuable antioxidants in functional food items. These results will be beneficial for achieving zero-discard rate of marine processing by-products and high efficiency of the skate-processing industry. In the future, *in vivo* studies using CSo and Pa-CP as antioxidant foods are needed.

Figures

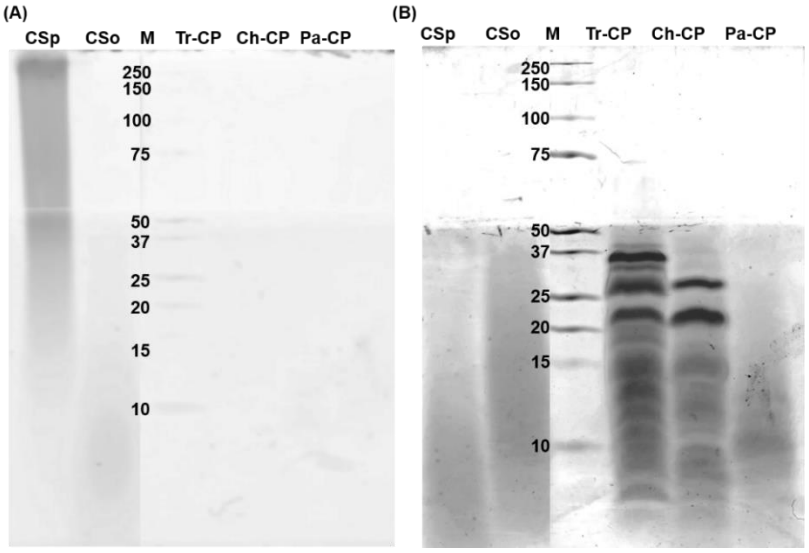


Fig. 1. Alcian blue (A)- and Coomassie Brilliant Blue (B)-stained Tricine-SDS-PAGE.

M, protein mark; CSp, chondroitin sulphate (CS) polysaccharides; CSo, thermally hydrolyzed CS oligosaccharides; Tr-CP, trypsin-hydrolyzed type II collagen peptides; Ch-CP, chymotrypsin-hydrolyzed type II collagen peptides; Pa-CP, papain-hydrolyzed type II collagen peptides.

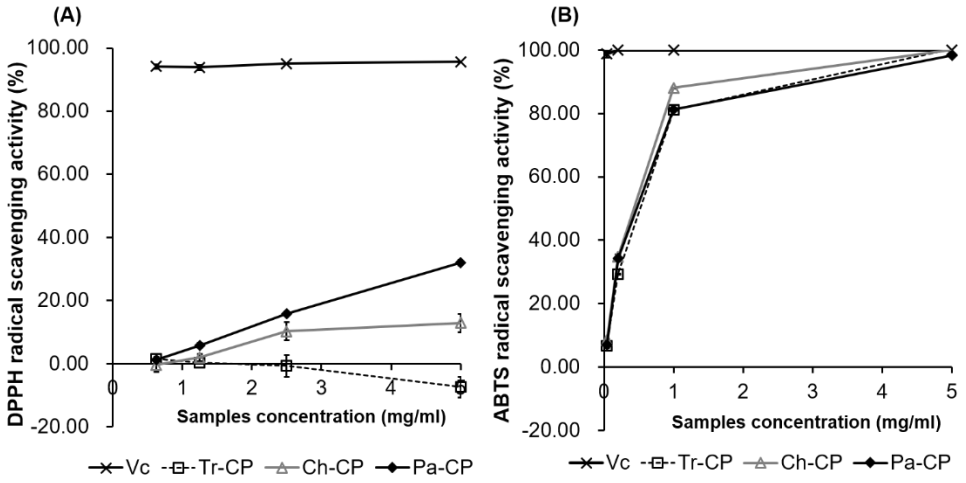


Fig. 2. DPPH (A) and ABTS (B) radical scavenging activities of enzyme-hydrolyzed type II collagen peptides (CPs).

Values are expressed as the mean and standard errors, respectively (n=3). Vc, vitamin C; Tr-CP, trypsin-hydrolyzed CP; Ch-CP, chymotrypsin-hydrolyzed CP; Pa-CP, papain-hydrolyzed CP.

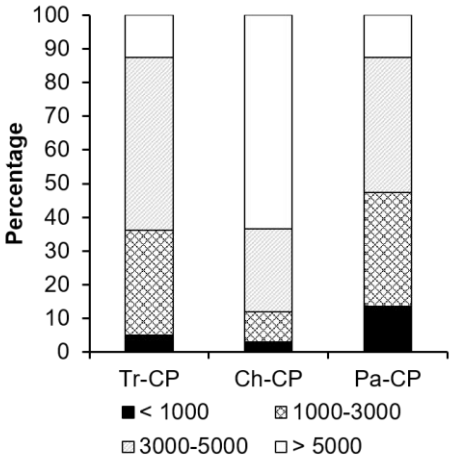


Fig. 3. Molecular weight distribution of enzyme-hydrolyzed type II collagen peptides (CPs).

Tr-CP, trypsin-hydrolyzed CP; Ch-CP, chymotrypsin-hydrolyzed CP; Pa-CP, papain-hydrolyzed CP.

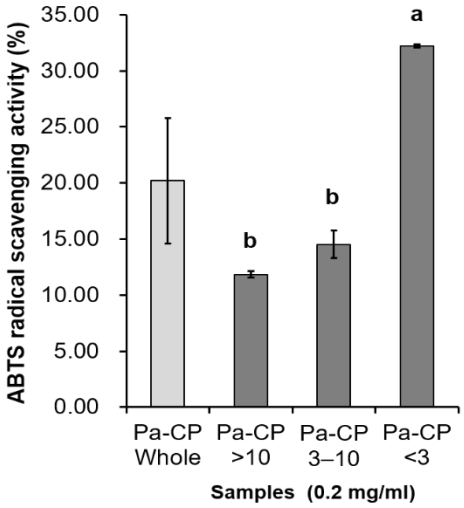


Fig. 4. ABTS radical scavenging activity of papain-hydrolyzed type II collagen peptides (Pa-CP) with different molecular weight segments.

The columns and bars show the mean values and standard errors, respectively (n=3). Different letters indicate statistical difference ($p < 0.01$, Tukey-Kramer test). Pa-CP Whole, whole Pa-CP; Pa-CP > 10, Pa-CP larger than 10000; Pa-CP 3–10, Pa-CP between 3000 to 10000; Pa-CP < 3, Pa-CP smaller than 3000.

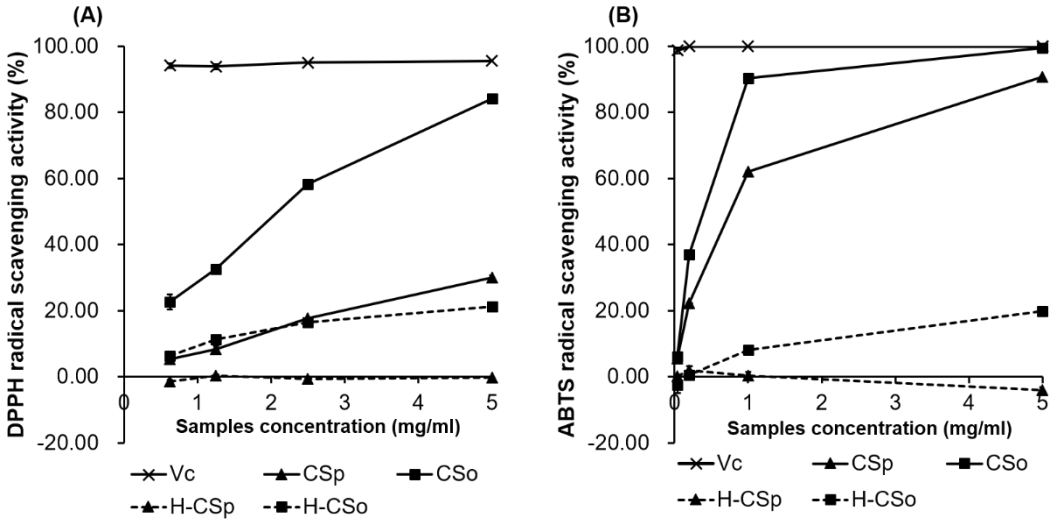


Fig. 5. DPPH (A) and ABTS (B) radical scavenging activities of different types of chondroitin sulfates.

Values are expressed as the mean and standard errors, respectively (n=3). CSo, thermally hydrolyzed chondroitin sulfate (CS) oligosaccharides; H-CSo, high-purity CS oligosaccharides; CSp, CS polysaccharides; H-CSp, high-purity purified CS polysaccharides.

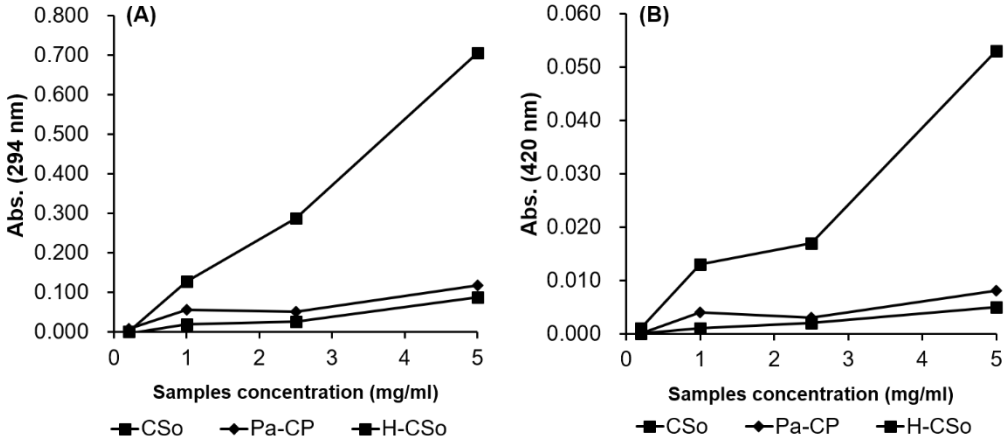


Fig. 6. UV-absorbance (A) and brown color (B) intensity of chondroitin sulfate oligosaccharides and papain-hydrolyzed collagen peptides.

CSo, thermally hydrolyzed chondroitin sulfate (CS) oligosaccharides; H-CSo, high-purity CS oligosaccharides; Pa-CP, papain-hydrolyzed type II collagen peptides.

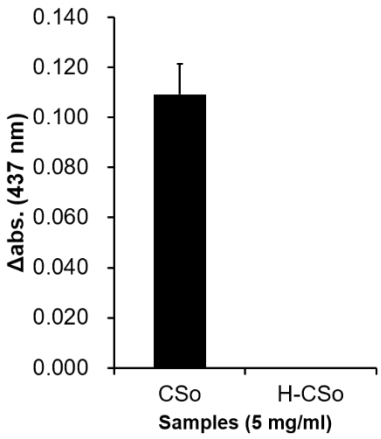


Fig. 7. Total flavonoid content of chondroitin sulfate (CS) oligosaccharides.

The columns and bars show the mean values and standard errors, respectively (n=3). CSo, thermally hydrolyzed CS oligosaccharides; H-CSo, high-purity CS oligosaccharides

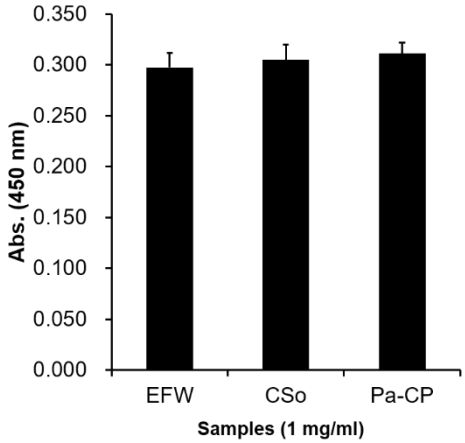


Fig. 8. Cytotoxicity of thermally hydrolyzed chondroitin sulfate (CS) oligosaccharides and papain-hydrolyzed type II collagen peptides.

Values are expressed as the mean and standard errors, respectively (n=10). EFW, endotoxin-free water; CSo, thermally hydrolyzed CS oligosaccharides; Pa-CP, papain-hydrolyzed type II collagen peptides. Sample concentration was 1 mg/ml.

Chapter IV

Wound healing activity of by-product of skate chondroitin sulfate production

1. Introduction

Wound healing is a complex and highly regulated process that can be divided into three phases: hemostasis and inflammation, proliferation, and remodeling (Broughton et al., 2006; Han et al., 2017). Failure to progress through these normal stages of healing results in chronic and non-healing wounds, such as leg ulcers, diabetic wounds, and pressure ulcers (Dhivya et al., 2015; Han & Ceilley, 2017). An essential feature of these wounds is oxidative stress caused by the inflammatory cells in the wound tissues that produce large amounts of reactive oxygen species (ROS), pro-inflammatory cytokines, and oxidases (cf. Kurahashi & Fujii, 2015; Schäfer & Werner, 2018). Although low ROS levels are required for defense against invading pathogens and modulating the signaling molecules, excessive ROS levels cause cellular apoptosis in the surrounding tissues and imbalanced redox homeostasis, resulting in chronic wounds (cf. Kurahashi et al., 2015; Schäfer et al., 2018).

Chronic wounds are the global health problem that cause significant discomfort and distress to patients. Even in the developed countries, almost 1.5% of the population

experiences problematic wounds, accounting for 2%–4% of all health care expenses (Ahmed et al., 2019). Thus, the market demands superior wound dressings that can achieve rapid healing at a reasonable cost. A very effective approach is the use of bioactive wound dressings in which the dressing materials contain bioactive compounds (Boateng et al., 2008; Dhivya et al., 2015); thus, the dressing not only covers the wound but also facilitates wound healing. Basal biomaterials (hydrogels, collagen, chitosan, and other polymers) form a natural tissue matrix (Boateng et al., 2008), whereas exogenous active compounds (antimicrobial agents, growth factors, and other wound-healing accelerators) play roles as key "wound-healing promoters" in the bioactive wound dressings (Boateng et al., 2008). For instance, peptides and saccharides are potent regulators of a variety of cellular behaviors, such as cell proliferation, migration, differentiation, and protein expression, and are therefore being developed as wound-healing promoters for bioactive wound dressings (Hubbell, 1999).

As shown in Chapter I, CS is a popular joint pain-related treatment that is used as a symptomatic slow-acting drug in Europe and as a dietary supplement in the United States (Volpi, 2007). Industrial CS production uses cartilage sources derived from terrestrial or marine animals; however, a large amount of the cartilage residue is wasted following CS extraction and purification, including type II collagen (C-II), non-collagenous proteins, and residual CS. Owing to the aging global population and the discovery of new CS bioactivities, such as an anti-obesity activity (Chapter II), a

demand for CS production has increased rapidly (Restaino et al., 2019; Vázquez et al., 2013). This has resulted in the rapid increase of the waste generated by a CS production. To realize zero-waste and maximize profit, these waste products must be used wisely rather than being discarded.

Due to the increase in CS production from skate (*Raja pulchra*) in northern Hokkaido, the by-product of skate CS production (BP-sCS) must be used wisely. Cartilage proteins are hydrolyzed during skate CS purification; therefore, BP-sCS contains a mixture of biomacromolecules, such as CS polysaccharide residues, C-II peptides, and non-collagenous peptides, alongside a small amount of minerals that bind to CS (Fig. 1). Since CS polysaccharides and peptides with a high molecular weight (MWt) display low absorbability in the skin and digestive system (Li et al., 2015; Shang et al., 2016; Shen & Mastsui, 2017), I hypothesized that BP-sCS could be used for wound healing as the compounds can directly come in contact with the wound site. CS has been reported to activate fibroblasts and their migration during wound healing (Zou et al., 2009), while peptides have been known to exhibit several biological activities related to wound healing, such as antioxidant activity, antimicrobial activity, and extracellular-matrix synthesis activation (Pal & Suresh, 2016). Consequently, it is highly possible that BP-sCS, which is a mixture of bioactive macromolecules, may promote wound-healing.

In this study, I examined the bioactivities of BP-sCS as a wound-healing promoter

for bioactive wound dressings. During the proliferative phase of wound healing, fibroblasts migrate to the wound site from surrounding tissue, become activated, proliferate, synthesize extracellular matrix, and finally differentiate into myofibroblasts to close the wound (Broughton, et al., 2006). At the same time, excessive ROS must be detoxified during chronic wound healing. Therefore, I focused on the antioxidant and fibroblast-activating roles of BP-sCS and examined the activities of pure CS polysaccharides and C-II peptides to determine the active components of BPs-CS.

2. Materials and methods

2.1. Materials

Skate cartilage, high-purity chondroitin sulfate polysaccharides sodium salt (H-CSp) and BP-sCS were supplied from Marukyo Bio Foods Co. Ltd. (Wakkanai, Hokkaido, Japan). CSp was isolated and purified from the cartilage of the skate *Raja pulchra*, and the remaining material was spray-dried to produce BP-sCS containing CSp, C-II peptides, non-collagenous peptides, minerals, and other materials (Fig. 1). Type II collagen was purified from skate cartilage according to the method of Chapter III, Section 2.2. The papain-hydrolyzed C-II peptides (Pa-CP) were prepared by hydrolyzing the purified C-II using papain (2.5% w/w) at 50°C for 4 h (Chapter III,

Section 2.2).

2.2. Antioxidant assays in tube

DPPH and ABTS radical scavenging assays were conducted as shown in Chapter III, Section 2.3.

2.3. Molecular weight distribution of peptides

Peptides and CSp residues in the BP-sCS were separated by ultrafiltration using the molecular weight cut off (MWCO) of 3000 (Merck Millipore, Darmstadt, Germany). A 5-ml aliquot of BP-sCS solution was centrifuged at 4,000 × *g* for 20 min and then eluted with 5 ml of deionized water at 4,000 × *g* for 20 min. This process was repeated several times to obtain the < 3000 segment, which has been predicted to contain only peptides, because the MWt of the H-CSp in BP-sCS is much larger than 3000 (Fig. 1). However, the separation also excludes peptides larger than 3000 in the BP-sCS; thus, the < 3000-segment of Pa-CP was also obtained to compare its bioactivity to the < 3000-segment of the BP-sCS. The collected segments were freeze-dried. The MWt distribution of < 3000 segments was determined using HPLC as described in Chapter III, Section 2.5.

2.4. Cell culture experiment

The mouse L929 fibroblast cell line from the RIKEN Cell Bank (Tsukuba, Japan) and the human skin TIG-113 fibroblast cell line from JCRB Cell Bank (Osaka, Japan) were cultured at 37°C with 5% CO_2. The culture media for the L929 and the TIG-113 cells was the minimum essential medium (MEM, Gibco, Grand Island, NY, USA) containing 1% penicillin/streptomycin (Thermo Fisher Scientific, Waltham, MA) with 5% or 10% fetal bovine serum (FBS, Lot. No 451456, Gibco), respectively. The medium was changed every 2–3 days, and cells were passaged when they reached 70%–80% confluency. Samples dissolved in endotoxin-free water (EFW) were added to the culture medium at various concentrations for different experiments, with EFW used as a negative control. The endotoxin levels in MEM and the samples (at 1000 μg/ml) were less than 1.0 EU/ml.

2.5. CCK-8 assay

Fibroblast viability/activity was assessed using the Cell Counting Kit-8 (CCK-8, Dojindo, Kumamoto, Japan) as described in Chapter II, Section 2.4. The incubation time for the assay was set to 30 min in this experiment.

2.6. Cell viability/activity assay under oxidative stress

The strong oxidant H_2O_2 (Wako Pure Chemical) and weak oxidant 2,2′-azobis(2-methylpropionamidine) dihydrochloride (AAPH, Tokyo Chemical Industry) were chosen to induce oxidative damage in the cells. Briefly, 100 µl of the L929 cell solution (2×10^3 cells/well) was seeded in each well of a 96-well plate. When the cells reached > 90% confluency, samples were added to the culture medium to produce a final concentration of 1000 µg/ml. After 24 h, the cells were exposed to H_2O_2 or AAPH for a further 24 h at a working concentration of 0.5 mM or 5 mM, respectively. After incubation, the cells were washed with the Hank's balanced salt solution (HBSS, Sigma-Aldrich, Saint Louis, MO, USA) and cell viability was assessed using the CCK-8 assay as described earlier, expressed as the relative absorbance normalized to that of the control well (no oxidant).

2.7. Measurement of intracellular ROS levels

Intracellular ROS formation was assessed according to the method described by Ahn et al. (2012), with minor modifications. The oxidation-sensitive dye H_2DCFDA was used as a probe as it diffuses through the cell membrane and is hydrolyzed into its

nonfluorescent form dichlorofluorescein (DCFH) by intracellular esterase. Then, DCFH reacts with the intracellular H_2O_2 to produce an oxidized form of DCFH, which is a green fluorescent dye. L929 cells (2×10^3 cells/well) were grown in a black/transparent 96-well microtiter plate until they reached > 90% confluency and were treated with the samples for 24 h. After the culture medium had been discarded, the cells were washed with HBSS and labeled with H_2DCFDA (20 μM; Sigma-Aldrich) in HBSS for 20 min in the dark at 37°C, and then washed with HBSS and incubated with 0.5 mM H_2O_2 in HBSS for 30 min in the dark at 37°C. Fluorescence was read at an excitation wavelength of 485 nm and an emission wavelength of 528 nm using a fluorescence microplate reader (WallAc ARVO 1420 Multilabel counter, PerkinElmer, Waltham, MA, USA). VC was used as a positive control. Data have been expressed as the relative fluorescence intensity normalized to that of the control well (no oxidant).

2.8. Fibroblast proliferation/metabolism assay

Fibroblast proliferation was assessed as per a method described previously in Chapter II, Section 2.4. Briefly, 250 μl of the L929-cell solution (5×10^3 cells/well) was seeded in each well of a 48-well plate. After 24 h, samples were added to the culture medium to produce a final concentration range of 1–1000 μg/ml. The CCK-8 assays were conducted on day 3 and day 7 after culture. Data have been expressed as the

relative absorbance normalized to that of the control well (EFW only).

2.9. Gene expression assay

Type I collagen gene expression was analyzed by real-time quantitative PCR (qPCR). Briefly, the L929 cells (5×10^3 cells/well) were seeded in a 48-well plate. After 24 h, the culture medium was replaced with medium containing 1000 μg/ml sample. After a further 3 days or 7 days, total RNA was extracted from each well using the ISOGEN II reagent (Nippon Gene, Tokyo, Japan) and quantified using a spectrophotometer (ND-1000, Thermo Fisher Scientific, Waltham, MA, USA). cDNA was synthesized from 500 ng total RNA using a Prime Script RT reagent kit with the gDNA Eraser Perfect Real Time (Takara Holdings, Ohtsu, Japan), according to the manufacturer's instructions. qPCR was performed using a Real-Time PCR system (LightCycler® Nano System, Basel, Switzerland), with synthesized cDNA diluted five times as the template. Amplification was carried out at a final volume of 15 μl, containing 1 μl of the cDNA template, 7.5 μl of 2X SYBR (Faststart universal SYBR green master, Roche, Basel, Switzerland), 1.5 μl of each primer (5 μM each), and 3.5 μl of sterilized water. PCR was performed as follows: 95°C for 10 min, followed by 40 cycles of 95°C for 10 s, 56°C for 10 s, and 72°C for 15 s. The reaction used primers for the type I procollagen α1 gene *Col1a1* (COL1A1-F: 5′-AAC CCG AGG TAT GCT

TGA TCT-3′, and COL1A1-R: 5′-CCA GTT CTT CAT TGC ATT GC-3′), and *Gapdh* (GAPDH-F: 5′-TCC CAC TCT TCC ACC TTC-3′, and GAPDH-R: 5′-CTG TAG CCG TAT TCA TTG TC-3′) (Kanazawa et al., 2008; Yoshimoto et al., 2009). Relative gene expression was calculated using the $2^{-\Delta\Delta CT}$ method with *Gapdh* as the internal control (Schmittgen & Livak, 2008). Data have been expressed as the relative values normalized to that of the control well (EFW only).

2.10. Scratch assay

The scratch assay was conducted using the methods described by Liang et al. (2007), with minor modifications. Briefly, L929 cells (1.2×10^4 cells/well) were seeded in 24-well plates with a reference point in each well, cultured until almost confluent, and a scratch generated through the reference point in the cell monolayer using a sterile 200 μl pipette tip. The wells were washed with HBSS to remove debris, and the culture medium containing each sample was added. For the scratch-oxidative stress tests, AAPH was added to the culture medium at a final concentration of 5 mM or 2.5 mM (Alvarez-Suarez et al., 2016). The scratches in each well were observed and photographed under a microscope (DMI600B, Leica, Wetzlar, Germany). The images acquired for each well were analyzed quantitatively using the ImageJ software (1.52a, National Institutes of Health, USA) and the repair rate (percentage wound closure)

calculated as follows:

$$\text{Repair rate (\%)} = [\text{area (0 h)} - \text{area } (x \text{ h})]/\text{area (0 h)} \times 100,$$

where area (0 h) and area (x h) indicate the scratch area at time 0 and time x (x = 6 h, 12 h, 24 h, 30 h, or 36 h), respectively.

2.11. Gel-contraction assay in a 3-D culture model

For the gel contraction assay, an *in vitro* 3D wound closure model according to the method of Zou et al. (2009) was used, with minor modifications. Porcine collagen (Cellmetrix type I-A, 3 mg/ml; Nitta Gelatin Inc., Osaka, Japan) was mixed with 10X MEM (Sigma-Aldrich) and reconstitution buffer (50 mM sodium hydroxide, 260 mM sodium hydrogen carbonate, and 200 mM HEPES) at a ratio of 8:1:1 on ice. After TIG-113 cells (2×10^5 cells/ml) were suspended in the collagen solution, 300 µl of the cell-collagen suspension was transferred into each well of a 24-well plate and incubated at 37°C for 30 min to allow the solution to form a gel. After gelation, 500 µl of culture medium containing 1000 µg/ml of sample was gently added to each well, and the gel was dissociated from the well by gently running the tip of a 200 µl pipette tip along its edge. After incubation for 48 h, the gel was photographed, and its area measured using the ImageJ software (1.52a, USA). Data have been expressed as the percentage of the

contracted gel area compared to the initial gel area. TIG-113 cell proliferation/metabolism was assessed using CCK-8 (see section 2.4) after the photographs had been taken.

2.12. Statistical analyses

Data have been expressed as the mean ± standard error. Statistical analyses were performed using the Student's *t*-test, the Dunnett's test, or the Steel-Dwass test after ANOVA with Microsoft Excel add-in statistical software (SSRI, Tokyo, Japan).

3. Results and discussions

3.1. Antioxidant activity of BP-sCS

3.1.1. Free-radical scavenging activity

The antioxidant activity of BP-sCS was assayed using the ABTS and the DPPH scavenging assays. BP-sCS displayed a strong antioxidant activity, particularly in the ABTS radical scavenging assay (Fig. 2A). At concentrations over 1 mg/ml, BP-sCS was able to scavenge almost all the ABTS radicals. Although CSp displayed no activity in the DPPH or the ABTS assays, Pa-CP was able to scavenge radicals in a dose-dependent

manner; therefore, type II CP, not CSp, is likely to be responsible for the free radical scavenging activity of BP-sCS.

Next, I separated CSp and the peptides in BP-sCS using a 3000 MWCO ultrafiltration membrane. Tricine-SDS-PAGE revealed that the < 3000 segment of BP-sCS contained only peptides (Fig. 3), which may include the type-II CP and the non-collagenous peptides. Similarly, I separated Pa-CP into two segments and compared the ABTS radical scavenging activity of the < 3000 BP-sCS and Pa-CP segments. Antioxidant activity was significantly higher in the < 3000 segment of BP-sCS than in that of Pa-CP (Fig. 4A), suggesting that the antioxidant activity of BP-sCS may be due to both type II CP and non-collagenous peptides.

I also analyzed the MWts distribution of the < 3000 BP-sCS and Pa-CP segments using size exclusion chromatography (Fig. 4B), finding that BP-sCS contained more < 1000 peptides and less 3000–5000 peptides than Pa-CP. Many studies have reported that peptides with a lower MWt display a stronger antioxidant activity (Agrawal et al., 2019; cf. Nwachukwu & Aluko, 2019; Zou et al., 2016), and it has been suggested that smaller peptides may expose more bioactive fragments via hydrolyzation (Zou et al., 2016). Therefore, the peptides with a lower MWt in BP-sCS may also be responsible for its high antioxidant activity.

3.1.2. Protection of cells from oxidative stress

H_2O_2 generates free radicals, and thus it is commonly used to induce cell death, and is therefore considered a good model of oxidative stress (Canas et al., 2007). In this study, I established an H_2O_2-induced oxidative stress model (Fig. 5A) in which the addition of 0.5 mM H_2O_2 significantly reduced cell viability/activity to approximately 30% that of the control cells, as quantified by the CCK-8 assay. Treating cells with 1000 μg/ml of BP-sCS significantly reduced the damage induced by H_2O_2, increasing their viability/activity to approximately 50% that of the control cells. In contrast, treatment with Pa-CP or CSp did not affect cell viability/activity.

I also developed another oxidative stress model using AAPH, which acted more slowly and had gentler effects than H_2O_2 (Fig. 5B). AAPH initiates free-radical reactions by generating radicals at a constant rate to initiate oxidation reactions at 37°C. Treatment with 5 mM AAPH for 24 h reduced cell viability to approximately 50% that of the control group, while treatment with BP-sCS or Pa-CP significantly increased cell viability/activity compared to that in the EFW group. CSp was again ineffective. Taken together, the results from the H_2O_2 and AAPH models indicate that peptides, but not H-CSp, in BP-sCS have significant cytoprotective activities against the oxidative stresses. This was found to be consistent with the previous studies in which peptides derived from the tilapia skin, lantern fish hydrolysate, and microalgae were found to exert cytoprotective effects under the AAPH- and the H_2O_2-induced oxidative stress (Chai et al., 2016; Hu et al., 2017; Zeng et al., 2018).

3.1.3. Reduction of intracellular ROS production

Next, I examined whether the compounds in BP-sCS could reduce the intracellular ROS production by H_2O_2 using a fluorescent probe whose fluorescence increases when free radicals are generated within a cell (Ahn et al., 2012).

Exposing the L929 cells to 0.5 mM H_2O_2 significantly increased the intracellular ROS production (Fig. 6), whereas ROS production was significantly reduced when the cells were treated with the positive control (VC) or 1000 μg/ml of BP-sCS. The same concentration of Pa-CP was also able to prevent intracellular ROS production, though it displayed no significant cell-protective effects against H_2O_2-induced oxidative stress. Surprisingly, 1000 μg/ml of H-CSp also significantly reduced the intracellular ROS production, despite showing no free-radical scavenging activity or cytoprotective activity against H_2O_2 or AAPH. These findings strongly suggest that CSp specifically affects the intracellular antioxidant system. It has previously been reported that CS-A induces the synthesis or increases the activity of antioxidant enzymes such as superoxide dismutase, catalase, and heme oxygenase-1 (Canas et al., 2007). Compared to the mammalian chondroitin sulfate, skate chondroitin sulfate contains more CS-C than CS-A, which may explain why H-CSp did not exert significant cytoprotective activity against the H_2O_2- or the AAPH-induced oxidative stress. A previous report indicated that CS formulations might influence the CS antioxidant activity (cf. Campo

et al., 2006). The antioxidant activity of CS-C might be lower than that of CS-A.

In these experiments, the sample-containing culture medium had already been changed to that without samples before H_2O_2 was added; thus, peptides and CS may have been transported into cells via cell surface transporters or membrane channels to exert their antioxidant activities. Alternatively, they may have bound cell-surface receptors to produce intracellular effects. Several peptide transporters (PEPTs) and CS receptors have been reported; for instance, PEPT-1 was found to be involved in the cellular uptake of peptides in skin keratinocytes (Kudo et al., 2016), while Zheng et al. (2018) reported that fish skin peptides failed to inhibit ROS production in the H_2O_2-exposed porcine enterocytes with PEPT1 knock-down. In addition, CS chain receptors such as the Toll-like receptor 2 and annexin 6 have been identified on the surface of fibroblasts (Takagi et al., 2002; Wu et al., 2018). These studies strongly suggest that the antioxidative effects of BP-sCS depend, at least in part, on the transporter- and the receptor-related signaling pathways.

3.2. Effect of BP-sCS on L929 fibroblast activity

3.2.1. Fibroblast proliferation/metabolism

To assess their effect on fibroblast proliferation/metabolism, the L929 cells were treated with 10 μg/ml, 100 μg/ml, or 1000 μg/ml of BP-sCS, Pa-CP, or CSp for up to

7 days (Fig. 7). No significant effects were observed after 3 days (Fig. 7A); however, Pa-CP and H-CSp significantly enhanced the L929 fibroblast proliferation/metabolism in a dose-dependent manner after 7 days (Fig. 7B). The lowest effective concentrations of Pa-CP and H-CSp were 10 μg/ml and 100 μg/ml, respectively, while BP-sCS also significantly activated fibroblast proliferation/metabolism at 1000 μg/ml. Thus, high BP-sCS concentrations promote fibroblast proliferation/metabolism, and its activity is mainly due to type-II CP and H-CSp.

Previously, I found that skate CS polysaccharides accelerated the 3T3-L1 fibroblast proliferation/metabolism (Chapter II, Section 3.3), while several studies have reported the fibroblast-proliferation activity of type I collagen-derived peptides. For example, collagen peptides from the Asian sea bass were found to promote the L929 fibroblast proliferation (Benjakul et al., 2018), whereas those from tilapia scales were shown to stimulate human skin fibroblast proliferation (Chai et al., 2010). However, this study is the first to report the effect of type-II peptides on fibroblast proliferation/metabolism. Since a biomaterial made of sturgeon collagen fibrils was shown to inhibit cell proliferation (Moroi et al., 2019), BP-sCS may be a good fibroblast-proliferation promoter for use in bioactive wound dressings.

3.2.2. Collagen mRNA expression

Type I collagen is secreted by skin fibroblasts during wound healing to construct a

new extracellular matrix (Broughton et al., 2006). In this study, I analyzed the type I collagen α1 chain (*Col1a1*) mRNA expression to investigate the extracellular matrix synthesis capacity of fibroblasts. Cell proliferation assays determined the effective BP-sCS dose (1000 μg/ml) for subsequent experiments. As shown in Fig. 8, the BP-sCS activated collagen synthesis faster than fibroblast proliferation/metabolism and significantly increased the *Col1a1* gene expression compared to that in the control after 3 days of culture. After 7 days, BP-sCS continued to enhance *Col1a1* expression but with no significant difference compared to that in the control group. Neither Pa-CP nor H-CSp showed a significant tendency to increase the *Col1a1* expression after 3 days. These results indicate that BP-sCS stimulates type I collagen synthesis at the mRNA transcriptional level, while the minimal effect of Pa-CP and H-CSp suggests that BP-sCS activity is mainly due to non-collagenous peptides. Several previous reports have demonstrated that non-collagenous peptides trigger collagen synthesis by fibroblasts (cf. Husein el Hadmed & Castillo, 2016; Zeng et al., 2018); however, to my knowledge, this is the first study to report the collagen-synthesis promoting activity of the fish cartilage-derived non-collagenous peptides.

3.2.3. Fibroblast migration

Scratch assay is particularly suitable for studying the effects of cell-matrix and cell-cell interactions on cell migration as it mimics cell migration during wound healing

in vivo (Liang et al., 2007). As shown in Fig. 9, treatment with BP-sCS, Pa-CP, or H-CSp (1000 μg/ml) tended to transiently and slightly increase the cell migration during the first 12 h, while the scratch had healed in all groups after 24 h. Recent studies have shown that collagen peptides and pure CS promote the migration of skin cells (fibroblasts or keratinocyte) (Hu et al., 2017; Kumar et al., 2019; Zou et al., 2009), while this study indicates that BP-sCS from skate cartilage has a weak fibroblast migration-promoting activity during wound healing.

Next, I examined fibroblast migration under oxidative stress to simulate conditions of chronic wounds. Treatment with 5 mM AAPH significantly reduced fibroblast migration and inhibited wound closure and was significantly counteracted by Pa-CP (Fig. 10A). A lower concentration of AAPH (2.5 mM) had a weaker inhibitory effect on wound closure (Fig. 10B). Compared to the EFW- and the H-CSp-treated groups, those treated with Pa-CP and BP-sCS displayed a higher wound repair rate, although the differences were insignificant. After treatment with 2.5 mM AAPH for 24 h, fibroblasts in the EFW and the CSp groups began to die and the site of the scratch enlarged, whereas after 48 h the fibroblasts in the control group (no AAPH) had made contact with each other and the scratch had healed completely (Fig. 10C). Conversely, the AAPH-stressed fibroblasts shrunk and had separated from each other, which could be the result of cell contraction and reduced cell number due to oxidative damage. Although the scratch in the BP-sCS and the Pa-CP groups did not heal, the AAPH-

stressed fibroblasts in these groups retained their normal morphology, and no further wound enlargement was observed (Fig. 10C). Therefore, BP-sCS may counteract the inhibitory effects of oxidative stress on fibroblast migration and wound closure, likely due to the effects of type-II CP (Pa-CP), which significantly enhances fibroblast migration under oxidative stress (Fig. 10A), consistent with the results of the antioxidant assay. Excessive ROS levels are an essential feature of chronic, non-healing wounds (cf. Schäfer & Werner, 2008); therefore, BP-sCS may be used to promote the healing of chronic wounds. A similar scratch-oxidative stress model previously demonstrated the antioxidant activity of honey, which protected the fibroblasts against oxidative damage and promoted wound healing and closure (Alvarez-Suarez et al., 2016). This study is the first to report the effects of fish peptides on fibroblast migration under oxidative stress simulating the effects of peptides on chronic wound healing.

3.2.4. Gel contraction

Wound contraction is a critical step in the remodeling phase of wound healing, during which fibroblasts in the wound site begin to synthesize collagen and transform into myofibroblasts (Broughton et al., 2006) that can contract the wound via traction forces between actin-myosin and collagen (cf. Brown, 2013). Previous studies have used fibroblast-collagen hydrogels to mimic the wound environment (Ngo et al., 2006), and measurement of the dimensional changes in these gels has allowed us to evaluate

the effect of certain factors on wound contraction in a 3D system (cf. Brown, 2013).

In this study, I used the human skin fibroblast TIG-113 cells in the gel-contraction assay since they retained the ability to differentiate into myofibroblasts. As shown in Fig. 11A, the gel-contraction area was approximately 25% after incubation for 48 h, with no significant differences observed between the groups. Since cell density relates to collagen gel contraction (cf. Brown, 2013; Ngo et al., 2006), and BP-sCS, Pa-CP, and H-CSp promotes the L929 fibroblast proliferation/metabolism, I also determined TIG-113 cell proliferation/metabolism using CCK-8 assays. There were no changes in cell proliferation/metabolism after incubation for 48 h (Fig. 11B); therefore, BP-sCS, Pa-CP, and H-CSp did not accelerate gel contraction but showed no adverse effects. A previous study reported that pure CS-C, but not CS-A, inhibits gel contraction by fibroblasts at a concentration of 1 μg/ml (Zou et al., 2009), a lower working concentration than that used in this study. CS polysaccharides are a mixture of non-, mono-, and di-sulfated disaccharides, and their functionality depends on their composition, which varies according to their species of origin. Although skate CS polysaccharides contain a higher proportion of CS-C than CS-A, I observed no suppressive effects of H-CSp on the gel-contraction activity of the TIG-113 cells. Skate CS also contains some non- and di-sulfated disaccharides; therefore, the effect of skate CS polysaccharides on gel contraction by fibroblasts may be related to these components.

In this study, the biomacromolecule content (high MWt peptides and CS

polysaccharides) of BP-sCS was almost 80% (Fig. 1). These biomacromolecules display poor bioavailability after oral administration (Shang et al., 2016; cf. Shen et al., 2017), and only hydrophobic molecules with a MWt of < 500 can passively diffuse through the skin (Li et al, 2015). Thus, BP-sCS should be combined with wound dressing materials that act outside the body and are unaffected by the skin or intestinal barriers. In this study, I clarified the interactions between the CS/peptides and skin fibroblasts and demonstrated that BP-sCS could actively promote skin wound healing.

4. Conclusion

This study is the first to compare the chronic wound healing bioactivities of skate H-CSp, type-II CP, and non-collagenous peptides. I found that the type-II CP and non-collagenous peptides displayed antioxidant activities, while H-CSp and type-II CP promoted fibroblast proliferation/metabolism, and non-collagenous peptides stimulated the matrix collagen expression. Therefore, BP-sCS, which is a combined preparation of these three substances, displayed all these activities and could be a superior wound-healing promoter for bioactive wound dressings. Although many studies have reported the activities and applications of CS or peptides as bioactive compounds, none have considered the industrial application of BP-sCS, a low-cost, environmentally friendly product that is uncontaminated with zoonosis pathogens and is subject to no religious

objections. These advantages make BP-sCS a highly competitive potential wound-healing promoter. In the future, *in vivo* studies using the wound-healing dressing or the cream that includes BP-sCS is needed. This study contributes toward a highly efficient, zero-waste fish-processing industry that produces not only foods but also active compounds for human health.

Figures

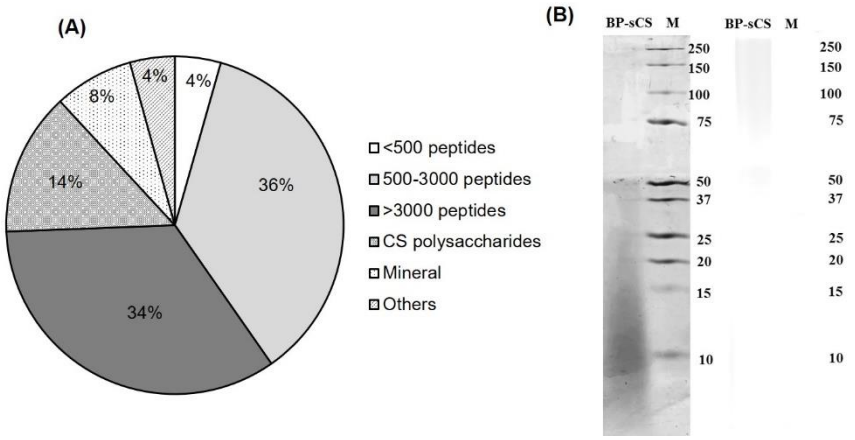


Fig. 1. Composition of the by-products of skate chondroitin sulfate (BP-sCS).

(A) BP-sCS contains CS polysaccharides, peptides, minerals, and others (lipid and water, etc.). The graph also shows the molecular weight distribution of the BP-sCS peptide fractions. (B) Tricine-SDS-PAGE stained with Alcian Blue (right, polysaccharides) and Coomassie Brilliant Blue (CBB; left, peptides). M, protein markers.

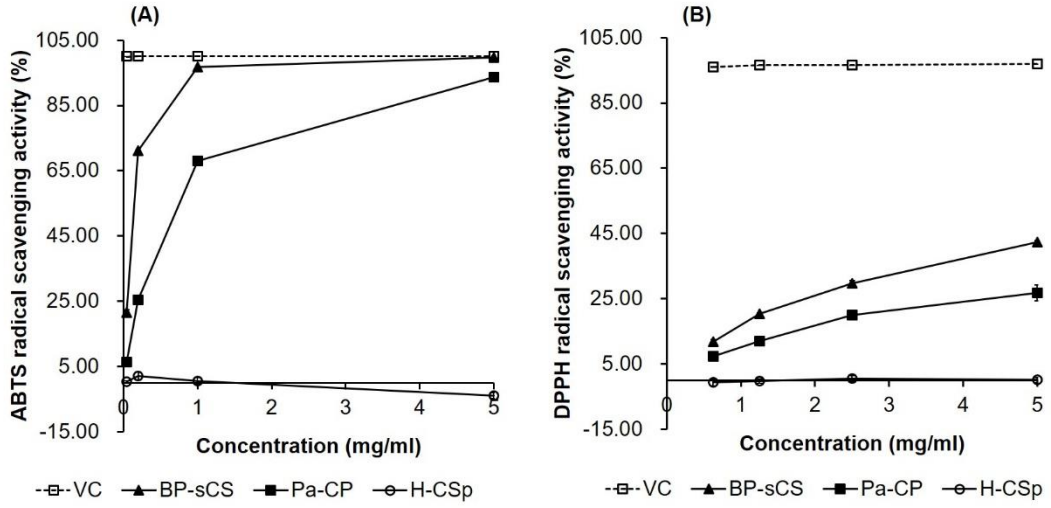


Fig. 2. ABTS (A) and DPPH (B) radical scavenging activities of the by-product of skate chondroitin sulfate (BP-sCS), the papain-hydrolyzed type II collagen peptides (Pa-CP), and the high-purity chondroitin sulfate polysaccharides (H-CSp).

Values have been expressed as the mean ± standard error (n=3).

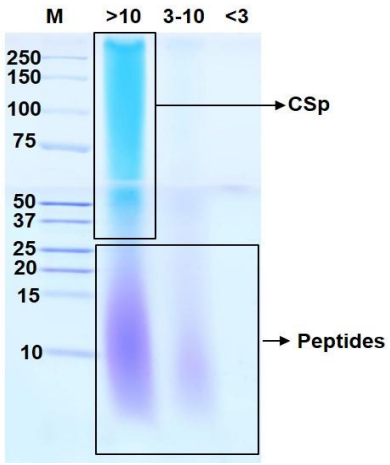


Fig. 3. Alcian blue- and Coomassie Brilliant Blue-stained Tricine-SDS-PAGE of three segments of the by-product of skate chondroitin sulfate (BP-sCS).

M, protein markers; > 10, BP-sCS segment of larger than 10000; 3–10, BP-sCS segment of between 3000 to 10000; < 3, BP-sCS segment of smaller than 3000.

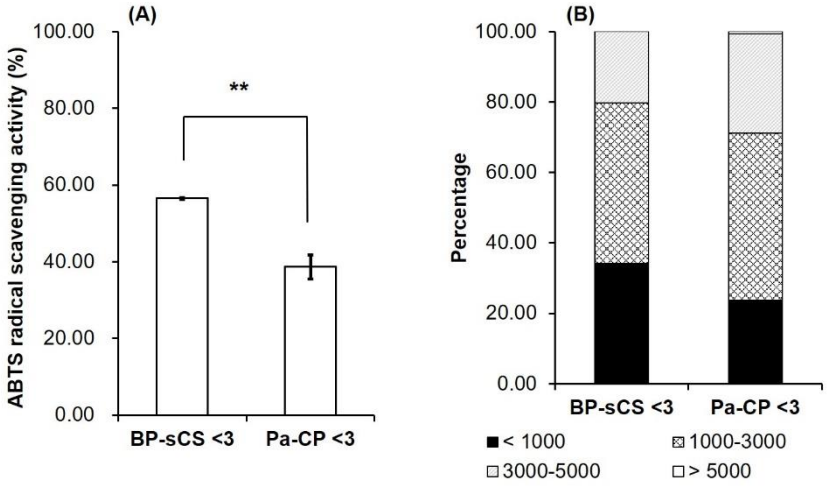


Fig. 4. ABTS radical scavenging activities (A) and molecular weight distributions (B) of < 3000 segments of the by-product of skate chondroitin sulfate (BP-sCS) and the papain-hydrolyzed type II collagen peptides (Pa-CP).

BP-sCS < 3, BP-sCS segment of less than 3000; Pa-CP < 3, Pa-CP segment of less than 3000. Columns and bars indicate the mean value ± standard error (n=3). ** $p < 0.01$, the Student's *t*-test.

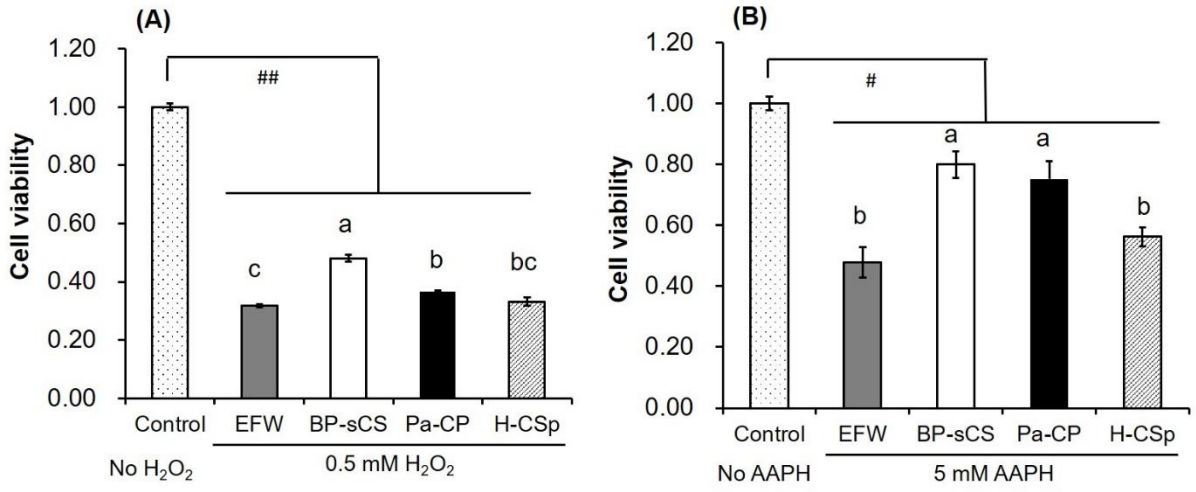


Fig. 5. Effects of the by-product of skate chondroitin sulfate (BP-sCS), the papain-hydrolyzed type II collagen peptides (Pa-CP), and the high-purity CS polysaccharides (H-CSp) against (A) H_2O_2- and (B) AAPH-induced oxidative stress on the L929 fibroblast proliferation/metabolism.

Control groups were not treated with H_2O_2 or AAPH. Oxidative stress was induced in all other groups using H_2O_2 (A) or AAPH (B). The sample concentration was 1000 μg/ml. EFW, endotoxin-free water. Columns and bars indicate the mean value ± standard error (n=12–16). # $p < 0.05$, ## $p < 0.01$ compared to the control group (the Steel-Dwass test). Different letters denote significant differences between groups ($p < 0.05$, the Steel-Dwass test).

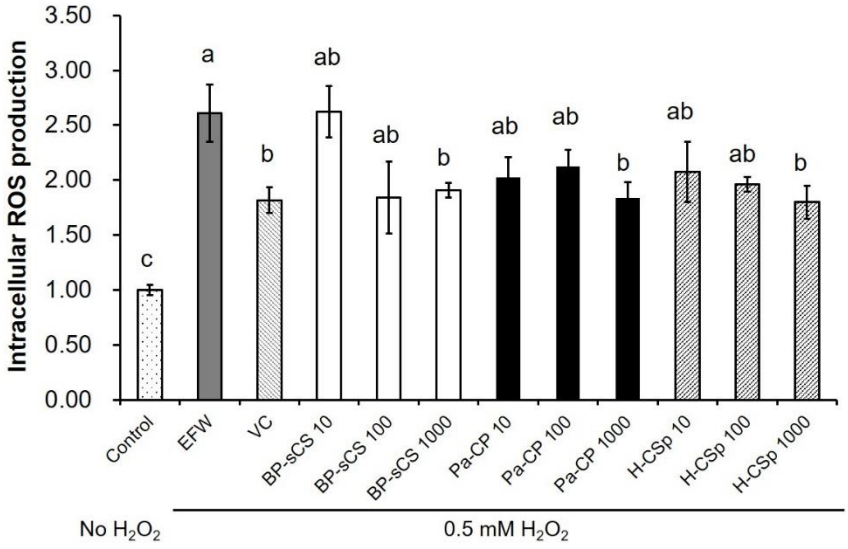


Fig. 6. Effects of the by-product of skate chondroitin sulfate (BP-sCS), the papain-hydrolyzed type II collagen peptides (Pa-CP), and the high-purity CS polysaccharides (H-CSp) on the H_2O_2-induced intracellular ROS production.

Control groups were not treated with H_2O_2. Oxidative stress was induced in all other groups using 0.5 mM H_2O_2. EFW, endotoxin-free water; VC, Vitamin C 200 μg/ml; BP-sCS 10, BP-sCS 10 μg/ml; BP-sCS 100, BP-sCS 100 μg/ml; BP-sCS 1000, BP-sCS 1000 μg/ml; Pa-CP 10, Pa-CP 10 μg/ml; Pa-CP 100, Pa-CP 100 μg/ml; Pa-CP 1000, Pa-CP 1000 μg/ml; H-CSp 10, H-CSp 10 μg/ml; H-CSp 100, H-CSp 100 μg/ml; H-CSp 1000, H-CSp 1000 μg/ml. Columns and bars indicate the mean value ± standard error (n=9–10). Different letters denote significant differences between groups ($p < 0.05$, the Steel-Dwass test).

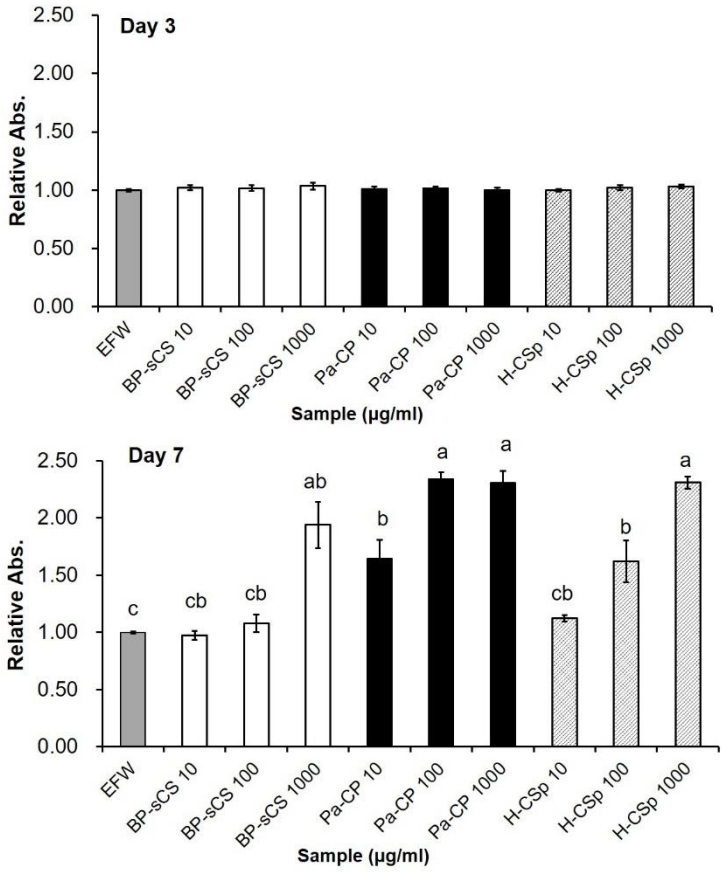


Fig. 7. Effect of the by-product of skate chondroitin sulfate (BP-sCS), the papain-hydrolyzed type II collagen peptides (Pa-CP), and the high-purity CS polysaccharides (H-CSp) on the L929 fibroblast proliferation/cell metabolism.

Values have been expressed relative to the corresponding endotoxin-free water (EFW) control. BP-sCS 10, BP-sCS 10 µg/ml; BP-sCS 100, BP-sCS 100 µg/ml; BP-sCS 1000, BP-sCS 1000 µg/ml; Pa-CP 10, Pa-CP 10 µg/ml; Pa-CP 100, Pa-CP 100 µg/ml; Pa-CP 1000, Pa-CP 1000 µg/ml; H-CSp 10, H-CSp 10 µg/ml; H-CSp 100, H-CSp 100 µg/ml; H-CSp 1000,H-CSp 1000 µg/ml. Columns and bars indicate the mean value ± standard error (n=6). Different letters denote significant differences between groups ($p < 0.05$, the Steel-Dwass test).

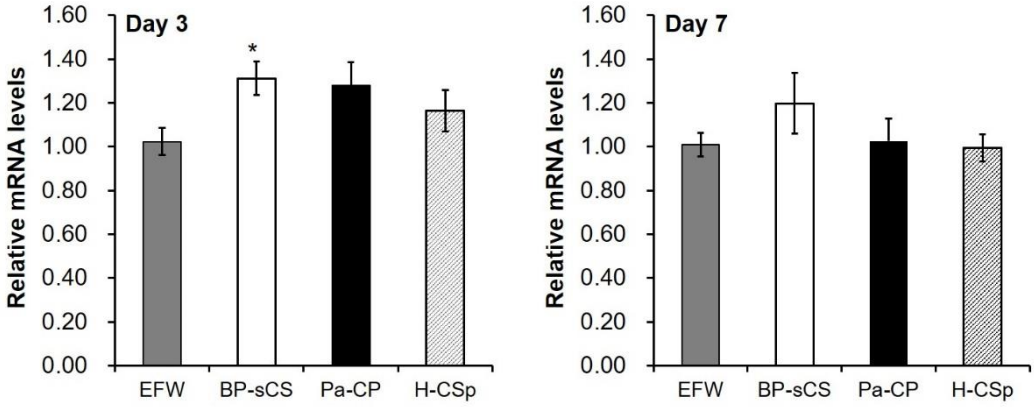


Fig. 8. Effect of the by-product of skate chondroitin sulfate (BP-sCS), the papain-hydrolyzed type II collagen peptides (Pa-CP), and the high-purity CS polysaccharides (H-CSp) on collagen mRNA expression in the L929 fibroblasts.

Values have been normalized to the internal control (*Gapdh*) and expressed relative to the corresponding endotoxin-free water (EFW) control. Sample concentration, 1000 μg/ml. Columns and bars indicate the mean value ± standard error (n=11–12). * $p < 0.05$, compared to the EFW control group (the Dunnett's test).

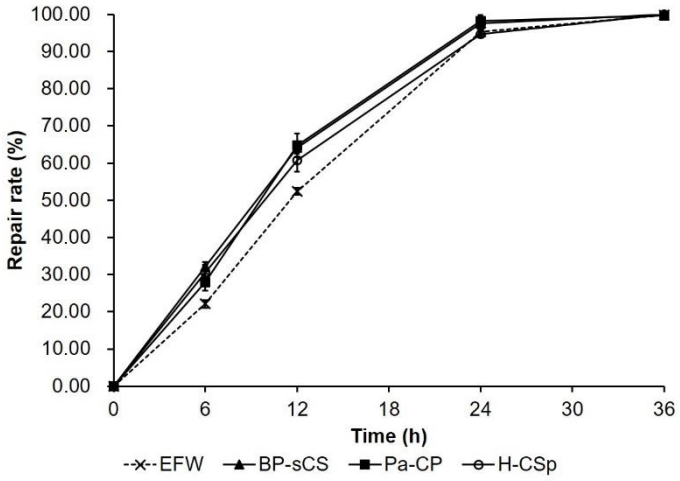


Fig. 9. Effect of the by-product of skate chondroitin sulfate (BP-sCS), papain-hydrolyzed type II collagen peptides (Pa-CP), and high purity CS polysaccharides (H-CSp) on L929 fibroblast migration and wound closure.

Control, EFW (endotoxin-free water) group. Sample concentration, 1000 μg/ml. Values are expressed as the mean ± standard error (n=5–6).

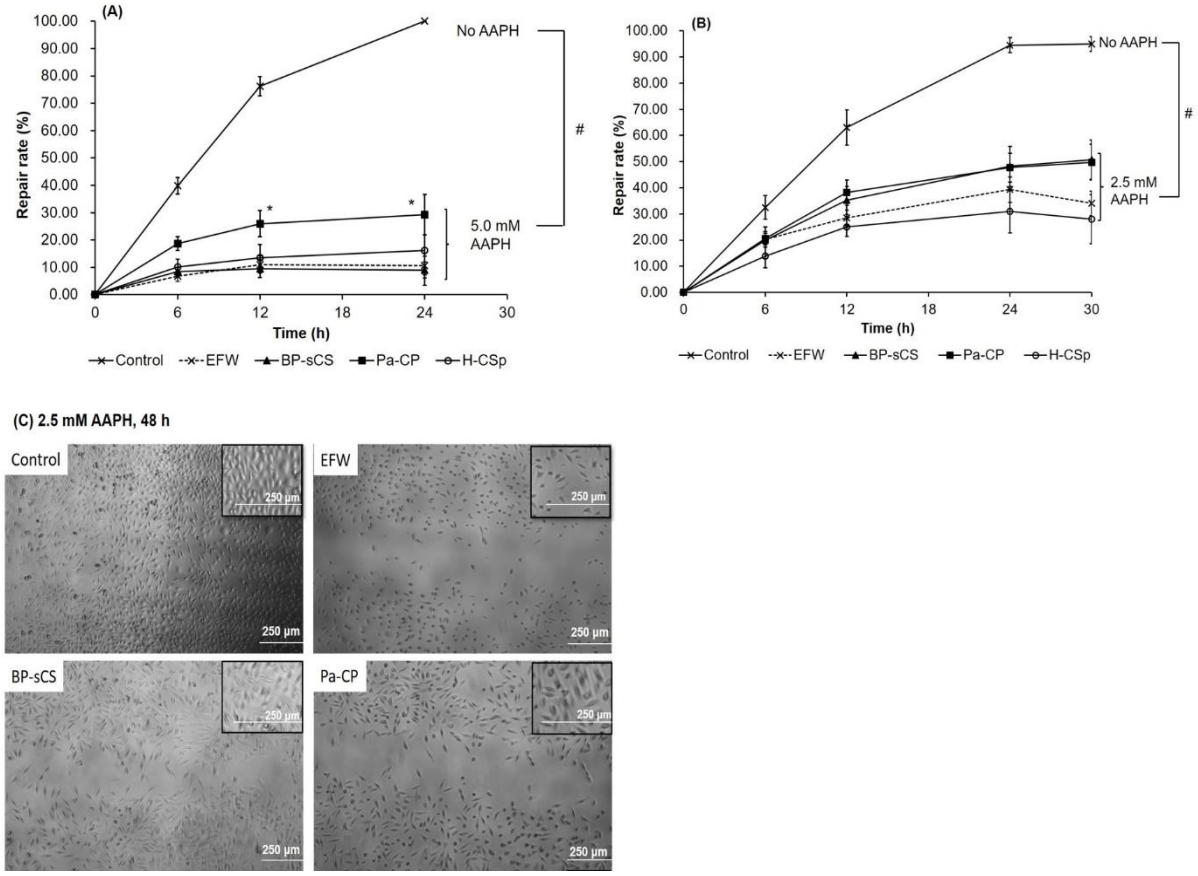


Fig. 10. Effect of the by-product of skate chondroitin sulfate (BP-sCS), the papain-hydrolyzed type II collagen peptides (Pa-CP), and the high-purity CS polysaccharides (H-CSp) on the L929 fibroblast migration and wound closure under an AAPH-induced oxidative stress.

(A, B) The control group was not treated with AAPH. All other groups were treated with 5.0 mM (A) or 2.5 mM (B) AAPH. Samples concentration, 1000 μg/ml. Values have been expressed as the mean ± standard error (n=5–6). # $p < 0.05$ compared to the control group (no AAPH; the Dunnett's test). *$p < 0.05$ compared to the endotoxin-free water (EFW) group (the Dunnett's test). (C) Photomicrographs of the L929 fibroblasts at 48 h in the scratch assay. Control, no AAPH; EFW, EFW with 2.5 mM AAPH; BP-sCS, 1000 μg/ml of BP-sCS with 2.5 mM AAPH; Pa-CP, 1000 μg/ml of Pa-CP with 2.5 mM AAPH. Bars, 250 μm in photos and enlarged photos.

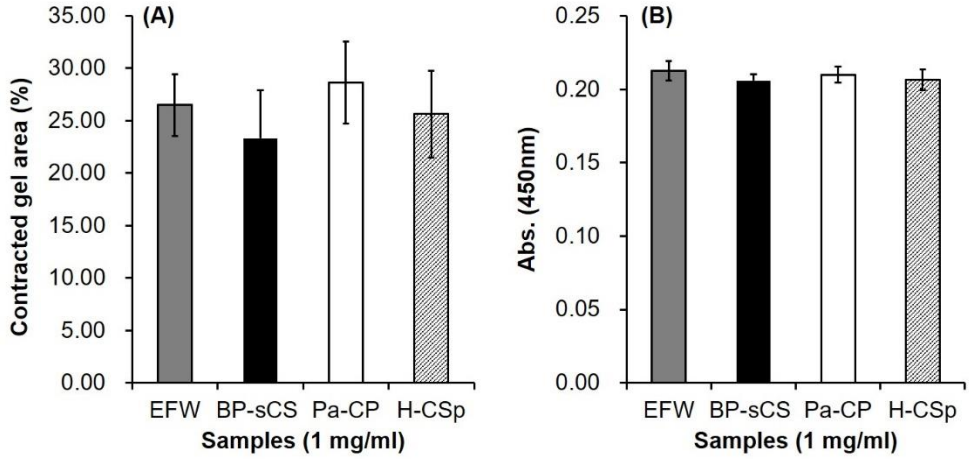


Fig. 11. Effect of the by-product of skate chondroitin sulfate (BP-sCS), the papain-hydrolyzed type II collagen peptides (Pa-CP), and the high-purity CS polysaccharides (H-CSp) on gel contraction (A) and cell proliferation/metabolism (B).

EFW, endotoxin-free water. Sample concentration, 1000 µg/ml. Columns and bars show the mean value ± standard error (n=4 in A and n=8 in B).

Chapter V

General discussion

In order to diversify skate-cartilage products, this thesis revealed the new biological activities of compounds contained in the cartilage of *Raja pulchra*. The significant findings of the studies in this thesis are as follows:

1) Skate CS has an anti-obesity activity.

Both CS polysaccharides and oligosaccharides suppressed pancreatic lipase activity as well as proliferation and lipid accumulation in mature adipocytes. Dietary intake of CS oligosaccharides could ameliorate obesity in the high-fat diet mice model. It prevented gaining in body weight, liver weight and adipose tissue weight, maintained lower food consumption, inhibited intestinal absorption of triglyceride, and adjusted the serum endotoxin level. The MWt of the CS affected the CS mode of action: CS polysaccharides had stronger lipase inhibitory activity, whereas CS oligosaccharides suppressed adipocyte lipid accumulation at a lower dose. Thus, a formulation containing both CSs may be more effective as an anti-obesity functional food.

2) Both type II collagen (C-II) peptides and thermally hydrolyzed CS oligosaccharides have antioxidant activity.

High free radical scavenging activity was observed in the < 3000 segment of the papain-hydrolyzed C-II peptides (Pa-CP) and thermally hydrolyzed CS oligosaccharides (CSo). The activity of CSo was mainly due to the intermediate and final products of the non-enzymatic browning reaction that occurred during the high-temperature hydrolysis. Furthermore, Pa-CP and CSo did not show cytotoxicity. Taken together, Pa-CP and CSo may act as antioxidants for functional foods owing to their high intestinal absorptivity.

3) The by-product of skate CS production (BP-sCS) could promote wound healing under oxidative stress.

BP-sCS showed free radical scavenging activity, protected fibroblast from oxidative stress, scavenged intracellular ROS, promoted fibroblast proliferation/metabolism, stimulated collagen synthesis by fibroblasts, and had no adverse effects on fibroblast migration and gel contraction. In addition, BP-sCS counteracted AAPH-induced oxidative stress damage that inhibited fibroblast migration. These effects of BP-sCS were due to cooperation among its ingredient biomacromolecules: C-II peptides, non-collagenous peptides, and CS polysaccharides. These findings indicate that BP-sCS could be a novel and superior wound-healing promoter for bioactive wound dressings.

The difficulty of commercial usage of fish by-products is the insufficient amount

of high-quality by-products and high costs for their supply (cf. Olsen et al., 2014). The realization of fish by-product usage needs the change of the entire supply chain to the one that includes the deep-processing of by-products. Although the commercial production of skate-CS containing functional foods for healthier joints has already implemented, present studies suggest that diversification of products having different functionality is possible. Here, three key aspects, sustainable skate production, the new fish-processing model, and the market demand, are discussed toward the future realization of more efficient usage of skate cartilage. After that, I discuss the general significance and influences of the fish cartilage products for our society.

1. Three key aspects toward the future realization of more efficient usage of skate cartilage by-products

1.1. Skate production and its sustainability

Sustainable fishery of skate is the prerequisite for the sustainable development of skate cartilage industry. However, in general, the low fecundity of cartilaginous fish makes low rates of population increase and low capacity of recovering from overfishing (Cavanagh & Gibson, 2007); and thus, precise resource management of skate species is required for their sustainable fisheries. For example, *Raja pulchra*, the major target of

the skate fisheries in Hokkaido, is oviparous, with a single egg capsules having multiple embryos (1–7) (Horimoto, 2020). The mature females produce only 200–500 egg capsules in one year (Horimoto, 2020). Due to overfishing, the catch of *R. pulchra* in Korea has been reduced by 90% in recent years, and the recovery from the overfishing is slow (Horimoto, 2020). The total skate catch of Hokkaido increased in 2016 and kept more than 800 tons from 2016 to 2018 (Horimoto, 2020). Therefore, its strict resource management is preferable in Hokkaido (Horimoto, 2020).

1.2. New fish-processing model to use up by-products toward the zero-discard

To realize further development of skate cartilage industry, the present fish processing model must be re-developed from the basis. As a first step, proper planning in the fish processing industry, to integrate the production of both primary products (usually fish meat) and secondary products (those from by-products), is essential, and this should cover the whole supply chain. The traditional fish processing factory has a primary product, and by-products (mixtures of non-edible parts) that are discarded; however, the latter could be treated as in-house sideline products or as new products for down-stream processing factories. Here I discuss four key elements necessary to implement this plan: zero-discard principle, sorting and grading of by-products, innovation in processing technology, and diversification of outputs.

The principle of zero-discard, which considers processing of the mainstream products and sideline cartilage by-products as a whole to exploit the entire fish body, is essential. Since fish by-products, including cartilage, quickly deteriorate, the processing of by-products sequentially after their production is desirable. For example, streamlined modern facilities for seafood processing have been successfully built in Norway (cf. Olsen et al., 2014; Stevens et al., 2018). They can manage over 650,000 tons of seafood by-products each year (Stevens et al., 2018). The sideline products in the Norwegian salmon industry include silage (animal feeds), fish oil, and protein hydrolysates (cf. Rustad et al., 2011; Stevens et al., 2018). Efficiency is maximized by the transportation of by-products directly from the slaughter line to the oil factory within hours (cf. Rustad et al., 2011). The processing expertise, technology, and infrastructure of the poultry industry provide useful insights for the aquaculture industry (cf. Jayathilakan et al., 2012; Stevens et al., 2018).

The value of food-grade by-products, such as those used directly for human consumption or for the extraction of bioactive compounds, is high (cf. Olsen et al., 2014). Therefore, sorting and grading of by-products is required during processing since by-products that are low-grade can only be used as hydrolysates or animal feeds, products that are much less profitable. As already stated in this study, cartilage, which contains multiple bioactive compounds, is a highly valuable by-product, and its separation from other by-products is essential. After sorting and grading, different types

of by-product are collected for potential conversion into multiple other products (Jayathilakan et al., 2012; Stevens et al., 2018). Unfortunately, most current by-product processing lines lack sorting and grading.

An appropriate by-product processing strategy is also crucial. Industrial production technologies should be low cost, high-efficiency, scalable, and environmentally friendly. For instance, large volumes of strong alkali or acid solution and chromatographic technologies are very challenging in use (cf. Vázquez et al., 2013). In contrast, the use of industrially available cheap enzymes, hydrothermal treatments (such as critical- or subcritical-water treatment), and membrane separation are more suitable technologies in large scale production.

The ideal model of fish processing is that a diverse range of products is produced from a single species, and sustainability is sought throughout the value chain. Stevens et al. (2018) reported that if maximizing by-product usage for human consumption the Scottish Atlantic salmon industry could increase food production from fish farming by over 60% in the UK. The resulting by-products could increase revenue by 803% and the industry bottom-line by over 5% without inputting more resources (Stevens et al., 2018). Other than as foods, salmon by-products could be processed into high-value consumables for human use, such as protein powder and hydrolysates, oil supplements, collagen and gelatin, polyunsaturated fatty acids, pharmaceutical products, and others (Stevens et al., 2018). CS and C-II could be obtained from salmon nasal cartilage, the

major by-product of the salmon industry. In the case of fish cartilage by-products, the co-production of CS and peptides would be an excellent strategy to maximize output; Shen et al. (2019) liquefied chicken sternal cartilage using hydrothermal treatment, hydrolyzed this using trypsin and papain, and separated CS and peptides using a membrane ultrafiltration system.

By introducing these four elements, I propose an ideal skate-cartilage processing flow (Fig. 1). In the skate-processing factory, fins are processed as the primary product (food), and other parts, including head, axial skeleton, viscera, skin, and blood, are obtained as by-products. The by-products are sorted and graded in the slaughter line. After the sorting, cartilage is transferred from the slaughter line to the sideline. At the same time, other by-products (skin, viscera, and blood) are also transferred to another sideline or down-stream processing factory.

The cartilage sideline branches into two ways. On the one way, CS polysaccharides are extracted and purified. The by-product of this step is BP-sCS and used as a wound-healing promoter for the bioactive wound dressing. CS oligosaccharides are produced from CS polysaccharides by thermal hydrolysis. Both CS polysaccharides and oligosaccharides are used as functional foods for healthier joints and anti-obesity. CS oligosaccharides can also be applied as antioxidant functional foods. On the other way, C-II is extracted and purified and then hydrolyzed to obtain collagen peptides. The by-products of this way contain CS polysaccharides and peptides of non-collagenous

proteins, but further studies are needed to realize the utilization of these by-products. As a result, diversified products (fins, CS, BP-sCS, C-II, and C-II peptides) will make the high efficiency of the skate-processing industry.

1.3. Market demand

An aging population is becoming a global issue. With aging, increasing numbers of people will suffer degenerative diseases, such as RA, Parkinson's disease, and Alzheimer's disease. As already shown in Chapter I, fish-cartilage products show high bioactivity for the treatment of degenerative diseases. For example, oral administration of fish-cartilage supplements (CS, C-II, or proteoglycans) improves arthritis symptoms (Trentham et al., 1993; Volpi, 2002). Fish-derived CS has the potential to be used as a treatment for diseases of the CNS due to its neuroprotective effects (Hashiguchi et al., 2011). Biomaterials for regenerative medicine also have enormous potential against degenerative diseases; for cartilage and bone regenerative medicine, fish C-II, CS, and their hybrid materials show great potential (Jeevithan et al., 2018; Varghese et al., 2008). Clarification of the functionality of skate C-II and CS as biomaterials for cartilage and bone regenerative medicine remains as a big challenge in the future.

Chronic diseases, such as obesity and hypertension, are also a growing threat to public health. Fish-cartilage products can be functional foods for chronic health

problems. Shark and sturgeon CSs have antithrombotic activity suitable for the prevention and treatment of thromboembolic diseases (Gui et al., 2015; Krichen et al., 2018). Skate (Chapter II) and salmon CSs (Han et al., 2000) have anti-obesity activity, which is worthy of anti-obesity functional foods. Fish cartilage CS and C-II including skate CS oligosaccharides and C-II peptides have antioxidant activity (Chapters III and IV; Ajisaka et al., 2016; Jeevithan et al., 2015), suggesting their suitability as antioxidants in health supplements or cosmetics.

The aging population and increases in degenerative and chronic diseases will stimulate the rapid growth of market demand for cartilage products. For instance, potential growth in the CS market has been predicted at 10% annually (Restaino et al., 2019). Moreover, fish-derived bioactive compounds are becoming increasingly popular due to their high safety and activity (cf. Schiraldi et al., 2010; cf. Subhan 2015). It seems inevitable that market demand for fish cartilage products will increase dramatically in the future; therefore, future research should be directed towards the development of high-quality cartilage products from fish by-products.

2. Significance and influences of fish-cartilage products for our society

Usage of fish-derived cartilage has high significance for tackling world problems. The bioactivity of fish cartilage products contributes to treatment of human health

problems as described above. Wise use of cartilage by-products is a "trash to treasure" transformation beneficial to the sustainable development of our society.

Fish cartilage products could contribute to improving the economic condition of poor households through livelihood diversification and income generation. If fish-cartilage processing forms an industrial chain from farming to market, it can influence related fishery or aquaculture industry. Extended downstream processing can develop the fish processing industry into the biotechnology industry. Such an industrial transformation is a way of increasing the income of fishery and aquaculture practitioners. The present experiments in this thesis clearly showed the possibility of the transformation of skate-processing industry in northern Hokkaido into the biotechnology industry that provides high-value products for human health.

The transformation of the aquaculture and fishery industries is in line with government policy in many countries. In the Thirteenth Five-Year Plan for Economic and Social Development (2016–2020) in China, the Chinese government planned a substantial reduction in the amount of capture fisheries, a decrease in the growth rate of aquaculture production in the country, and a transformation and upgrade of the fisheries and aquaculture sector (FAO 2018). The plan aims to improve product quality and to optimize the industry structure, including the processing sector. In Europe, the downstream processing of fisheries by-catch is encouraged by governments (Sotelo et al., 2016; Vázquez et al., 2018). Industry transformation is dependent on innovations in

fish utilization and processing. In many countries, innovations are being made in areas like processing and packaging technology, the efficient use of raw materials, and product diversification (FAO, 2018).

Moreover, new industries can activate regional areas economically. In Japan, young people are pouring into big cities like Tokyo, due to weaker regional economic conditions. Population loss, especially of young people, further weakens regional economies. This negative cycle will eventually lead to the decline of local towns, as witnessed in New Zealand and Germany (Lovell et al., 2018; Wirth et al., 2016). The traditional fisheries industries, such as fishing and aquaculture, have limited appeal to young people and are less profitable. Developing high value-added and high-technology new industries can create new jobs and high profits, attract talent inflow, and activate the local economy. Material fish of the present studies came from northern Hokkaido, where is one of the most severe regions of decreasing population in Japan. The data of the present experiments in this thesis are likely to be beneficial for activating the local economy there.

In conclusion, the present thesis clarified new bioactivities of skate cartilage by-products and assessed their possible applications. Skate by-products are low-cost, environmentally friendly, no contamination with zoonosis, and no religious objections. These advantages indicate that skate by-products could be competitive, valuable

products. The present thesis will be beneficial to achieve the zero-discard, highly efficient skate-processing industry that will activate the regional economy in the future.

Figure

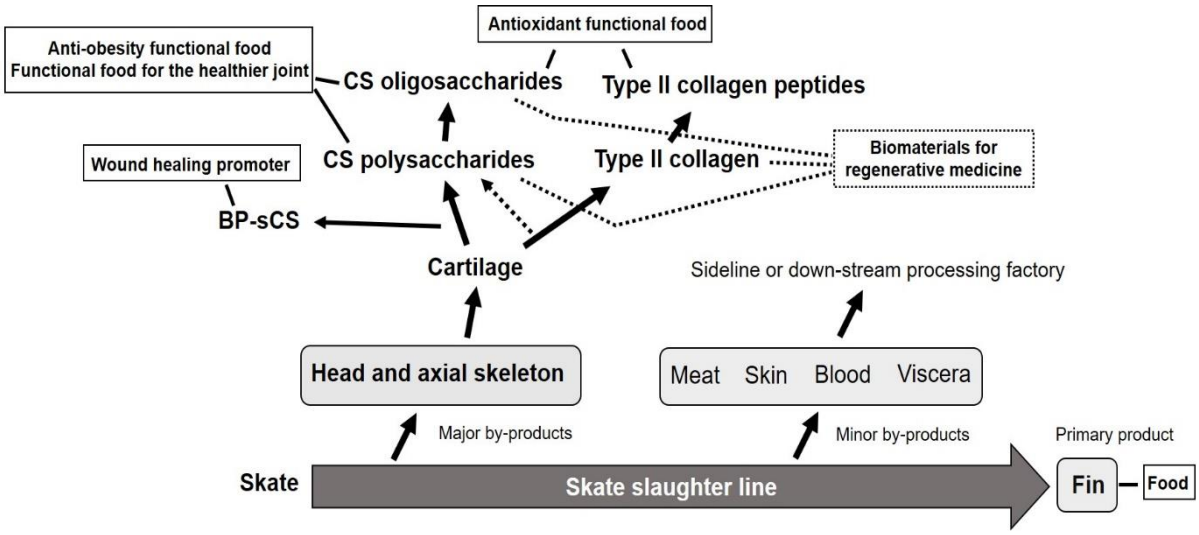


Fig. 1. Proposed skate-cartilage processing flow chart

Dotted lines and the dotted arrow indicate future tasks.

References

Agrawal, H., Joshi, R., Gupta, M., 2019. Purification, identification and characterization of two novel antioxidant peptides from finger millet (*Eleusine coracana*) protein hydrolysate. Food Res. Int., 120, 697–707.

Ahmed, T. A., Suso, H. P., Maqbool, A., Hincke, M. T., 2019. Processed eggshell membrane powder: Bioinspiration for an innovative wound healing product, Mat. Sci. Eng. C, 95, 192–203.

Ahn, C. B., Je, J. Y., Cho, Y. S., 2012. Antioxidant and anti-inflammatory peptide fraction from salmon by-product protein hydrolysates by peptic hydrolysis, Food Res. Int., 49, 92–98.

Ajandouz, E. H., Tchiakpe, L. S., Ore, F. D., Benajiba, A., Puigserver, A., 2001. Effects of pH on caramelization and Maillard reaction kinetics in fructose-lysine model systems. J. Food Sci., 66, 926–931.

Ajisaka, K., Oyanagi, Y., Miyazaki, T., Suzuki, Y., 2016. Effect of the chelation of metal cation on the antioxidant activity of chondroitin sulfates. Biosci. Biotech. Bioch., 80, 1179–1185.

Alvarez-Suarez, J. M., Giampieri, F., Cordero, M., Gasparrini, M., Forbes-Hernández, T. Y., Mazzoni, L., Afrin, S., Beltran-Ayala, P., Gonzalez-Paramas, A. M., Santos-Buelga, C., Varela-Lopez, A., Quiles, J. L., Battion, M., 2016. Activation of AMPK/Nrf2 signalling by Manuka honey protects human dermal fibroblasts

against oxidative damage by improving antioxidant response and mitochondrial function promoting wound healing. J. Funct. Foods, 25, 38–49.

Amiri, A., Memarpoor-Yazdi, M., Shanbedi, M., Eshghi, H., 2013. Influence of different amino acid groups on the free radical scavenging capability of multi walled carbon nanotubes. J. Biomed. Mater. Res. Part A, 101, 2219–2228.

Arai, H., Kashiwagi, S., Nagasaka, Y., Uchida, K., Hoshii, Y., Nakamura, K., 1999. Oxidative modification of apolipoprotein E in human very-low-density lipoprotein and its inhibition by glycosaminoglycans. Arch. Biochem. Biophys., 367, 1–8.

Arima, K., Fujita, H., Toita, R., Imazu-Okada, A., Tsutsumishita-Nakai, N., Takeda, N., Nakao, Y., Wang, H., Kawano, M., Matsushita, K., Tanaka, H., Morimoto, S., Nakamura, A., Kitagaki, M., Hieda, Y., Hatto, R., Watanabe, A., Yumura, T., Okuhara, T., Hayashi, H., Shimizu, K., Nakayama, K., Masuda, S., Ishihara, Y., Yoshioka, S., Yoshioka, S., Shirade, S., Tanaka, H., 2013. Amounts and compositional analysis of glycosaminoglycans in the tissue of fish. Carbohyd. Res., 366, 25–32.

Asano, K., Yoshimura, S., Nakane, A., 2013. Alteration of intestinal microbiota in mice orally administered with salmon cartilage proteoglycan, a prophylactic agent. PLoS One, 8, e75008.

Barnett, M. L., Kremer, J. M., St. Clair, E. W., Clegg, D. O., Furst, D., Weisman, M., Fletcher, M. J. F., Chasan-Taber, S., Finger, E., Morales, A., Le, C. H., 1998.

Treatment of rheumatoid arthritis with oral type II collagen: results of a multicenter, double-blind, placebo-controlled trial. Arth. Rheum., 41, 290–297.

Bastos, D. H. M., Gugliucci, A., 2015. Contemporary and controversial aspects of the Maillard reaction products. Curr. Opin. Food Sci., 1, 13–20.

Benjakul, S., Karnjanapratum, S., Visessanguan, W., 2018. Hydrolysed collagen from *Lates calcarifer* skin: its acute toxicity and impact on cell proliferation and collagen production of fibroblasts. Int. J. Food Sci. Tech., 53, 1871–1879.

Benjakul, S., Visessanguan, W., Phongkanpai, V., Tanaka, M., 2005. Antioxidative activity of caramelisation products and their preventive effect on lipid oxidation in fish mince. Food Chem., 90, 231–239.

Birk, D. E., Silver, F. H., 1984. Collagen fibrillogenesis in vitro: comparison of types I, II, and III. Arch. Biochem. Biophys. 235, 178–185.

Bjornsson, T. D., Nash, P. V., Schaten, R., 1982. The anticoagulant effect of chondroitin-4-sulfate. Thromb. Res. 27, 15–21.

Blanco, M., Fraguas, J., Sotelo, C., Pérez-Martín, R., Vázquez, J., 2015. Production of chondroitin sulphate from head, skeleton and fins of *Scyliorhinus canicula* by-products by combination of enzymatic, chemical precipitation and ultrafiltration methodologies. Mar. drugs, 13, 3287–3308.

Boateng, J. S., Matthews, K. H., Stevens, H. N., Eccleston, G. M., 2008. Wound healing dressings and drug delivery systems: a review. J. Pharm. Sci., 97, 2892–2923.

Bronzi, P., Chebanov, M., Michaels, J. T., Wei, Q., Rosenthal, H., Gessner, J., 2019. Sturgeon meat and caviar production: Global update 2017. J. Appl. Ichthyol., 35, 257–266.

Broughton, G., Janis, J. E., Attinger, C. E., 2006. The basic science of wound healing, Plast. Reconstr. Surg., 117, 12S–34S.

Brown, R. A., 2013. In the beginning there were soft collagen-cell gels: towards better 3D connective tissue models? Exp. Cell Res., 319, 2460–2469.

Bu, Y., Elango, J., Zhang, J., Bao, B., Guo, R., Palaniyandi, K., Rohinson, J. S., Geevaretuam, J., Regenstein, J. M., Wu, W., 2017. Immunological effects of collagen and collagen peptide from blue shark cartilage on 6T-CEM cells. Process Biochem., 57, 219–227.

Calderon, L., Collin, E., Murphy, M., O'Halloran, D., Pandit, A., 2010. Type II collagen-hyaluronan hydrogel-a step towards a scaffold for intervertebral disc tissue engineering. Eur. Cells Mater., 20, 134–148

Calvo, J. C., Rodbard, D., Katki, A., Chernick, S., Yanagishita, M., 1991. Differentiation of 3T3-L1 preadipocytes with 3-isobutyl-1-methylxanthine and dexamethasone stimulates cell-associated and soluble chondroitin 4-sulfate proteoglycans. J. Biol. Chem., 266, 11237-11244.

Campo, G. M., Avenoso, A., Campo, S., Ferlazzo, A. M., Calatroni, A., 2006. Antioxidant activity of chondroitin sulfate. Adv. Pharmacol., 53, 417–431.

Canas, N., Valero, T., Villarroya, M., Montell, E., Verges, J., García, A. G., Lopez, M. G., 2007. Chondroitin sulfate protects SH-SY5Y cells from oxidative stress by inducing heme oxygenase-1 via phosphatidylinositol 3-kinase/Akt. J. Pharmacol. Exp. Ther., 323, 946–953.

Cantley, M. D., Rainsford, K. D., Haynes, D. R. 2013. Comparison of the ability of chondroitin sulfate derived from bovine, fish and pigs to suppress human osteoclast activity *in vitro*. Inflammo. Pharmacol., 21, 407–412.

Cani, P. D., Possemiers, S., Van de Wiele, T., Guiot, Y., Everard, A., Rottier, O., Geurts, L., Naslain, D., Neyrinck, A., Lambert, D. M., Muccioli, G. G., Delzenne1, N. M., 2009. Changes in gut microbiota control inflammation in obese mice through a mechanism involving GLP-2-driven improvement of gut permeability. Gut, 58, 1091–1103.

Cao, H., Shi, F. X., Xu, F., Yu, J. S., 2013. Molecular structure and physicochemical properties of pepsin-solubilized type II collagen from the chick sternal cartilage. Eur. Rev. Med. Pharmacol. Sci., 17, 1427–1437.

Cao, H., Xu, S. Y., 2008. Purification and characterization of type II collagen from chick sternal cartilage. Food Chem., 108, 439–445.

Cavanagh, R. D., Gibson, C. 2007. Overview of the conservation status of cartilaginous fishes (chondrichthyans) in the Mediterranean Sea. IUCN, Gland, Switzerland and Malaga, Spain. vi + 42 pp.

Chai, H. J., Wu, C. J., Yang, S. H., Li, T. L., Pan, B. S., 2016. Peptides from hydrolysate of lantern fish (*Benthosema Pterotum*) proved neuroprotective *in vitro* and *in vivo*. J. Funct. Foods, 24, 438–449.

Chai, H. J., Li, J. H., Huang, H. N., Li, T. L., Chan, Y. L., Shiau, C. Y., Wu, C. J., 2010. Effects of sizes and conformations of fish-scale collagen peptides on facial skin qualities and transdermal penetration efficiency. J. BioMed Res., 2010, 757301.

Chen, L., Bao, B., Wang, N., Xie, J., Wu, W., 2012. Oral administration of shark type II collagen suppresses complete Freund's adjuvant-induced rheumatoid arthritis in rats. Pharmaceuticals, 5, 339–352.

Cho, Y. G., Cho, M. L., Min, S. Y., Kim, H. Y., 2007. Type II collagen autoimmunity in a mouse model of human rheumatoid arthritis. Autoimmun. Rev., 7, 65–70.

Cowman, M. K., Slahetka, M. F., Hittner, D. M., Kim, J., Forino, M., Gadelrab, G., 1984. Polyacrylamide-gel electrophoresis and Alcian Blue staining of sulphated glycosaminoglycan oligosaccharides. Biochem. J., 221, 707–716.

Cumming, M. H., Hall, B., Hofman, K., 2019. Isolation and characterisation of major and minor collagens from hyaline cartilage of Hoki (*Macruronus novaezelandiae*). Mar. drugs, 17, 223–239.

Dai, M., Sui, B., Xue, Y., Liu, X., Sun, J., 2018. Cartilage repair in degenerative osteoarthritis mediated by squid type II collagen via immunomodulating activation of M2 macrophages, inhibiting apoptosis and hypertrophy of

chondrocytes. Biomaterials, 180, 91–103.

Dhivya, S., Padma, V. V., Santhini, E., 2015. Wound dressings – a review, BioMed., 5, 22–27.

Egea, J., García, A. G., Verges, J., Montell, E., López, M. G., 2010. Antioxidant, antiinflammatory and neuroprotective actions of chondroitin sulfate and proteoglycans. Osteoarthr. Cartilage, 18, S24–S27.

FAO, 2014. International plan of action for conservation and management of sharks, http://www.fao.org/ipoa-sharks/en/

FAO, 2016. The state of world fisheries and aquaculture. http://www.fao.org/state-of-fisheries-aquaculture

FAO, 2018. The state of world fisheries and aquaculture. http://www.fao.org/3/i9540en/i9540en.pdf

FAO, Cultured Aquatic Species Information Programme. http://www.fao.org/fishery/culturedspecies/Salmo_salar/en

Farrugia, T. J., Oliveira, A. C., Knue, J. F., Seitz, A. C., 2015. Nutritional content, mercury, and trace element analyses of two skate (*Rajidae*) species in the Gulf of Alaska. J. Food Compos. Anal., 42, 152–163.

Felician, F. F., Xia, C., Qi, W., Xu, H., 2018. Collagen from marine biological sources and medical applications. Chem. Biodiverse., 15, e1700557.

Fertala, A., Sieron, A. L., Hojima, Y., Ganguly, A., Prockop, D. J., 1994. Self-assembly

into fibrils of collagen II by enzymic cleavage of recombinant procollagen II. Lag period, critical concentration, and morphology of fibrils differ from collagen I. J. Biol. Chem. 269, 11584–11589.

Ferraro, V., Cruz, I. B., Jorge, R. F., Malcata, F. X., Pintado, M. E., Castro, P. M., 2010. Valorisation of natural extracts from marine source focused on marine by-products: A review. Food Res. Int., 43, 2221–2233.

Francioli, S. E., Candrian, C., Martin, K., Heberer, M., Martin, I., Barbero, A., 2010. Effect of three-dimensional expansion and cell seeding density on the cartilage-forming capacity of human articular chondrocytes in type II collagen sponges. J. Biomed. Mater. Res. A, 95, 924–931.

Garza, A. L., Milagro. F., Boque N., Campión. J., Martínez. J., 2011. Natural inhibitors of pancreatic lipase as new players in obesity treatment. Planta Med., 77, 773–785.

Gao, Y., Li, B., Kong, W., Yuan, L., Guo, L., Li, C., Fan, H., Fan, Y., Zhang, X., 2018. Injectable and self-crosslinkable hydrogels based on collagen type II and activated chondroitin sulfate for cell delivery. Int. J. Biol. Macromol., 118, 2014–2020.

Gui, M., Song, J., Zhang, L., Wang, S., Wu, R., Ma, C., Li, P., 2015. Chemical characteristics and antithrombotic effect of chondroitin sulfates from sturgeon skull and sturgeon backbone. Carbohyd. Polym., 123, 454–460.

Halim, N. R. A., Yusof, H. M., Sarbon, N. M., 2016. Functional and bioactive properties of fish protein hydrolysates and peptides: A comprehensive review. Trends Food

Sci. Tech., 51, 24–33.

Hall, B.,1982. Bone in the cartilaginous fishes. Nature, 298, 324–324.

Han, G., Ceilley, R., 2017. Chronic wound healing: a review of current management and treatments, Adv. Ther., 34, 599–610.

Han, L. K., Kimura, Y., Okuda, H., 1999. Reduction in fat storage during chitin-chitosan treatment in mice fed a high-fat diet. Int. J. Obesity, 23, 174–179.

Han, L. K., Sumiyoshi, M., Takeda, T., Chihara, H., Nishikiori, T., Tsujita, T., Kimura, Y., Okuda, H., 2000. Inhibitory effects of chondroitin sulfate prepared from salmon nasal cartilage on fat storage in mice fed a high-fat diet. Int. J. Obesity, 24, 1131–1138.

Han, L. K., Sumiyoshi, M., Takeda, T., Chihara, H., Nishikiori, T., Tsujita, T., Kimura, Y., Okuda, H., 2000. Inhibitory effects of chondroitin sulfate prepared from salmon nasal cartilage on fat storage in mice fed a high-fat diet. Int. J. Obesity, 24, 1131–1138.

Hashiguchi, T., Kobayashi, T., Fongmoon, D., Shetty, A. K., Mizumoto, S., Miyamoto, N., Nakamura, T., Yamada, S., Sugahara, K., 2011. Demonstration of the hepatocyte growth factor signaling pathway in the *in vitro* neuritogenic activity of chondroitin sulfate from ray fish cartilage. BBA-Gen. Subjects, 1810, 406–413.

Hashim, P., Ridzwan, M. M., Bakar, J., Hashim, M. D., 2015. Collagen in food and beverage industries. Int. Food Res. J., 22, 1–8.

Herbage, D. A. N. I. E. L., Bouillet, J. O. S. E. T. T. E., Bernengo, J. C., 1977. Biochemical and physiochemical characterization of pepsin-solubilized type-II collagen from bovine articular cartilage. Biochem. J., 161, 303–312.

Hirose, S., Asano, K., Nakane, A., 2017. Attenuation of obesity-induced inflammation in mice orally administered with salmon cartilage proteoglycan, a prophylactic agent. Biochem. Bioph. Res. Co., 484, 480–485.

Horimoto, T., 2020. Series Fisheries Management and Marine Environment. Studies on the ecology and resource management of the skate (Kasube) in Hokkaido. Hokusuishi Dayori, 100, 17–19. (in Japanese). 堀本高矩, 2020. 資源管理・海洋環境シリーズ“未詳資源”かすべに挑む, 北水試だより, 100, 17–19.

Hu, Z., Yang, P., Zhou, C., Li, S., Hong, P., 2017. Marine collagen peptides from the skin of Nile Tilapia (*Oreochromis Niloticus*): Characterization and wound healing evaluation. Mar. Drugs, 15, 102–113.

Hubbell, J. A., 1999. Bioactive biomaterials, Curr. Opin. Biotech., 10, 123–129.

Husein el Hadmed, H., Castillo, R. F., 2016. Cosmeceuticals: peptides, proteins, and growth factors. J. Cosmet. Dermatology, 15, 514–519.

Im, A. R., Park, Y., Kim, Y. S., 2010. Isolation and characterization of chondroitin sulfates from sturgeon (*Acipenser sinensis*) and their effects on growth of fibroblasts. Biol. Pharm. Bull., 33, 1268–1273.

Imada, K., Oka, H., Kawasaki, D., Miura, N., Sato, T., Ito, A., 2010. Anti-arthritic action

mechanisms of natural chondroitin sulfate in human articular chondrocytes and synovial fibroblasts. Biol. Pharm. Bull., 33, 410–414.

Jayathilakan, K., Sultana, K., Radhakrishna, K., Bawa, A. S., 2012. Utilization of byproducts and waste materials from meat, poultry and fish processing industries: a review. J. Food Sci. Tec., 49, 278–293.

Jeevithan, E., Bao, B., Bu, Y., Zhou, Y., Zhao, Q., Wu, W., 2014. Type II collagen and gelatin from silvertip shark (*Carcharhinus albimarginatus*) cartilage: Isolation, purification, physicochemical and antioxidant properties. Mar. Drugs, 12, 3852–3873.

Jeevithan, E., Sanchez, C., de Val, J. E. M. S., Henrotin, Y., Wang, S., Motaung, K. S. C. M., Guo, R., Wang C., Robinson, J., Regenstein J. M., Bao, B., Wu, W., 2018. Cross-talk between primary osteocytes and bone marrow macrophages for osteoclastogenesis upon collagen treatment. Sci. Rep., 8, 5318.

Jeevithan, E., Zhang, J., Bao, B., Palaniyandi, K., Wang, S., Wenhui, W., Robinson, J. S., 2016a. Rheological, biocompatibility and osteogenesis assessment of fish collagen scaffold for bone tissue engineering. Int. J. Biol. Macromol., 91, 51–59.

Jeevithan, E., Zhang, J., Bao, B., Shujun, W., JeyaShakila, R., Wu, W. H., 2016b. Biocompatibility assessment of type-II collagen and its polypeptide for tissue engineering: effect of collagen's molecular weight and glycoprotein content on tumor necrosis factor (Fas/Apo-1) receptor activation in human acute T-

lymphocyte leukemia cell line. RSC Adv., 6, 14236–14246.

Jeevithan, E., Zhang, J., Wang, N., He, L., Bao, B., Wu, W., 2015. Physico-chemical, antioxidant and intestinal absorption properties of whale shark type-II collagen based on its solubility with acid and pepsin. Process Biochem., 50, 463–472.

Ju, J. H., Cho, M. L., Jhun, J. Y., Park, M. J., Oh, H. J., Min, S. Y., Cho, Y. G., Hwang, S. Y., Kwok S. K., Seo, S. H., Yoon, C. H., Park, S. H., Kim, H. Y., 2008. Oral administration of type-II collagen suppresses IL-17-associated RANKL expression of $CD4^+$ T cells in collagen-induced arthritis. Immunol. Lett., 117, 16–25.

Kakizaki, I., Tatara, Y., Majima, M., Kato, Y., Endo, M., 2011. Identification of proteoglycan from salmon nasal cartilage. Arch. Biochem. Biophys., 506, 58–65.

Kanazawa, I., Yamaguchi, T., Yano, S., Yamauchi, M., Sugimoto, T., 2008. Metformin enhances the differentiation and mineralization of osteoblastic MC3T3-E1 cells via AMP kinase activation as well as eNOS and BMP-2 expression. Biochemi. Biophysi. Res. Commun., 375, 414–419.

Kiani, C., Liwen, C. H. E. N., Wu, Y. J., Albert, J. Y., Burton, B. Y., 2002. Structure and function of aggrecan. Cell Res., 12, 19–32.

Knudson, C. B., Knudson, W., 2001. Cartilage proteoglycans. Semin. Cell Dev. Biol., 12, 69–78

Krichen, F., Bougatef, H., Sayari, N., Capitani, F., Amor, I. B., Koubaa, I., Maccari F., Mantovani V., Galeotti F., Volpi N., Bougatef, A., 2018. Isolation, purification and

structural characterestics of chondroitin sulfate from smooth hound cartilage: *in vitro* anticoagulant and antiproliferative properties. Carbohyd. Polym., 197, 451–459.

Kroh, L. W., 1994. Caramelisation in food and beverages. Food Chem., 51, 373–379.

Kobayashi, T., Kakizaki, I., Nozaka, H., Nakamura, T., 2017. Chondroitin sulfate proteoglycans from salmon nasal cartilage inhibit angiogenesis. Biochem. Bioph. Rep., 9, 72–78.

Kudo, M., Katayoshi, T., Kobayashi-Nakamura, K., Akagawa, M., Tsuji-Naito, K., 2016. H^+/peptide transporter (PEPT2) is expressed in human epidermal keratinocytes and is involved in skin oligopeptide transport. Biochem. Bioph. Res. Co., 475, 335–341.

Kumar, L. V., Shakila, R. J., Jeyasekaran, G., 2019. *In vitro* anti-cancer, anti-diabetic, Anti-inflammation and wound healing properties of collagen peptides derived from Unicorn Leatherjacket (*Aluterus Monoceros*) at different hydrolysis. Tur. J. Fish. Aquat. Sci., 19, 551–560.

Kurahashi, T., Fujii, J., 2015. Roles of antioxidative enzymes in wound healing, J. Dev. Biol., 3, 57–70.

Kwok, J. C. F., Warren, P., Fawcett, J. W., 2012. Chondroitin sulfate: a key molecule in the brain matrix. Int. J. Biochem. Cell B., 44, 582–586.

Lee, C. R., Grodzinsky, A. J., Spector, M., 2003. Biosynthetic response of passaged

chondrocytes in a type II collagen scaffold to mechanical compression. J. Biomed. Mater. Res. A, 64, 560–569.

Li, H., Low, Y. S. J., Chong, H. P., Zin, M. T., Lee, C. Y., Li, B., Leolukman, M., Kang, L., 2015. Microneedle-mediated delivery of copper peptide through skin, Pharm. Res., 32, 2678–2689.

Li, S., Li, J., Mao, G., Hu, Y., Ye, X., Tian, D., Linhardt, R.J., Chen, S., 2018. Fucosylated chondroitin sulfate oligosaccharides from *Isostichopus badionotus* regulates lipid disorder in C57BL/6 mice fed a high-fat diet. Carbohyd. Polym., 201, 634–642.

Li, X. R., Chi, C. F., Li, L., Wang, B., 2017. Purification and identification of antioxidant peptides from protein hydrolysate of scalloped hammerhead (*Sphyrna lewini*) cartilage. Mar. Drugs, 15, 61–77.

Li, Z., Wang, B., Chi, C., Gong, Y., Luo, H., Ding, G., 2013. Influence of average molecular weight on antioxidant and functional properties of cartilage collagen hydrolysates from *Sphyrna lewini*, *Dasyatis akjei* and *Raja porosa*. Food Res. Int., 51, 283–293.

Liang, C. C., Park, A. Y., Guan, J. L., 2007. *In vitro* scratch assay: a convenient and inexpensive method for analysis of cell migration *in vitro*, Nat. Protoc., 2, 329–333.

Liang, Q., Wang, L., Sun, W., Wang, Z., Xu, J., Ma, H., 2014. Isolation and

characterization of collagen from the cartilage of Amur sturgeon (*Acipenser schrenckii*). Process Biochem., 49, 318–323

Liu, P., Huang, M., Song, S., Hayat, K., Zhang, X., Xia, S., Jia, C., 2012. Sensory characteristics and antioxidant activities of Maillard reaction products from soy protein hydrolysates with different molecular weight distribution. Food Bioprocess Tech., 5, 1775-1789.

Lopes, C., Antelo, L. T., Franco-Uría, A., Alonso, A. A., Pérez-Martín, R., 2015. Valorisation of fish by-products against waste management treatments–Comparison of environmental impacts. Waste Manage., 46, 103–112.

Lovell, S. A., Gray, A., Boucher, S. E., 2018. Economic marginalization and community capacity: How does industry closure in a small town affect perceptions of place? J. Rural Studies, 62, 107–115.

Maccari, F., Galeotti, F., Volpi, N., 2015. Isolation and structural characterization of chondroitin sulfate from bony fishes. Carbohyd. Polym., 129, 143–147.

Marine Stewardship Council, https://www.msc.org/what-you-can-do/eat-sustainable-seafood/fish-to-eat/hoki

Martel-Pelletier, J., Farran, A., Montell, E., Vergés, J., Pelletier, J. P., 2015. Discrepancies in composition and biological effects of different formulations of chondroitin sulfate. Molecules, 20, 4277–4289.

Melgar-Lesmes, P., Garcia-Polite, F., Del-Rey-Puech, P., Rosas, E., Dreyfuss, J. L.,

Montell, E., Verges, J., Edelman, E.R., Balcells, M., 2016. Treatment with chondroitin sulfate to modulate inflammation and atherogenesis in obesity. Atherosclerosis, 245, 82–87.

Meng D., 2019. Studies on the efficient utilization of bester sturgeon by-products. pp.145, Ph.D. thesis, Hokkaido University.

Meng, D., Li, W., Ura, K., Takagi, Y., 2020. Effects of phosphate ion concentration on *in-vitro* fibrillogenesis of sturgeon type I collagen. Int. J. Biol. Macromol., 148, 182–191.

Merly, L., Smith, S. L., 2013. Collagen type II, alpha 1 protein: a bioactive component of shark cartilage. Int. Immunopharmacol., 15, 309–315.

Miyazaki, T., Miyauchi, S., Anada, T., Tawada, A., Suzuki, O., 2015. Chondroitin sulfate-E binds to both osteoactivin and integrin αVβ3 and inhibits osteoclast differentiation. J. Cell. Biochem., 116, 2247–2257.

Mizuta, S., Hwang, J. H., Yoshinaka, R., 2003. Molecular species of collagen in pectoral fin cartilage of skate (*Raja kenojei*). Food Chem., 80, 1–7.

Moroi, S., Miura, T., Tamura, T., Zhang, X., Ura, K., Takagi, Y., 2019. Self-assembled collagen fibrils from the swim bladder of Bester sturgeon enable alignment of MC3T3-E1 cells and enhance osteogenic differentiation. Mat. Sci. Eng. C, 104, 109925.

Morris, M. C., Gilliam, E. A., Button, J., Li, L., 2014. Dynamic modulation of innate

immune response by varying dosages of lipopolysaccharide (LPS) in human monocytic cells. J. Biol. Chem., 289, 1–11.

Murado, M. A., Fraguas, J., Montemayor, M. I., Vázquez, J. A., González, P., 2010. Preparation of highly purified chondroitin sulphate from skate (*Raja clavata*) cartilage by-products. Biochem. Eng. J., 49, 126–132.

Murota, I., Taguchi, S., Sato, N., Park, E. Y., Nakamura, Y., Sato, K., 2014. Identification of antihyperuricemic peptides in the proteolytic digest of shark cartilage water extract using *in vivo* activity-guided fractionation. J. Agr. Food Chem., 62, 2392–2397.

Nadanaka, S., Clement, A., Masayama, K., Faissner, A., Sugahara, K., 1998. Characteristic hexasaccharide sequences in octasaccharides derived from shark cartilage chondroitin sulfate D with a neurite outgrowth promoting activity. J. Biol. Chem., 273, 3296–3307.

Nair, M. B., Baranwal, G., Vijayan, P., Keyan, K. S., Jayakumar, R., 2015. Composite hydrogel of chitosan–poly (hydroxybutyrate-co-valerate) with chondroitin sulfate nanoparticles for nucleus pulposus tissue engineering. Colloid Surface B, 136, 84–92.

Ngo, P., Ramalingam, P., Phillips, J. A., Furuta, G. T., 2006. Collagen gel contraction assay, In Cell-Cell Interactions, 103–109.

Nie, S., Huang, J., Hu, J., Zhang, Y., Wang, S., Li, C., Marcone, M., Xie, M., 2013.

Effect of pH, temperature and heating time on the formation of furan in sugar–glycine model systems. Food Sci. Human Wellness, 2, 87–92.

Nishimoto, S., Takagi, M., Wakitani, S., Nihira, T., Yoshida, T., 2005. Effect of chondroitin sulfate and hyaluronic acid on gene expression in a three-dimensional culture of chondrocytes. J. Biosci. Bioeng., 100, 123–126.

Nishimura, M., Miyamoto, N., Nishihira, J., 2018. Daily oral chondroitin sulfate oligosaccharides for knee joint pain in healthy subjects: a randomized, blinded, placebo-controlled study. The Open Nutr. J., 12, 10–20.

Novoa-Carballal, R., Pérez-Martín, R., Blanco, M., Sotelo, C. G., Fassini, D., Nunes, C., Coimbra, M., Silva, T. H., Reis, R. L., Vázquez, J. A., 2017. By-products of *Scyliorhinus canicula*, *Prionace glauca* and *Raja clavata*: A valuable source of predominantly 6S sulfated chondroitin sulfate. Carbohyd. Polym., 157, 31–37.

Nwachukwu, I. D., Aluko, R. E., 2019. Structural and functional properties of food protein-derived antioxidant peptides. J. Food Biochem., 43, e12761.

Olsen, R. L., Toppe, J., Karunasagar, I., 2014. Challenges and realistic opportunities in the use of by-products from processing of fish and shellfish. Trends Food Sci. Tech., 36, 144–151.

Ono, H. K., Yoshimura, S., Hirose, S., Narita, K., Tsuboi, M., Asano, K., Nakane, A., 2018. Salmon cartilage proteoglycan attenuates allergic responses in mouse model of papain-induced respiratory inflammation. Mol. Med. Rep., 18, 4058–4064.

Pal, G. K., Suresh, P. V., 2016. Sustainable valorisation of seafood by-products: recovery of collagen and development of collagen-based novel functional food ingredients, Innov. Food Sci. Emerg., 37, 201–215.

Pan, X., Zhao, Y. Q., Hu, F. Y., Wang, B., 2016. Preparation and identification of antioxidant peptides from protein hydrolysate of skate (*Raja porosa*) cartilage. J. Funct. Foods, 25, 220–230.

Pontis, J. A., Costa, L. A. M. A. D., Silva, S. J. R. D., Flach, A., 2014. Color, phenolic and flavonoid content, and antioxidant activity of honey from Roraima, Brazil. Food Sci. Tech., 34, 69–73.

Raabe, O., Reich, C., Wenisch, S., Hild, A., Burg-Roderfeld, M., Siebert, H. C., Arnhold, S., 2010. Hydrolyzed fish collagen induced chondrogenic differentiation of equine adipose tissue-derived stromal cells. Histochem. Cell Biol., 134, 545–554.

Restaino, O. F., Finamore, R., Diana, P., Marseglia, M., Vitiello, M., Casillo, A., Bedini, E., Parrilli, M., Corsaro, M. M., Trifuoggi, M., Rosa, M. D., Schiraldi, C., 2017. A multi-analytical approach to better assess the keratan sulfate contamination in animal origin chondroitin sulfate. Anal. Chim. Acta, 958, 59–70.

Restaino, O. F., Finamore, R., Stellavato, A., Diana, P., Bedini, E., Trifuoggi, M., Rosa, M. D., Schiraldi, C., 2019. European chondroitin sulfate and glucosamine food supplements: a systematic quality and quantity assessment compared to

pharmaceuticals. Carbohyd. Polym., 114984.

Rustad, T., Storrø, I., Slizyte, R., 2011. Possibilities for the utilisation of marine by-products. Int. J. Food Sci. Tech., 46, 2001–2014.

Schäfer, M., Werner, S., 2008. Oxidative stress in normal and impaired wound repair, Pharmacol. Res., 58, 165–171.

Schägger, H., Von, J. G., 1987. Tricine-sodium dodecyl sulfate-polyacrylamide gel electrophoresis for the separation of proteins in the range from 1 to 100 kD. Anal. Biochem., 166, 368–379.

Schiraldi, C., Alfano, A., Cimini, D., Rosa, M. D., Panariello, A., Restaino, O. F., Rosa, M. D., 2012. Application of a 22L scale membrane bioreactor and cross-flow ultrafiltration to obtain purified chondroitin. Biotechnol. Progr., 28, 1012–1018.

Schiraldi, C., Cimini, D., De Rosa, M., 2010. Production of chondroitin sulfate and chondroitin. Appl. Microbiol. Biot., 87, 1209–1220.

Schmittgen, T. D., Livak, K. J., 2008. Analyzing real-time PCR data by the comparative CT method. Nat. Protoc., 3, 1101–1103.

Seidel, R., Blumer, M., Pechriggl, E. J., Lyons, K., Hall, B. K., Fratzl, P., Weaver J. C., Dean, M. N., 2017. Calcified cartilage or bone? Collagens in the tessellated endoskeletons of cartilaginous fish (sharks and rays). J. Struct. Biol., 200, 54–71.

Shang, Q., Shi, J., Song, G., Zhang, M., Cai, C., Hao, J., Li, G., Yu, G., 2016. Structural modulation of gut microbiota by chondroitin sulfate and its oligosaccharide. Int. J.

Biol. Macromol., 89, 489–498.

Shen, Q., Zhang, C., Jia, W., Qin, X., Cui, Z., Mo, H., Richel, A., 2019. Co-production of chondroitin sulfate and peptide from liquefied chicken sternal cartilage by hot-pressure. Carbohyd. Polym., 115015.

Shen, W., Matsui, T., 2017. Current knowledge of intestinal absorption of bioactive peptides. Food Funct., 8, 4306–4314.

Sila, A., Bougatef, A., 2016. Antioxidant peptides from marine by-products: Isolation, identification and application in food systems. J. Funct. Foods, 21, 10–26.

Silvipriya, K. S., Kumar, K. K., Bhat, A. R., Kumar, B. D., John, A., Lakshmanan, P., 2015. Collagen: Animal sources and biomedical application. J Appl. Pharm. Sci., 5, 123–127.

Song, Y., Kim, M., Woo, M., Baek, J. M., Kang, K. H., Kim, S. H., Roh S. S., Park C. H., Jeong K. S., Noh, J. S., 2017. Chondroitin sulfate-rich extract of skate cartilage attenuates lipopolysaccharide-induced liver damage in mice. Mar. Drugs, 15, 178–192.

Sotelo, C. G., Comesaña, M. B., Ariza, P. R., Pérez-Martín, R. I., 2016. Characterization of collagen from different discarded fish species of the West coast of the Iberian Peninsula. J. Aquatic Food Prod. Tec., 25, 388–399.

Stabler, T. V., Montell, E., Vergés, J., Huebner, J. L., Kraus, V. B., 2017. Chondroitin sulfate inhibits monocyte chemoattractant protein-1 release from 3T3-L1

adipocytes: a new treatment opportunity for obesity-related inflammation? Biomarker insights, 12, 1–4.

Stevens, J. R., Newton, R. W., Tlusty, M., Little, D. C., 2018. The rise of aquaculture by-products: Increasing food production, value, and sustainability through strategic utilisation. Mar. Policy, 90, 115–124.

Su, G., Zheng, L., Cui, C., Yang, B., Ren, J., Zhao, M., 2011. Characterization of antioxidant activity and volatile compounds of Maillard reaction products derived from different peptide fractions of peanut hydrolysate. Food Res. Int., 44, 3250–3258.

Subhan, F., Ikram, M., Shehzad, A., Ghafoor, A., 2015. Marine collagen: an emerging player in biomedical applications. J. Food Sci. Tech., 52, 4703–4707.

Surapaneni, L., Huang, G., Bodine, A. B., Brooks, J., Podila, R., Haley-Zitlin, V., 2014. Correlations between chondroitin sulfate physicochemical properties and its in-vitro absorption and anti-inflammatory Activity. arXiv, 1412, 5562.

Takagi, H., Asano, Y., Yamakawa, N., Matsumoto, I., Kimata, K., 2002. Annexin 6 is a putative cell surface receptor for chondroitin sulfate chains. J. Cell Sci., 115, 3309–3318.

Tao, J., Zhao, Y. Q., Chi, C. F., Wang, B., 2018. Bioactive peptides from cartilage protein hydrolysate of spotless smoothhound and their antioxidant activity *in vitro*. Mar. Drugs, 16, 100–118.

Trentham, D. E., Dynesius-Trentham, R. A., Orav, E. J., Combitchi, D., Lorenzo, C., Sewell, K. L., Hafler, D. A., Weiner, H. L., 1993. Effects of oral administration of type II collagen on rheumatoid arthritis. Science, 261, 1727–1730.

Uchisawa, H., Okuzaki, B. I., Ichita, J., Matsue, H., 2001. Binding between calcium ions and chondroitin sulfate chains of salmon nasal cartilage glycosaminoglycan. In International Congress Series, 1223, 205–220.

Varghese, S., Hwang, N. S., Canver, A. C., Theprungsirikul, P., Lin, D. W., Elisseeff, J., 2008. Chondroitin sulfate based niches for chondrogenic differentiation of mesenchymal stem cells. Matrix Biol., 27, 12–21.

Vázquez, J., Fraguas, J., Novoa-Carvallal, R., Reis, R., Antelo, L., Pérez-Martín, R., Valcarcel, J., 2018. Isolation and chemical characterization of chondroitin sulfate from cartilage by-products of blackmouth catshark (*Galeus melastomus*). Mar. Drugs, 16, 344–359.

Vázquez, J. A., Fraguas, J., Novoa-Carballal, R., Reis, R. L., Pérez-Martín, R. I., Valcarcel, J., 2019. Optimal isolation and characterisation of chondroitin sulfate from rabbit fish (*Chimaera monstrosa*). Carbohyd. Polym., 210, 302–313.

Vázquez, J., Rodríguez-Amado, I., Montemayor, M., Fraguas, J., González, M., Murado, M., 2013. Chondroitin sulfate, hyaluronic acid and chitin/chitosan production using marine waste sources: Characteristics, applications and eco-friendly processes: A review. Mar. Drugs, 11, 747–774

Volpi, N., 2002. Oral bioavailability of chondroitin sulfate (Condrosulf®) and its constituents in healthy male volunteers. Osteoarthr. Cartilage, 10, 768–777.

Volpi, N., 2007. Analytical aspects of pharmaceutical grade chondroitin sulfates. J. Pharm. Sci., 96, 3168–3180.

Volpi, N., 2019. Chondroitin Sulfate Safety and Quality. Molecules, 24, 1447.

Volpi, N., Bolognani, L., Conte, A., Petrini, M., 1993. Effects of chondroitin sulfates with different structures on leukemia cells: U-937 cell proliferation and differentiation. Leukemia Res., 17, 789–798.

Wahli, W., Michalik, L., 2012. PPARs at the crossroads of lipid signaling and inflammation. Trends Endocrin. Metabo., 23, 351-363.

Wang, J., Zhang, L., Jin, Z., 2016. Separation and purification of low-molecular-weight chondroitin sulfates and their anti-oxidant properties. Bangladesh J. Pharmacol., 11, S61–S67.

Wijesekara, I., Pangestuti, R., Kim, S. K., 2011. Biological activities and potential health benefits of sulfated polysaccharides derived from marine algae. Carbohyd. Polym., 84, 14–21.

Witten, P. E., Huysseune, A., Hall, B. K., 2010. A practical approach for the identification of the many cartilaginous tissues in teleost fish. J. Appl. Ichthyol., 26, 257–262.

Wirth, P., Elis, V., Müller, B., Yamamoto, K., 2016. Peripheralisation of small towns in

Germany and Japan–Dealing with economic decline and population loss. J. rural studies, 47, 62–75.

Wu, F., Zhou, C., Zhou, D., Ou, S., Liu, Z., Huang, H., 2018. Immune-enhancing activities of chondroitin sulfate in murine macrophage RAW 264.7 cells. Carbohyd. Polym., 168, 611–619.

Xu, H., Wang, J., Zhang, X., Li, Z., Wang, Y., Xue, C., 2015. Inhibitory effect of fucosylated chondroitin sulfate from the sea cucumber *Acaudina molpadioides*, on adipogenesis is dependent on Wnt/β-catenin pathway. J. Bios. Bioeng., 119, 85–91.

Yamada, S., Matsushima, K., Ura, H., Miyamoto, N., Sugahara, K. 2013. Mass preparation of oligosaccharides by the hydrolysis of chondroitin sulfate polysaccharides with a subcritical water microreaction system. Carbohyd. Rre., 371, 16–21.

Yamagata, M., Kimata, K., Oike, Y., Tani, K., Maeda, N., Yoshida, K., Shimomura Y., Yoneda M., Suzuki, S., 1987. A monoclonal antibody that specifically recognizes a glucuronic acid 2-sulfate-containing determinant in intact chondroitin sulfate chain. J. Biol. Chem., 262, 4146–4152.

Yang, J., Ren, J., Song, J., Liu, F., Wu, C., Wang, X., Gong, L., Li, W., Xiao, F., Yan, F., Chen, L., 2013. Glucagon-like peptide 1 regulates adipogenesis in 3T3-L1 preadipocytes. Int. J. Mol. Med., 31, 1429–1435.

Yoshimoto, M., Heike, T., Chang, H., Kanatsu-Shinohara, M., Baba, S., Varnau, J. T.,

Shinoharac, T., Yoder, M. C., Nakahata, T., 2009. Bone marrow engraftment but limited expansion of hematopoietic cells from multipotent germline stem cells derived from neonatal mouse testis. Exp. Hematol., 37, 1400–1410.

Zeng, Q., Fan, X., Zheng, Q., Wang, J., Zhang, X., 2018. Anti-oxidant, hemolysis inhibition, and collagen-stimulating activities of a new hexapeptide derived from *Arthrospira* (*Spirulina*) *platensis*. J. Appl. Phycol., 30, 1655–1665.

Zhang, L., Lu, Y., 2012. Inhibitory activities of extracts from *Cleistocalyx operculatus* flower buds on pancreatic lipase and α-amylase. Eur. Food Res. Technol., 235, 1133–1139.

Zhang, Q., Li, J., Liu, C., Song, C., Li, P., Yin, F., Xiao, Y., Li, J., Jiang, W., Zong, A., Zhang, X., Wang, F., 2015. Protective effects of low molecular weight chondroitin sulfate on amyloid beta (Aβ)-induced damage *in vitro* and *in vivo*. Neuroscience, 305, 169–182.

Zhang, X., Adachi, S., Ura, K., Takagi, Y., 2019. Properties of collagen extracted from Amur sturgeon *Acipenser schrenckii* and assessment of collagen fibrils in vitro. Int. J. Biol. Macromol., 137, 809–820.

Zhang, X., Azuma, N., Hagihara, S., Adachi, S., Ura, K., Takagi, Y., 2016. Characterization of type I and II procollagen α1chain in Amur sturgeon (*Acipenser schrenckii*) and comparison of their gene expression. Gene, 579, 8–16.

Zhang, X., Ookawa, M., Tan, Y., Ura, K., Adachi, S., Takagi, Y., 2014. Biochemical

characterisation and assessment of fibril-forming ability of collagens extracted from Bester sturgeon *Huso huso*× *Acipenser ruthenus*. Food Chem., 160, 305–312.

Zhao, L., Liu, M., Wang, J., Zhai, G., 2015. Chondroitin sulfate-based nanocarriers for drug/gene delivery. Carbohyd. Polym., 133, 391–399.

Zheng, L., Wei, H., Yu, H., Xing, Q., Zou, Y., Zhou, Y., Peng, J., 2018. Fish skin gelatin hydrolysate production by ginger powder induces glutathione synthesis to prevent hydrogen peroxide induced intestinal oxidative stress via the Pept1-p62-Nrf2 cascade. J. Agr. Food Chem., 66, 11601–11611.

Zhu, W., Ji, Y., Wang, Y., He, D., Yan, Y., Su, N., Zhang, C., Xing, X. H., 2018. Structural characterization and in vitro antioxidant activities of chondroitin sulfate purified from *Andrias davidianus* cartilage. Carbohyd. Polym., 196, 398–404.

Zou, T. B., He, T. P., Li, H. B., Tang, H. W., Xia, E. Q., 2016. The structure-activity relationship of the antioxidant peptides from natural proteins, Molecules, 21, 72–86.

Zou, X. H., Jiang, Y. Z., Zhang, G. R., Jin, H. M., Hieu, N. T. M., Ouyang, H. W., 2009. Specific interactions between human fibroblasts and particular chondroitin sulfate molecules for wound healing. Acta Biomater., 5, 1588–1595

Acknowledgments

Upon the completion of this thesis, I am grateful to those who have offered me encouragement and support during the course of my study.

Special acknowledgment is given to my respectable supervisor Prof. Yusuaki Takagi, for his patient guidance, constructive suggestions and constant encouragement throughout in my study and life. His profound insight about my research taught me so much. He provided me with beneficial help and offered me precious comments during the whole process of my PhD course.

I would like to express particular thanks to members of my thesis reading committee Prof. Shiniji Adachi, Prof. Hiroki Saeki, and Associate Prof. Kazuhiro Ura, Faculty of the Fisheries Sciences, for spending their time on careful reading of my thesis and their valuable comments, as well as for their instruction and generous support during these years.

I would like to present my thanks to all members in our laboratory for their help and kindness. They gave me an enjoyable life in Japan.

Finally, I would like to express my gratitude to my parents and friends who have provided me great encouragement and support. Thanks for the life during the exchange student to PhD student in Hokkaido University that is the most wonderful and lucky time, which living in the city I like, having people I like and doing the things I like.